2018

CONSEQUENCES OF ARYL HYDROCARBON RECEPTOR ACTIVATION: THYMIC ATROPHY AND THERAPEUTIC LIPOSOMAL NANOPARTICLES

Joanna Michelle Kreitinger

CONSEQUENCES OF ARYL HYDROCARBON RECEPTOR ACTIVATION:

THYMIC ATROPHY AND THERAPEUTIC LIPOSOMAL NANOPARTICLES

By

JOANNA MICHELLE KREITINGER

Bachelor of Arts in Organismal Biology and Ecology, University of Montana, Missoula, 2012

Dissertation

Presented in partial fulfillment of the requirements
for the degree of

Doctor of Philosophy
in Cellular, Molecular & Microbial Biology

The University of Montana
Missoula, MT

Fall 2018

For approval by:
Scott Whittenburg, Dean of the Graduate School

Dr. David M. Shepherd
Department of Biomedical and Pharmaceutical Sciences

Dr. Scott Wetzel
Division of Biological Sciences

Dr. Celine Beamer
Department of Biomedical and Pharmaceutical Sciences

Dr. Jesse Hay
Division of Biological Sciences

Dr. Mike Minnick
Division of Biological Sciences

Kreitinger, Joanna Ph.D., Fall 2018 Cellular, Molecular & Microbial Biology

CONSEQUENCES OF ARYL HYDROCARBON RECEPTOR ACTIVATION: THYMIC ATROPHY AND REGENERATION

Chairperson: Dr. David M. Shepherd

Abstract

The Aryl hydrocarbon Receptor (AhR) is a ligand-activated transcription factor best known for its role in xenobiotic metabolism of environmental pollutants. Activation of the AhR by its prototypical ligand 2,3,7,8-tetrachlorodibenzo-pdioxin (TCDD) leads to pronounced thymic atrophy and severe immunosuppression. Studies of AhR activation can have dual applications: to better understand AhR-mediated immunotoxicity and to harness its immunomodulatory effects for therapeutic use. Here, we first aimed to determine whether AhR-mediated thymic atrophy was ligand-dependent through the use of dietary and endogenously sourced ligands, indole-3-carbinol (I3C) and 2-(19 H-indole-39 -carbonyl)-thiazole-4-carboxylic acid methyl ester (ITE) respectively. We also aimed to identify key mediators of TCDD-induced thymic atrophy through the use of lineage-specific Cre-lox conditional knockout mice. We hypothesized that AhR activation induces thymic atrophy in a ligand-dependent manner and AhR expression within CD11c+ DCs is necessary for thymic atrophy by TCDD. In vivo exposure of ITE and I3C yielded dramatically different thymic outcomes with ITE resulting in severe thymic atrophy similar to TCDD while I3C did not induce atrophy. Through the use of Cre-Lox conditional knockout mice under lineage-specific promoters, we identified a requisite role for AhR activation in CD11c+ cells for TCDD-induced thymic atrophy. We next aimed to apply current understanding of AhR-mediated immune suppression in the development of a liposomal nanoparticle (LNP) delivery system for concentrated delivery of AhR-agonist, ITE, to dendritic cells. Dendritic cells are exquisitely sensitive to AhR activation and promote the generation of regulatory T cells. ITE is a potent inducer of AhR activation; however, it is rapidly metabolized and systemic exposure to high doses can have undesirable effects. Therefore, we hypothesized that the generation and delivery of AhR agonist-loaded liposomal nanoparticles would activate the AhR in dendritic cells leading to a phenotype similar to TCDD, and result in cell-specific uptake when administered *in vivo*. LNP maintained high ITE entrapment, were of optimal size for dendritic cell uptake, induced AhR-responsive genes *in vitro*, and were preferentially taken up by splenic APCs. Together, this work furthers our understanding of AhR-mediated thymic atrophy, and presents a novel AhR agonist delivery system for therapeutic application of the AhR.

ACKNOWLEDGMENTS

I owe many thanks to my committee members: Dr. Scott Wetzel, Dr. Michael Minnick, Dr. Jesse Hay, Dr. Celine Beamer, and Dr. David Shepherd for guidance, feedback, and encouragement during my graduate work. Special thanks go to Dr. Shepherd, for advising me throughout the past five years. Together we had many accomplishments and I appreciate the opportunities afforded to me throughout my doctoral training. Thank you, Dr. Beamer, for teaching me laboratory skills and being available for questions during my doctoral training. Thank you, Dr. Wetzel, for introducing me to laboratory research as an undergraduate student.

Thank you to my Shepherd Lab-mates for the lending of hands, providing many laughs, not breaking all the instruments, and making sometimes-tedious bench work more enjoyable. Thank you to my graduate peers, many of who have become close friends, for the unending support and for sharing in, and normalizing, all that is the graduate school experience.

I would like to thank Britten Postma, Pam Shaw, Kelly Carrick, Jess Wexler and Lou Herritt for my training in animal techniques, data collection and analysis, and answering so many questions of mine. Thank you to DBS office administration for helping with forms and questions. I would also like to thank Gretchen McCaffery for the immensely helpful one-on-one writing sessions and workshops provided throughout my doctoral training. I want to extend a sincere thank you to Jody Anderson, an amazing woman of P.E.O., for providing me with the opportunity to become a National P.E.O. Scholar—it was truly a highlight of my graduate education. Thank you, Dr. Sarj Patel, for being so available as I prepared for my qualifying exams. Thank you, Andrij Holian, for writing many letters of recommendation for fellowships and scholarships.

Thank you to my incredible family and friends for being there for me in the most exciting moments, the most challenging moments, and everything in between. Lastly, I have to acknowledge my son, who I fondly and all too often refer to as my best cell culture and my greatest experiment.

TABLE OF CONTENTS

LIST OF FIGURES

Chapter 1.

Chapter 2.

Chapter 3.

LIST OF TABLES

CHAPTER 1: INTRODUCTION

This study describes the effects of aryl hydrocarbon receptor (AhR) activation on the thymus. Chapter 1 will: 1) introduce the AhR and its numerous ligands, 2) introduce the basic structure of the thymus and its role as a primary immune organ and 3) describe dendritic cells and their basic role within the immune system.

THE ARYL HYDROCARBON RECEPTOR

DISCOVERING THE AHR

While multiple scientific advances coalesced into the discovery of the Aryl hydrocarbon Receptor (AhR), a common theme existed; namely the necessity to understand mechanisms of xenobiotic toxicity. Specifically, the discovery that polycyclic aromatic hydrocarbons (PAHs) appeared to induce their own metabolism drove the ultimate discovery of a receptor that could bind these compounds. First described by Allan Conney in the 1950's, and originally termed the BP hydroxylase, due to its induced expression following exposure to benzo(a)pyrene (BaP), the receptor's name was broadened to Aryl hydrocarbon Hydroxylase (AhH) in the 1970's with the discovery that multiple PAHs were suitable ligands (Figure 1.1) (Okey et al. 1979; Wright et al. 2017; Yao and Denison 1992).

Up until the late 1970's, the AhR was still seen as a hydroxylase that was acted on *by* a receptor; the AhR itself being identified as a receptor had not yet come to fruition. A monumental contribution to AhR research came with the discovery that 2,3,7,8 tetrachlorodibenzo-p-dioxin (TCDD), a halogenated aromatic hydrocarbon, could bind mammalian hepatocytes (Kouri et al. 1974). Following this discovery, TCDD was also determined to induce metabolism in tissues and systems previously found unable to do so with PAHs. These landmark studies enabled the ultimate identification of an "induction receptor" in 1976 by Poland, Glover, and Kende (Harper et al. 2006). Soon after, the receptor was termed Ah Receptor after Okey and Nebert documented its receptor-like activity (Wright et al. 2017; Yao and Denison 1992). Formally known as the Aryl

hydrocarbon Receptor, and with its prototypical ligand discovered, AhR research and its impacts across multiple disciplines, including immunology, were just beginning.

Figure 1. 1 AhR Timeline of Discovery

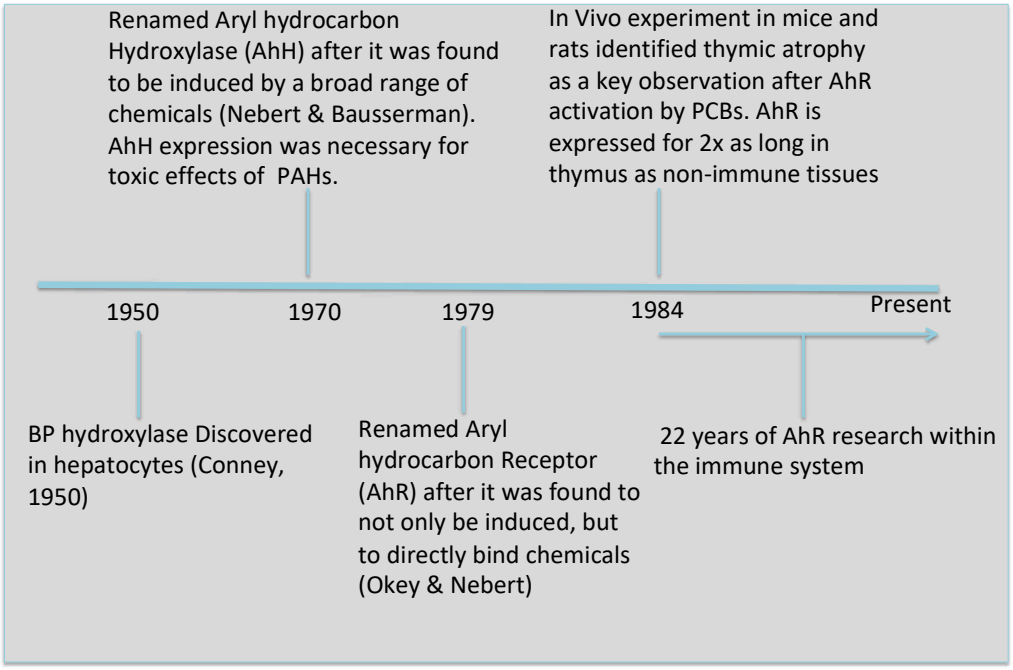

Figure 1. 1 AhR Timeline of Discovery

A brief timeline of key events that led to the discovery of the AhR and AhR research in the field of immunology.

AHR SIGNALING PATHWAYS

The AhR is a cytosolic, ligand-activated transcription factor in the basic helix-loop-helix/Per-Arnt-Sim (bHLH/PAS) protein family. In mammals, the AhR is ubiquitous with temporal, cellular, and tissue-specific expression. Greatest AhR expression occurs in the liver, thymus, lung, kidney, spleen, and placenta (Harper et al. 2006). Studies have shown that the AhR plays important roles beyond xenobiotic metabolism, including roles in hematopoiesis, immune system biology, neural differentiation, and liver formation (Wright et al. 2017).

In its inactive state, the AhR is found in the cytosol complexed to a host of chaperone proteins including XAP2, HSP90, and AIP. Upon ligand binding, a conformational change releases the chaperone proteins and exposes the nuclear localization sequence (Figure 1.2). The ligand:AhR is transported into the nucleus where it heterodimerizes with another bHLH/PAS protein, the Aryl hydrocarbon Receptor Nuclear Transporter (ARNT, HIF1β) (Yao and Denison 1992). Ligand:AhR/ARNT complexes specifically recognize and bind dioxin/xenobiotic responsive elements (DRE/XRE) in the promoter region of AhR-inducible genes (Dolwick et al. 1993). The mere presence of the DRE consensus sequence, 5'-TNGCGTG-3', upstream of a gene can be used to determine whether the gene is AhR-responsive, and most AhR-responsive genes have multiple DRE in the promoter region (Swanson et al. 1995).

The most common and consistent transcriptional target of the AhR canonical pathway following TCDD exposure is Cytochrome P450, family 1, subfamily A, polypeptide 1 (Cyp1a1), a phase I metabolizing enzyme. Within the promoter region of murine Cyp1a1, there are eight putative DREs and five of these are conserved between mouse, rat, and human (Li et al. 2014; Nukaya and Bradfield 2009). Therefore, measuring Cyp1a1 gene expression is both an accurate and a translational readout of AhR activation. Importantly, the AhR transcribes a host of other genes with cell/tissue specificity including indoleamine-2,3 dioxygenase 1 and 2 (IDO 1 and 2), isoforms of transforming growth factor beta (TGFβ), and retinaldehyde dehydrogenases (RALDH) (Vogel et al. 2008).

Having discussed the AhR canonical pathway, it is necessary to briefly address the AhR non-canonical pathway, which is also shown in Figure 1.2. The AhR non-canonical pathway occurs through alternative binding of nuclear AhR independent of ARNT and can result in expression of genes needed to maintain homeostasis (Wright et al. 2017). Less is currently understood regarding the interactions and implications of the non-canonical pathway.

Figure 1. 2 AhR signaling pathways.

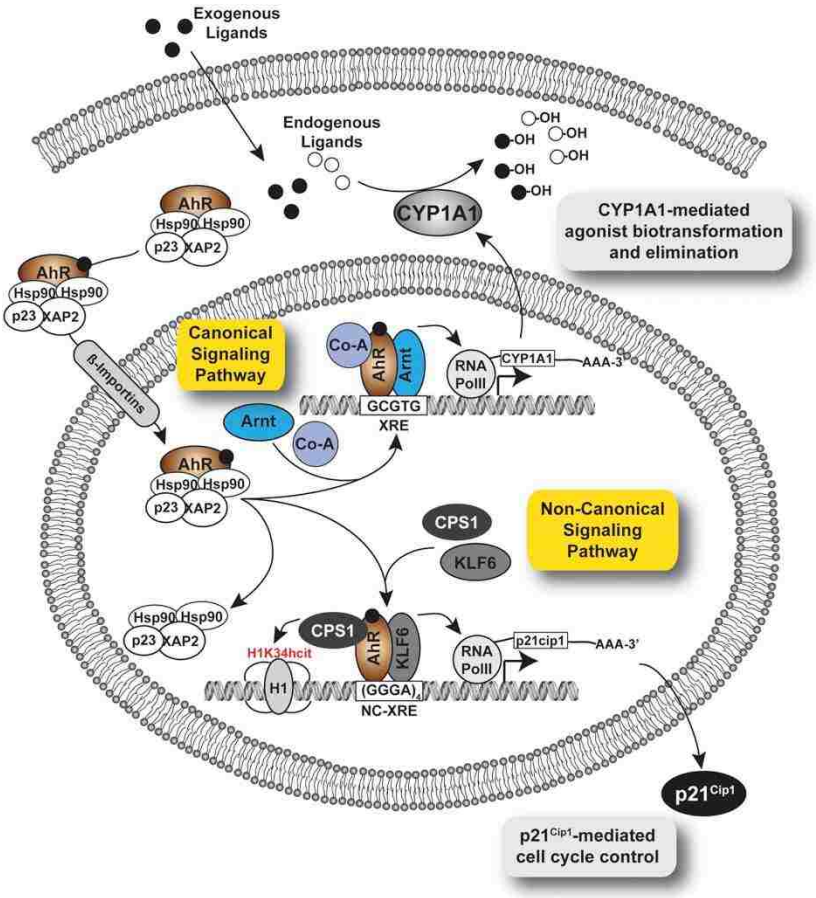

Figure 1.2 AhR signaling pathways.
A diagram of protein interactions involved in the AhR canonical and non-canonical signaling pathways. In the canonical AhR signaling pathway, a ligand diffuses into the cell and binds cytosolic AhR complex, which triggers dissociation of chaperone proteins. The ligand-bound AhR translocates to the nucleus where it binds ARNT enabling binding to canonical DREs and triggering transcription of the AhR gene battery. In the non-canonical signaling pathway, the ligand-bound, nuclear AhR binds proteins independent of ARNT. RelB in the nucleus thereby allows binding to NF-kB response elements. (Wright et al. 2017)

AHR ALLELES

In the early years of AhR research, there were conflicting results regarding protein and ligand binding, which can now be attributed to the use of mouse strains with different AhR alleles. These alleles include AhR^{b-1}, AhR^{b-2}, AhR^{b-3}, and AhR^{d} (Smith et al. 2018). C57Bl/6 mice carry the best-studied allele: AhR^{b-1}, which readily binds TCDD with high affinity. DBA/J mice, however, carry the AhR^{d} allele with a 10x lower binding affinity for TCDD due to an $alanine^{375}$ to valine substitution in the ligand-binding domain (Ema et al. 1994). Additionally, the AhR demonstrates both basal and inducible expression that is dependent on tissue and cell type. In mammals, organs known to have the highest basal AhR expression levels include the liver, lung, kidney, spleen, placenta, and thymus (Harper et al. 2006). Within the immune system, AhR is expressed basally by a majority of cells types, and increased AhR expression occurs with exposure to xenobiotics, mitogens, antigens, and cytokines (Pohjanvirta 2011)

Importantly, AhR^{b-1} mouse models have so far been the predominant source for our current understanding of the AhR, but there are differences between the AhR^{b-1} allele expressed in mice and the AhR expressed in most humans, which share 85% sequence homology. The human AhR binds to TCDD more similar to the AhR^{d} mouse allele with ~10x lower affinity than murine AhR^{b-1}. Interestingly, human AhR has a similar mutation to murine AhR^{d} with an amino acid substitution in the ligand-binding domain, and some research suggests that the human AhR may bind endogenous compounds with greater affinity than exogenous compounds (Hubbard et al. 2016).

AHR LIGANDS

While TCDD is the prototypical AhR ligand, due to its high binding affinity, numerous compounds are known to bind and activate the AhR. AhR ligand interactions that are best understood involve planar, hydrophobic, highly toxic environmental compounds within the halogenated aromatic hydrocarbons (HAHs) and polycyclic aromatic hydrocarbons (PAHs); however, the increased interest in AhR in multiple fields has resulted in a continual identification of AhR ligands beyond the classical, exogenous HAHs.

Classical ligands do not vary far from the prototypical AhR ligand, TCDD, and generally take planar conformations with multiple benzene rings and act as AhR agonists. Importantly, a broad range of non-classical ligands, those that vary substantially from TCDD, can readily bind the AhR (Figure 1.3)(Pohjanvirta 2011). Notably, compounds with demonstrated antagonistic properties also directly bind the AhR, and can result in ligand-selective antagonism. Notably, 2-methyl-2H-pyrazole-3-carboxylic acid (2-methyl-4-o-tolylazo-phenyl)-amide (CH223191) can block binding of TCDD and other halogenated aromatic hydrocarbons (HAH), without blocking binding of non-HAH ligands (Pohjanvirta 2011).

While TCDD is an exogenous compound, endogenous compounds have also been identified. The earliest and arguably most notable is 2-(1′H-indole-3′-carbonyl)-thiazole-4-carboxylic acid methyl ester (ITE), which was isolated from porcine lungs in 2002, and found to bind AhR^b with moderate affinity (3nM ITE vs .27nM TCDD) (Song et al. 2002). The identification of an endogenous ligand was a pivotal finding as the AhR is a

highly conserved protein and its roles in xenobiotic metabolism and immune modulation are likely more recent adaptive functions.

Diet is a prominent source of AhR ligands—from both bioaccumulation of TCDD in fatty tissue of animals and from plant-derived ligands such as Indole-3-carbinol (I3C). In fact, one study analyzing body burden of TCDD-equivalents (TEQs) found plant-based dietary ligands to be a greater contributor (96% of TEQ) than TCDD to total body burden in humans (Connor and Finley 2003). Notably, ligand affinity, an important factor, was not addressed in this analysis, but it highlights the need to study a variety of ligands beyond TCDD, including those from dietary sources.

Figure 1. 3 A representative panel of AhR ligands

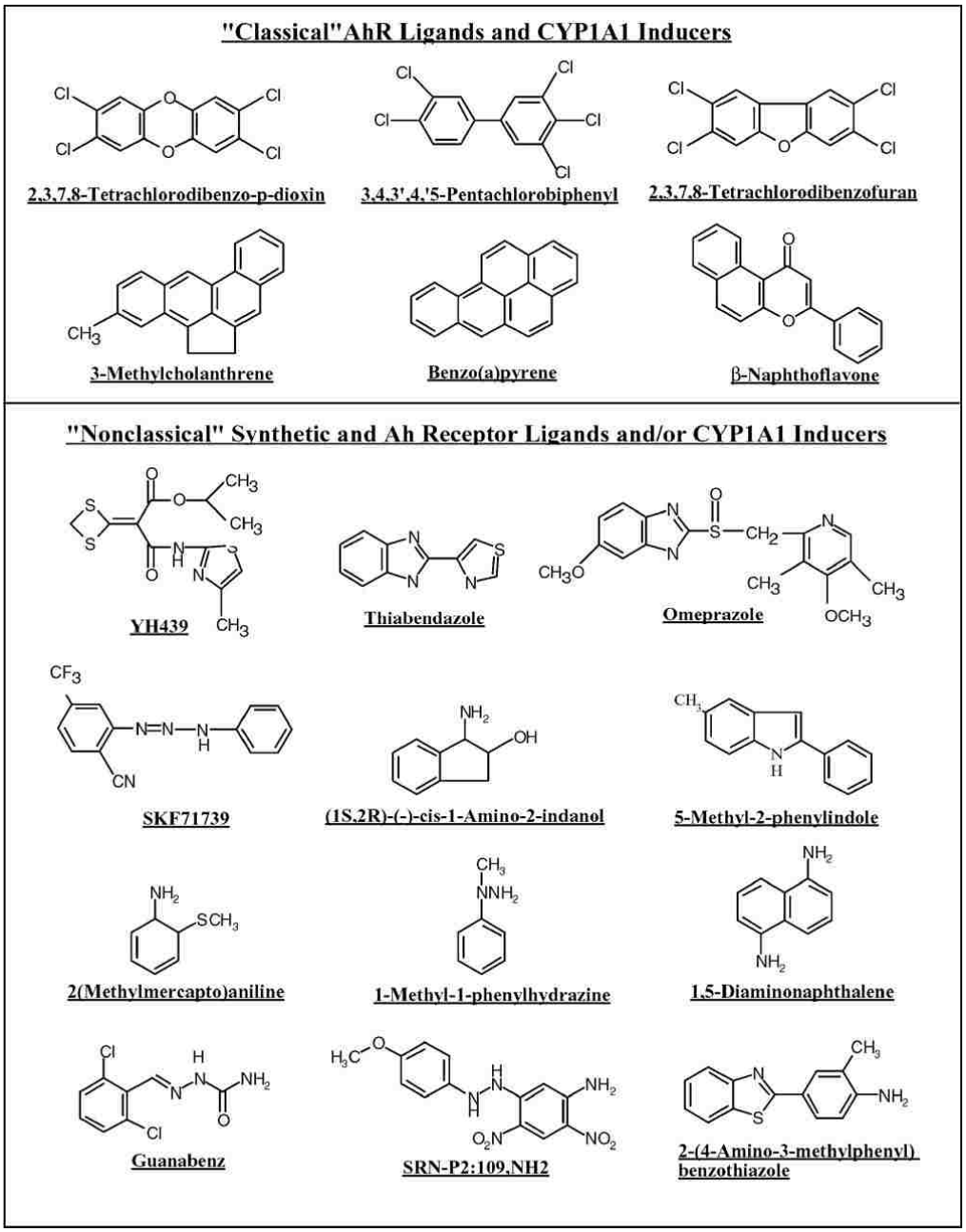

Figure 1.3 A Representative Panel of AhR ligands.
A panel of known AhR ligands intended to show their variation and similarity (Denison and Nagy 2003).

AHR-INDUCED IMMUNOSUPPRESSION

In 1984, thymic expression of the AhR in Sprague-Dawley rats was determined to occur at high levels for twice as long (42 days vs. 21 days) after parturition as compared to non-immune tissues such as liver and lungs (Nikolaidis et al. 1988). These observations led to further investigation of AhR activity in immune organs, and the discovery that AhR activation had adverse effects on thymic function. In 1985, PCBs acting through the AhR were found to cause severe thymic atrophy and humoral immune suppression (Hanieh 2014). The succession of rapid discoveries throughout the 1980s broadened the expanse of AhR-mediated suppression within the immune system to include: reduction in splenic lymphocyte number and function in mice, reduced humoral antibody response in mice and rats, and overall reduction in ability of mice to fight certain infections (Goudot et al. 2017).

With a potential link made between the AhR and observed suppression of the immune system, immunologists entered into a field, which to this point had predominantly been pioneered by toxicologists and biochemists. The interweaving of discoveries from these disciplines has both expanded our understanding of the AhR signaling pathway and of the immense complexity of the innate and adaptive immune responses.

Innate immune cells strongly vary in AhR expression (Figure 1.4), ranging from high, constitutive expression, to low, conservatively inducible expression. The outcome of AhR activation on promotion or regulation of immune responses also appears to vary by cell type and maturation phase. Interestingly, both inflammatory and regulatory genes have an abundance of AhR responsive elements within their promoter regions, and it has

been shown that cross-talk between AhR and NF-κB results in multiple pro-inflammatory signals (Goudot et al. 2017). Neutrophils, and most granulocytes are not thought to express the AhR at significant levels and appear to be predominantly influenced by AhR activation through an indirect mechanism.

Antigen presenting cells, macrophages and dendritic cells, constitutively express the AhR at relatively high levels and show further AhR expression upon activation and maturation (Kreitinger et al. 2016). It has also been shown in vitro that AhR activation in monocytes selectively promotes differentiation of murine monocyte-derived DCs through induction of BLIMP-1 (Goudot et al. 2017), while impairing differentiation of monocyte-derived Macs. Additionally, AhR deficiency correlated with a reduced frequency of monocyte-derived DCs in vivo (Goudot et al. 2017). Dendritic cells are highly responsive to AhR activation and demonstrate AhR-mediated alterations to maturation, protein expression, and gene induction. Specifically, AhR activation results in an increase in immature dendritic cells as marked by moderate CD11c and MHII expression. AhR-activated dendritic cells show increased frequency and density of co-stimulatory molecules as well as increased expression of regulatory genes, including Indoleamine 2,3-dioxygenase-1,-2 (IDO-1,-2) and transforming growth factor beta (TGFβ). AhR-induced regulatory DCs are potent inducers of Foxp3+ regulatory T cells, while direct exposure of naïve T cells to AhR activation appears to induce non-Foxp3+ Tregs (Bankoti et al. 2010c; Benson and Shepherd 2011b; Gagliani et al. 2015; Qiu et al. 2012).

Natural killer cells, which are thought to have basal expression of AhR, are reported to have reduced bacterial clearance and tumor cell recognition capacity in $AhR^{-/-}$ mice. These studies also suggest that NK cells are, in part, directly affected by AhR

activation with a modest immune enhancement function (Winans et al. 2015). Conversely, there are also reports showing AhR-mediated immunosuppressive NK cell function, which suggests that additional environmental, or maturational components may be involved in AhR-mediated effects on NK cells (Kreitinger et al. 2016).

Innate lymphoid cells (ILCs), which play an important role in mucosal immunity, were shown to have compromised bacterial clearance through reduced IL-22 expression when ILCs lacked AhR (Pearse 2006). While AhR research in ILCs is relatively minimal, current literature suggests AhR activation in ILC subsets may be necessary for infection clearance within mucosa. AhR impacts CD4+ T cell subsets, both directly and indirectly, to different ends; variation in AhR expression levels is a probable explanation. Th1 and Th2 cells, which are thought to have minimal AhR expression, show AhR-mediated immune deviation. Specifically, Th1 cells become the dominant subset over Th2 cells through GATA binding protein-3 (GATA-3) inhibition in naïve T cells (Kreitinger et al. 2016). Th17 cells, which are known to express high levels of AhR, are shown to undergo rapid expansion upon direct AhR activation. Interestingly, with influences from AhR activation and subsequent TGFβ signaling, new research shows that inflammatory Th17 cells can undergo transdifferentiation to Tr1 cells, a Foxp3- regulatory T cell subset (Pearse 2006). CD4+ Foxp3+ regulatory T cells (Tregs) moderately express the AhR, and AhR activation in DCs significantly increases regulatory T cell frequency and effector functions indirectly (Kreitinger et al. 2016). Within CD8+ T cells, recent discoveries have found that AhR activation by xenobiotics during development has long-lasting effects on CD8+ frequencies through an epigenetic mechanism, ultimately reducing antiviral capacities (Pearse 2006). At this time, AhR expression in B cells is not well

understood. It has been documented by numerous studies that AhR activation by xenobiotics reduces antibody production and overall humoral immunity; however, it has not been determined whether this reduction in humoral immunity is due to direct AhR activation in B cells. Altered antibody production has been associated with both CD4+ T cell and DC AhR activation.

Figure 1. 4 AhR Expression in Immune Cells

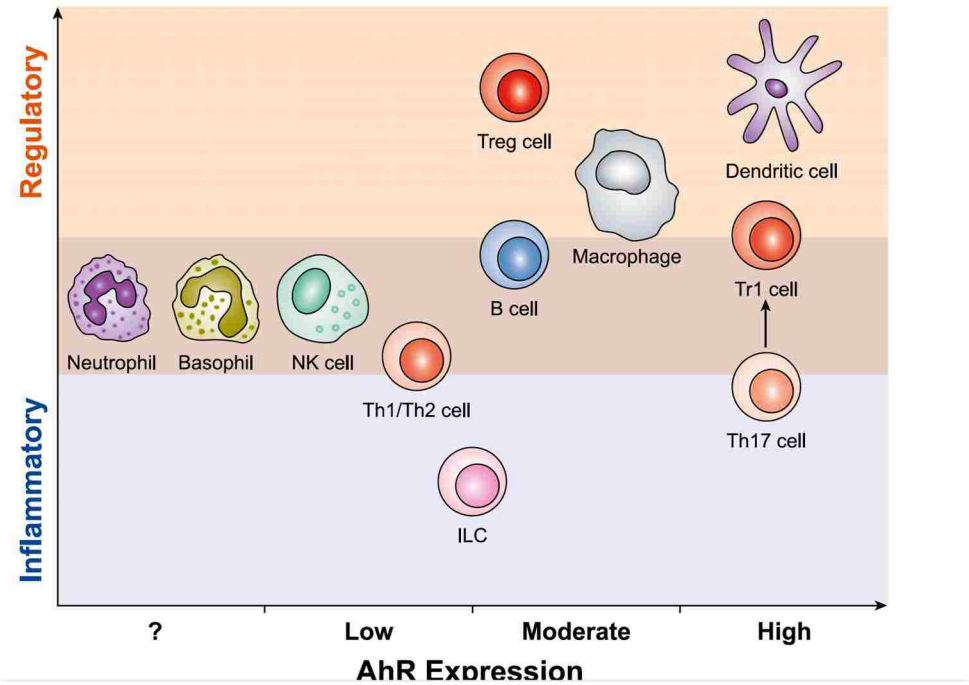

Figure 1.4 AhR Expression in Immune Cells.
AhR expression (x-axis) and outcomes of AhR activation (y-axis) by immune cell type. Importantly, AhR expression by cell type is based on mRNA and not protein expression. (Kreitinger et al. 2016)

THE THYMUS

A PRIMARY IMMUNE ORGAN

The thymus is a multi-lobed primary immune organ that rests directly above the heart. The thymus and bone marrow compose the mammalian primary immune organs with important roles in development, differentiation, and education of competent immune cells. From primary immune organs, immature immune cells seed most tissues of the periphery including secondary lymphoid tissues such as the spleen and lymph nodes, sites of mucosa, and skin to form the innate and adaptive immune systems.

STRUCTURE AND ORGANIZATION

Both hematopoietic and non-hematopoietic cells constitute the thymus. Stromal elements including epithelial cells and fibroblasts, as well as dendritic cells, organize the thymus into two functionally distinct microenvironments: cortex and medulla (Figure 1.5). The cortex, which is the more outer tissue of the thymus, has a high cellular density predominantly composed of small, immature thymocytes (Murphy and Weaver 2016; Pearse 2006). The cortex is an area of rapid cell division and cell death with lymphoblasts undergoing mitosis and large numbers of thymocytes undergoing apoptosis. There are relatively low numbers of epithelial cells in the cortex and relatively high numbers of macrophages in order to phagocytize apoptotic bodies (Murphy and Weaver 2016; Pearse 2006).

The medulla is the more central portion of the thymus and has a lower cell density than the cortex (Murphy and Weaver 2016; Pearse 2006). Cells that have passed the first stage of selection, discussed in detail below, will migrate to the medulla where they

interact with dendritic cells and medullary thymic epithelial cells (mTECs) and undergo the second stage of selection. Cells undergo turnover much less rapidly than in the cortex and will leave the medulla as fully functional naïve T cells.

Figure 1. 5 Thymus Organization.

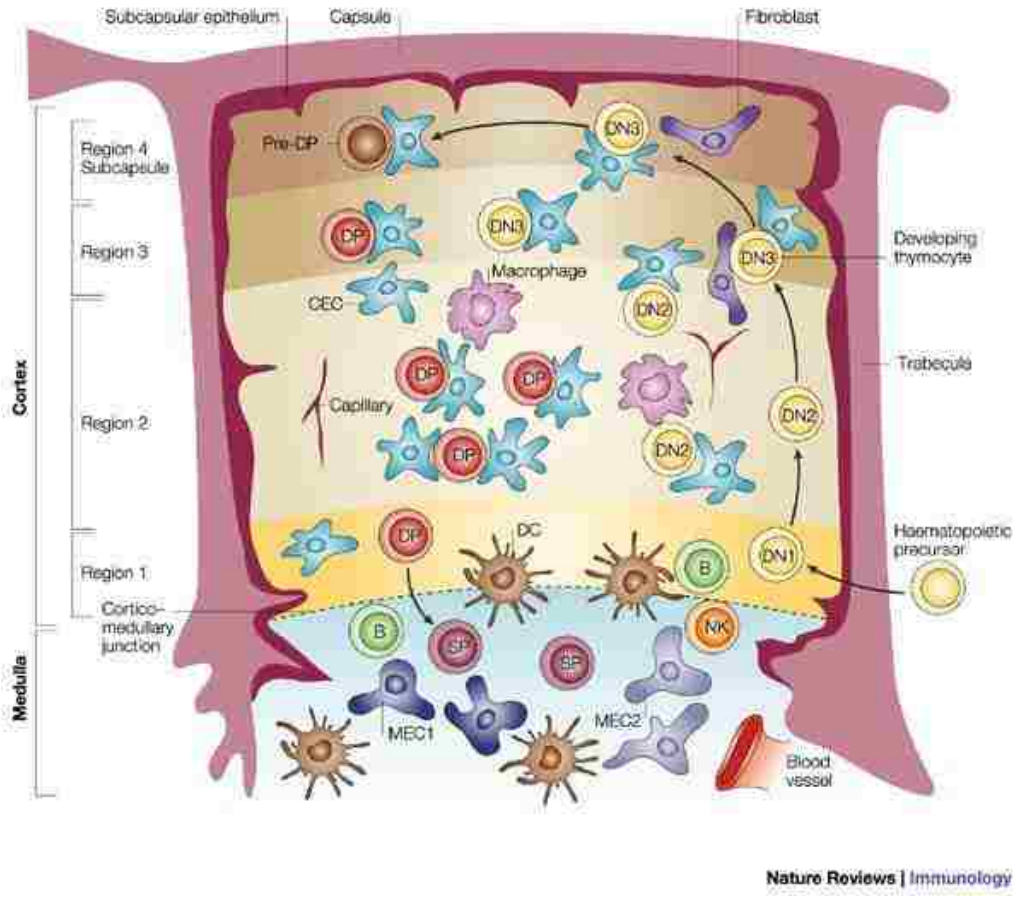

Figure 1.5 Thymus Organization.
A diagram of thymic organization and thymocyte development. (Blackburn and Manley 2004)

T CELL SELECTION

T cells, a key component of adaptive immune responses, are produced in the thymus. Once in the thymus, CD3-, T cell Receptor- (TCR), CD4-/CD8- (double-negative, DN) lymphoid precursors interact with thymic stroma and undergo necessary commitment to either

the αβ or λδ T cell lineage through TCR gene rearrangement. αβ T cells, which compose a majority of thymocytes, undergo strict selection events that can be tracked by surface protein expression of CD4 and CD8 co-receptors (Figure 1.6) (Savino 2006).

First, CD4+ CD8+ thymocytes (double-positive, DP), which make up a majority of thymocytes, undergo positive selection in the cortex where only cells with TCRs that can recognize self-peptide:self-MHC presented by cortical epithelial cells (cTECs) will survive. Most cells do not express receptors that can recognize self-peptide complexes and therefore most DP thymocytes die. Cells that have successfully passed positive selection will undergo negative selection, which occurs in the medulla and is facilitated by medullary epithelial cells (mTECs) and dendritic cells (DCs), to ensure that they do not recognize self antigens too strongly. A small niche of self-recognizing thymocytes is not negatively selected, but instead is driven toward a regulatory phenotype leading to thymic Tregs.

Cells that fail negative selection undergo programmed cell death, and are predisposed to Bim-mediated apoptosis. For the ~2% of cells that successfully navigate positive and negative selection, down-regulation of either CD4 or CD8 corresponds with the cell's ability to recognize extracellular antigen bound to MHC II or self-peptides bound to MHCI, respectively (Murphy and Weaver 2016). These successfully

recombined CD4+ or CD8+ single positive (SP) naïve T cells will then leave the thymus to seed the periphery. Overall, these critical selection events ensure only centrally tolerant and functional, immature T cells develop. Unlike αβ T cells, γδ T cells are a distinct but minor lineage that does not undergo positive and negative selection. Some γδ T cell receptors may recognize antigen directly, in a way similar to antibodies, and are not restricted to antigen presented on Major Histocompatibility Complexes (MHC) like αβ T cells. γδ T cells are currently not well studied, but it is understood that γδ T cells leave the thymus to seed peripheral tissues, such as the dermis, in waves or bursts that correspond with development (Murphy and Weaver 2016).

Figure 1. 6 Thymocyte Maturation.

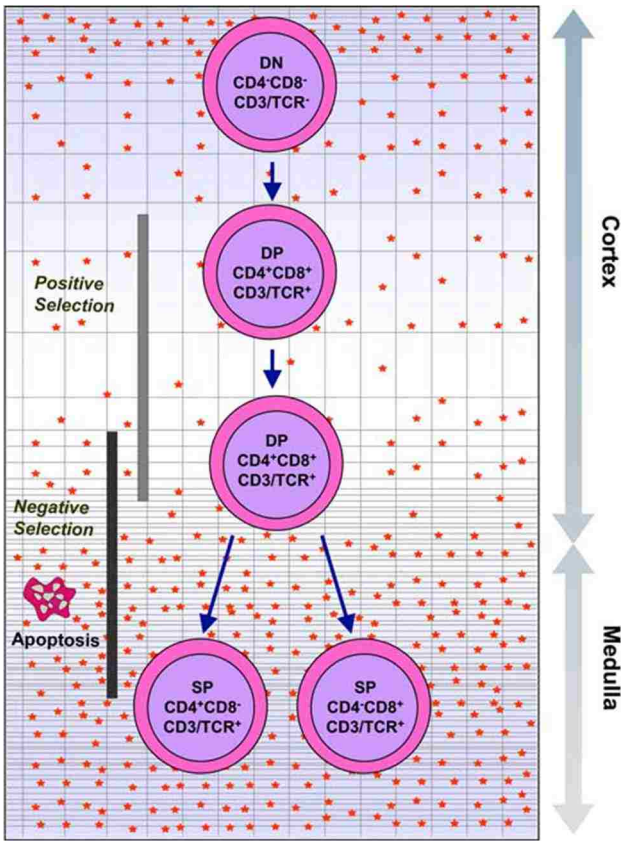

Figure 1.6 Thymocyte Maturation.

Diagram of thymic selection where thymocytes transition from CD4/CD8 double negative (DN) to double positive (DP) to single positive (SP) (Savino et. al, 2006).

THYMIC ATROPHY

Thymic atrophy is the severe shrinking of thymic tissue and occurs for a variety of reasons. Age-related thymic atrophy is considered a natural process where the thymus begins a slow, steady decline after adolescence. Numerous studies suggest that age-related thymic atrophy is due to alterations in the stromal compartment, predominantly epithelial cells, and corresponds with reduced Foxn1, a transcriptional regulator necessary for thymic epithelial cell (TEC) development (Cepeda and Griffith 2017; Lepletier et al. 2015; Masters et al. 2017). Interestingly, during age-related thymic atrophy, thymic tissue is replaced by an increased deposition of adipose tissue (Cepeda and Griffith 2017).

Age-related thymic atrophy decreases thymic output of naïve T cells, which leads to a narrowing of peripheral TCR repertoires (Murray et al. 2003; Surh and Sprent 2000). As fewer naïve T cells are produced within the aged thymus, the periphery continues to expand peripheral T cells, which leads to a skewed ratio of naive T cells to memory T cells. Consequently, the reduced output of naïve T cells and corresponding expansion of peripheral T cells leads to a systemic reduction in the diversity of TCR repertoires over time.

Notably, T cell output by an aged thymus is not completely inhibited, but naïve T cells that are successfully formed exhibit a high potential for senescence, marked by increased CD57 expression, and show a limited response upon exposure to antigenic stimuli (Mo et al. 2003). Additional phenotypic differences in naïve T cells generated by aged-thymi include reduced CD62L, a lymph node-homing protein and the chemokine CCR7, which suggests these T cells may not properly mobilize to relevant lymphoid

tissues (Haynes and Swain 2006). Together, these alterations would lead to defective responses to primary antigen exposures, such as new pathogens or vaccinations, as well as novel, endogenous tumor antigens.

Conversely, aged-thymi are also associated with autoimmune diseases that develop in geriatric patients (Prelog 2006). As previously discussed, the thymus strictly selects against self-reactive T cells prior to their entry into the periphery, a process largely controlled by thymic DCs and TECs; however, these stromal cell populations undergo substantial loss during age-induced atrophy, resulting in an increase in auto-reactive T cell escape, and ultimately a weakening of central tolerance corresponding with chronic inflammation (Coder et al. 2015).

Importantly, aging is not the only factor able to induce thymic atrophy. In fact, periodic and stochastic thymic atrophy can occur from infection, pharmaceuticals, including chemotherapies and high-dose antibiotics, some cancers and tumors, pregnancy, and exposure to toxicants such as TCDD (Cepeda and Griffith 2017). These forms of thymic atrophy appear to differ from, and may exacerbate, age-related thymic atrophy in that they are often transient with partial recovery/regeneration occurring once the contributing factor or insult is removed.

AHR AND THYMUS

The thymus expresses high levels of AhR (Carlstedt-Duke 1979) and thymic atrophy by TCDD was first noted in a 1970's study where multiple laboratory rodent species were exposed to TCDD via gastric intubation (Harris et al. 1973; Poland and Glover 1975). It was a key study in the 1980's that connected AhR activation to the

drastic alterations of a primary immune organ, becoming a key turning point in AhR research that peaked the interest of immunotoxicologists. Additionally, thymic atrophy and nutmeg liver became hallmark signs of exposure to exogenous AhR ligands, and it was long thought that the profound suppression of T cell-mediated immune responses was in part due to disrupted T cell development within the atrophied thymus.

Immunological studies assessed alterations to thymic cells in adult mice, as well as in utero and in vitro fetal thymic cultures (Esser and Welzel 1993; Holladay et al. 1991; Lutz et al. 1998; Poland and Glover 1975). These studies determined that the thymus was directly affected by TCDD, predominantly through a significant depletion of CD4+CD8+ double positive (DP) thymocytes (Esser and Welzel 1993; Holladay et al. 1991; Silverstone et al. 1994b). This loss of DP thymocytes was believed, at the time, to underlie the profound suppression of peripheral T cell responses following exposure to TCDD and dioxin-like compounds.

Interestingly, while TCDD-induced thymic atrophy is largely due to a loss of DP thymocytes, developing thymocytes have relatively low basal AhR expression as measured through mRNA, suggesting the DP loss is an indirect effect of AhR activation (Figure 1.7). Importantly, hematopoietic and non-hematopoietic cells constitute the thymus, and thymic precursors seed the thymus from bone marrow. Studies suggested that TCDD affected thymocytes from bone marrow (Silverstone et al. 1994b); however, the contributions of AhR expression within hematopoietic and non-hematopoietic cells remained a key question.

Staples et al. (1998) performed bone marrow chimera studies where they irradiated AhR^{+} mice and $AhR^{-/-}$ mice to deplete bone marrow derived cells. Chimeras

were created with AhR^{+} mice receiving $AhR^{-/-}$ bone marrow, and $AhR^{-/-}$ mice receiving AhR^{+} bone marrow prior to TCDD exposure. Interestingly, only mice that had AhR expression in bone marrow underwent thymic atrophy. This key finding determined that AhR expression in hematopoietic cells was necessary to induce thymic atrophy following TCDD exposure. Notably, the hematopoietic compartment is highly heterogeneous (Figure 1.7) and a key question that has remained unanswered since these early studies is whether AhR expression within specific cell types of the hematopoietic compartment is responsible for thymic atrophy.

Figure 1. 7 AhR Expression within the hematopoietic compartment.

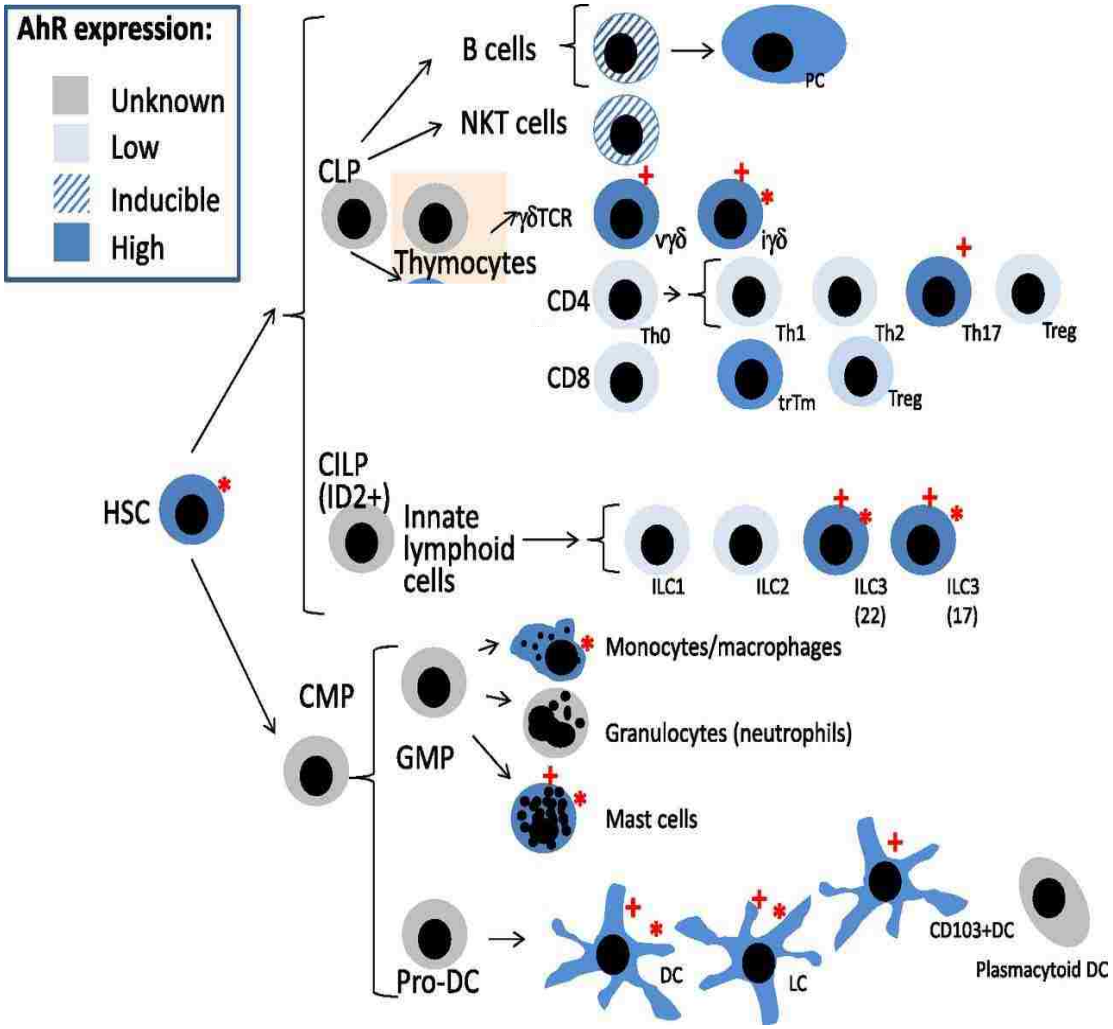

Figure 1.7. A diagram of AhR expression in cells of the hematopoietic compartment (Esser and Rannug 2015) . Shades of blue represent AhR expression potential consolidated from studies using qPCR and Western blot analysis. Plus signs (+)denote cells where AhR activation has been described to alter the function of the cell. Asterisks (*) denote cells in which AhR is suggested to play a role in lineage-specific differentiation.

DENDRITIC CELLS

PROFESSIONAL ANTIGEN PRESENTING CELLS

Just as research in the 1970's was leading to the discovery of the AhR, research by Ralph Steinman during this time was leading to the identification of dendritic cells (DCs) (Merad et al. 2013). DCs are described as professional antigen-presenting cells for their ability to phagocytize, internally process, and present antigen bound to surface proteins called major histocompatibility complexes (MHC). In mice, MHCI are loaded with short peptides derived from intracellular proteins while MHCII are able to accommodate slightly longer peptides from extracellular proteins. These antigen:MHC complexes act as a key form of communication between DCs and T cells.

According to the three-signal hypothesis (Figure 1.8), DCs employ cognate and soluble interactions to orchestrate three key signals when communicating with T cells (Kambayashi and Laufer 2014). First, peptide-loaded MHC on the surface of DCs interact with T cell receptor (TCR) complexes. Second, surface proteins on the DCs including CD80 and CD86 or CD40, interact with CD28 or CD40L on the T cell to provide co-stimulatory signals. Last, cytokines produced by dendritic cells act as soluble instructors to influence the fate and response of antigen-specific T cells. Together, these interactions result in both positive and negative signaling cascades in the T cells that ultimately result in differentiation, cellular proliferation, and/or activation-induced cell death. This emphasizes the critical role that DCs play in T-cell differentiation, homeostasis, activation, acquisition of effector functions, and apoptosis.

Together, T cells and dendritic cells interact with B cells to promote antigen-specific antibody responses through B cell proliferation and isotype (class) switching. While B cells can recognize soluble antigens independently of dendritic cells, the presentation of antigen by dendritic cells is crucial for the development of efficient humoral responses. AhR activation has long been shown to disrupt humoral immune responses, predominantly through reduced IgG expression. Interestingly, IgA expression is enhanced with AhR activation and some of our work that has been previously presented, but not to be discussed at length in this dissertation, suggests the effects on Ig secretion is, in-part, due to AhR activation within dendritic cells.

Figure 1. 8 The Three-signal Hypothesis

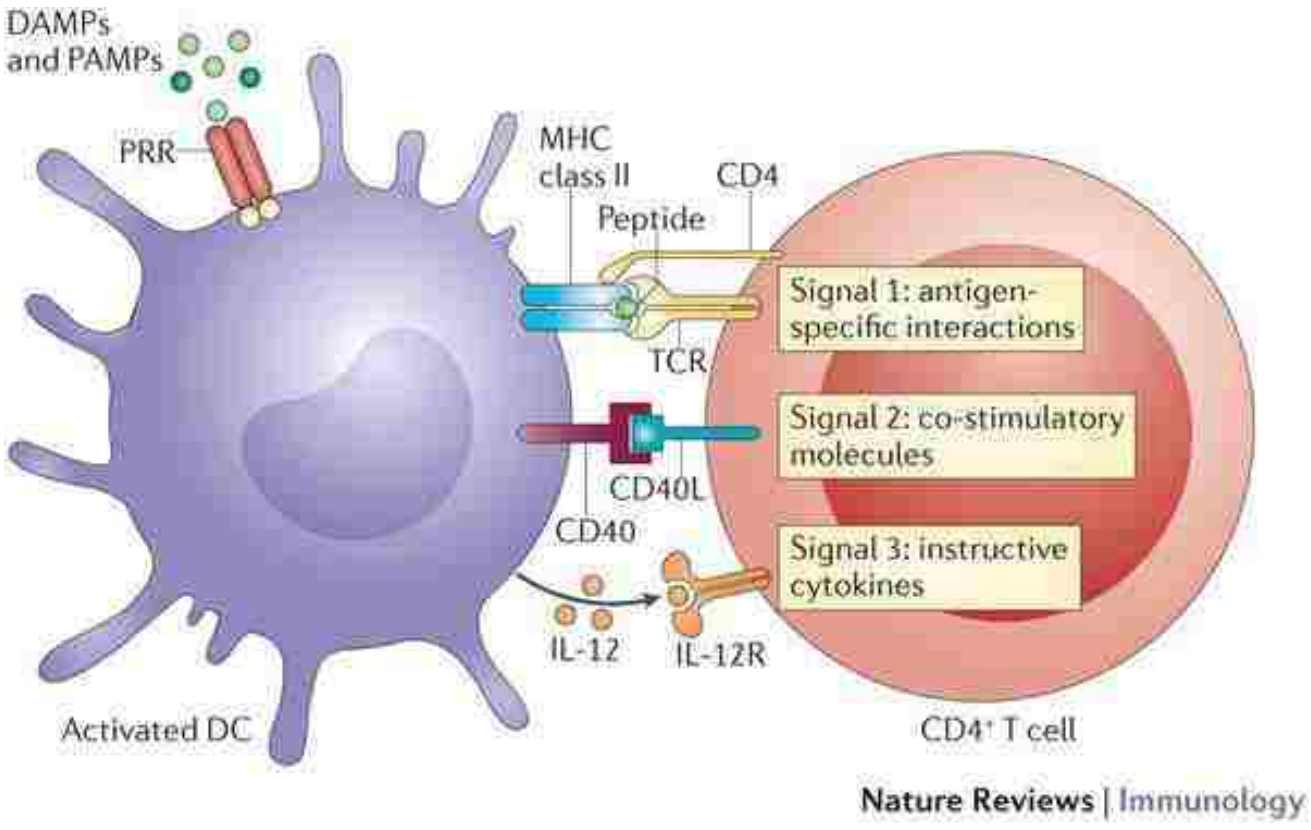

Figure 1. 8 The Three-signal Hypothesis. Within this hypothesis, signal 1 is formed by the cognate interactions of MHC on dendritic cells with TCR and TCR co-receptor on T cells. Signal 2 is also a cognate interaction between co-stimulatory molecules including CD40-CD40L, CD80/86-CD28/CD3, while signal three includes soluble factors including cytokines such as inflammatory IL-12 or inhibitory IL-10. (Kambayashi and Laufer 2014)

DIVERGENT FUNCTIONS OF DCS

DCs can acquire diverse activation, maturation, and functional states that correspond with a dichotomy in immune responses (Figure 1.9). Stimulatory, or inflammatory DCs, release inflammatory cytokines including IFNγ, TNFα, and IL-6 to drive inflammatory T cell responses required for protection against pathogens and tumors. However, aberrant stimulatory DC presence can promote the development of autoimmune pathologies. Conversely, DCs can adopt a regulatory phenotype through signals within their microenvironment, such as TGFβ, IL-10, or compounds that bind and activate the AhR. Regulatory DCs play an important role in organ homeostasis through inhibition of T cell activation and promotion of regulatory T cell differentiation and/or maintenance and provide a promising potential route for therapeutic immune suppression.

Figure 1. 9 Divergent DC Functions

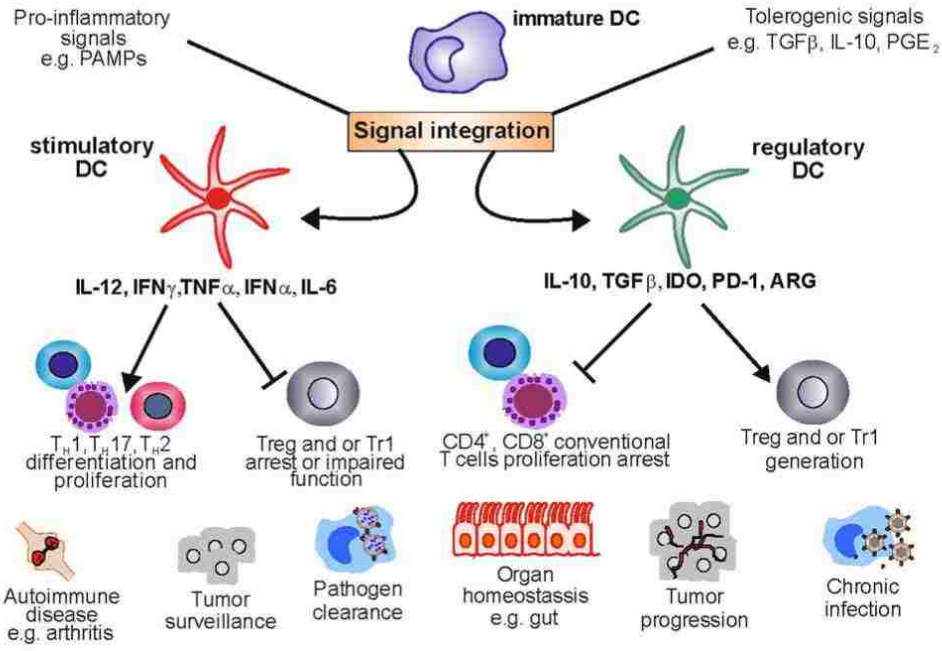

Figure 1.9 Divergent DC Functions

Diagram depicting signal integration in immature DCs and subsequent stimulatory versus regulatory DC outcomes. Schmidt et al., 2012. Frontiers in Immunol. 3 (274); 1-17.

DCs IN THE THYMUS

DCs play another key role in the formation of the adaptive immune system through interactions with developing thymocytes in the thymus. In mice, hematopoietic DCs, which share a common lineage marker, CD11c, can be divided into numerous subsets dependent on tissue and location. Within the thymus, DC populations consist of conventional DCs (cDCs) and plasmacytoid DCs (pDCs). Studies using parabiotic mice congenic for CD45.1 or CD45.2 established that thymic cDCs can be subdivided into two populations with different developmental origins. Resident, thymus-derived cDCs (cDC1), identified by expression of CD11c+ CD8α+ Sirpα-, arise from precursors within the thymus. Migratory cDCs (cDC2) identified by expression of CD11c+CD8α- Sirpα+, are present in circulation prior to seeding the thymus (Proietto et al. 2008a).

cDC1 and cDC2 were shown to be equally competent at performing negative selection of DP thymocytes while plasmacytoid DCs were not as effective at negative selection (Atibalentja et al. 2011). cDC2 may participate in thymic selection through presentation of processed antigen taken up while in the periphery, or by transfer of peptides from cDC1 and thymic epithelial cells once they have migrated into the thymus from the periphery (Allan et al. 2006; Atibalentja et al. 2011; Knight et al. 1998). Additionally, both thymic cDC1s and sDC2s show an ability to induce CD4+ CD25+ Foxp3+ regulatory T cells (Tregs) from naïve T cells in culture (Proietto et al. 2008a).

AhR AND DC

Of immune cells with AhR mRNA levels currently characterized, DCs are considered to be one of the highest expressers (Figure 1.4 and 1.7) (Esser and Rannug

2015). AhR activation in DCs by TCDD is associated with alterations to antigen presentation and costimulatory molecules, including ICAM-1, CD24, CD86, and CD40 (Vorderstrasse and Kerkvliet 2001). Steady-state DCs, a term for DCs cultured in vitro with granulocyte macrophage-colony stimulating factor (GM-CSF) instead of Flt3-ligand, showed reduced MHC class II, CD86, CD80, and CD54 and were associated with increased generation of CD4+ Foxp3+ Tregs in vitro (Simones and Shepherd 2011) .

Dietary compounds, indole-3-carbinol (I3C) and indirubin-3-oxime (IO) were found to reduce expression of CD40, CD54, and CD11c while increasing MHCII and CD80 on murine CD11c+ DCs in vitro. These dietary compounds also altered gene expression with increased mRNA for genes, including ALDH1A, IDO, and TGFβ. These genes code for proteins that are able to metabolize available tryptophan, reducing its availability for proliferating immune cells and initiating class switching of antibody isotypes, and are implicated in the regulatory DC phenotype and the generation of regulatory cells (Quintana et al. 2010c). These dietary compounds also reduced DC production of pro-inflammatory cytokines: tumor necrosis factor alpha (TNFα), IL-1β, IL-12, and IL-6 while increasing IL-10 protein levels (Benson and Shepherd 2011b). Importantly, unlike TCDD, the effects of dietary ligands were partially mediated by the AhR (Benson and Shepherd 2011b) .

While these effects of AhR activation were observed in steady-state DCs (Simones and Shepherd 2011), it was also necessary to determine whether these effects could occur in DCs within an inflammatory environment. In vitro generation of inflammatory DCs exposed to LPS or CpG showed marked reduction in inflammatory signaling when exposed to TCDD (Bankoti et al. 2010a; Bankoti et al. 2010b).

Importantly, AhR expression and consequences of AhR activation in murine DCs is highly translational as AhR expression occurs at high levels in human DCs and human DCs exposed to AhR agonists lead to suppressed T cell responses through reduced Th1 and Th17 polarization (Platzer et al. 2009; Wang et al. 2014).

DCs are an immune cell population that is highly susceptible to AhR activation by an array of ligands and are present in most tissues. Considering the important role of DCs in thymocyte selection and the numerous, broad effects of AhR activation in DCs, the consequences of AhR activation on DCs in thymus and their potential role in AhR-induced thymic atrophy is of key interest.

SPECIFIC AIMS

AHR-MEDIATED THYMIC ATROPHY

Within the thymus, AhR activation by TCDD results in a dramatic loss of developing thymocytes, which is associated with reduced frequency of double positive (DP, $CD4^+CD8^+$) thymocytes, and relative increases in the frequency of double negative (DN, $CD4^-CD8^-$) and single positive ($CD4^+$ SP and $CD8^+$ SP) thymocytes (Kamath et al. 1998; Kamath et al. 1997; Lundberg et al. 1990). Multiple mechanisms may contribute to the loss of thymocytes, including reduced proliferation of DN precursor thymocytes (Lai et al. 1994), enhanced apoptosis via Fas:FasL interactions at the DP stage (Camacho et al. 2005b), and more rapid emigration of thymocytes to the periphery (Temchura et al. 2005). It is of keen interest to determine whether these effects are due to AhR activation within the developing thymocytes and/or in other thymic cell populations of the thymus. Studies using murine bone marrow chimeras showed that thymic atrophy by TCDD is dependent on AhR activation within the hematopoietic compartment (Staples et al. 1998); however, the hematopoietic compartment is highly heterogeneous, and the specific immune cell contributor(s) have not yet been identified. Preliminary data from our laboratory suggest that AhR activation in CD11c+ cells, a lineage marker for DCs, plays a requisite role in TCDD-induced thymic atrophy. To corroborate these initial findings, it is necessary to evaluate the role of AhR expression in other key lineages of the hematopoietic compartment.

Additionally, while TCDD is the prototypical AhR ligand due to its demonstrated high binding affinity, the AhR is a highly promiscuous receptor known to bind an array of compounds (Pohjanvirta 2011). Dietary compounds such as indole-3-carbinol (I3C) and endogenous compounds such as 2-(1*H*-Indol-3-ylcarbonyl)-4-thiazolecarboxylic acid methyl ester (ITE) can bind and activate the AhR, and ligand-specific effects are known to occur (Pohjanvirta 2011; Song et al. 2002). Of late, there has been substantial interest in harnessing AhR-mediated immunosuppression for treatment of inflammatory diseases (Quintana et al. 2010a); however, TCDD is highly toxic and natural AhR ligands are gaining traction as promising alternatives. Therefore, it is also of great interest and relevance to assess thymic atrophy in response to AhR ligands beyond TCDD. *Thus, the*

first aim of this dissertation was to evaluate thymic atrophy by a select panel of ligands and determine the role of AhR activation within hematopoietic cell lineages for TCDD-mediated thymic atrophy.

AGONIST-LOADED LIPOSOMAL NANOPARTICLES FOR THERAPEUTIC ACTIVATION OF THE AHR.

AhR activation is a potent immune-modulator and shows immense promise in the treatment of autoimmune diseases (Quintana et al. 2010a). However, it is well documented that the effects of AhR activation during an immune response vary based on the target cell (Esser and Rannug 2015; Kreitinger et al. 2016; Stockinger et al. 2014) and that AhR activation can result in drastically different outcomes, from increasing inflammatory responses to promoting immune regulation or tolerance (Lee et al. 2015b). Harnessing the immunosuppressive effects of AhR activation within specific immune cell populations through a targeted delivery system would enable treatment of immune and inflammatory diseases while circumventing the deleterious effects of systemic AhR activation and subsequent non-specific immune modulation. Specifically, DCs constitutively express AhR at high levels, are keenly sensitive to AhR expression by multiple ligands, and adopt a regulatory phenotype that directly induces Tregs, making them an attractive target for AhR agonists (Quintana et al. 2010c; Simones and Shepherd 2011).

While AhR activation in DCs holds immense promise for treatment of autoimmune and inflammatory diseases, TCDD is highly toxic and exhibits a long half-life in humans; properties that make TCDD undesirable for pharmaceutical use (Harris et al. 1973; Kerkvliet 2012; Miniero et al. 2001). Natural AhR ligands, such as ITE, are more desirable for therapeutic purposes; however, natural ligands are more rapidly metabolized than TCDD and thus require higher and more frequent doses (Abron et al. 2018; Benson and Shepherd 2011b; Song et al. 2002). Importantly, packaging compounds within nanoparticles has been shown to improve drug solubility and potency, reduce off-target effects, and protect the drugs against metabolic degradation (Akbarzadeh et al. 2013). Liposomal nanoparticles (LNPs) are biodegradable and

biocompatible delivery systems for enhanced therapeutic benefits, both *in vitro* and *in vivo*, and are considered to be the most successful drug-carrier system to date (Bozzuto and Molinari 2015). Taken together, it is of keen interest to develop ITE-loaded LNPs and to evaluate ITE-loaded LNPs for biological effects in dendritic cells. *Thus, the second aim of this dissertation was to generate ITE-loaded LNP, to assess LNP uptake efficiency, cytotoxicity, and phenotypic changes in bone marrow derived dendritic cells in vitro, and to evaluate biodistribution of LNPs in vivo.*

Specific Aim 1: Evaluate thymic atrophy by a select panel of ligands and determine the requirement of AhR activation within hematopoietic cell lineages for TCDD-mediated thymic atrophy.

> **Hypothesis:** *AhR activation induces thymic atrophy in a ligand-dependent manner and AhR expression within CD11c+ DCs is necessary for thymic atrophy by TCDD.*

Specific Aim 2: Generate ITE-loaded LNP, assess LNP uptake efficiency, cytotoxicity, and phenotypic changes in bone marrow derived dendritic cells (BMDCs) *in vitro*, and evaluate biodistribution of LNP *in vivo*.

> **Hypothesis:** *We hypothesize that delivery of AhR agonist-loaded liposomal nanoparticles will activate the AhR leading to a BMDC phenotype similar to TCDD, and result in cell-specific uptake in vivo.*

REFERENCES

Abron JD, Singh NP, Mishra MK, et al. (2018) An endogenous aryl hydrocarbon receptor (AhR) ligand, ITE induces regulatory T cells (Tregs) and ameliorates experimental colitis. Am J Physiol Gastrointest Liver Physiol doi:10.1152/ajpgi.00413.2017

Akbarzadeh A, Rezaei-Sadabady R, Davaran S, et al. (2013) Liposome: classification, preparation, and applications. Nanoscale research letters 8(1):102

Allan RS, Waithman J, Bedoui S, et al. (2006) Migratory dendritic cells transfer antigen to a lymph node-resident dendritic cell population for efficient CTL priming. Immunity 25(1):153-162

Atibalentja DF, Murphy KM, Unanue ER (2011) Functional redundancy between thymic CD8α+ and Sirpα+ conventional dendritic cells in presentation of blood-derived lysozyme by MHC class II proteins. The Journal of Immunology 186(3):1421-1431

Bankoti J, Burnett A, Navarro S, Miller AK, Rase B, Shepherd DM (2010a) Effects of TCDD on the fate of naive dendritic cells. Toxicol Sci 115(2):422-34 doi:10.1093/toxsci/kfq063

Bankoti J, Rase B, Simones T, Shepherd DM (2010b) Functional and phenotypic effects of AhR activation in inflammatory dendritic cells. Toxicol Appl Pharmacol 246(1-2):18-28 doi:10.1016/j.taap.2010.03.013

Bankoti J, Rase B, Simones T, Shepherd DM (2010c) Functional and phenotypic effects of AhR activation in inflammatory dendritic cells. Toxicology and applied pharmacology 246(1):18-28

Benson JM, Shepherd DM (2011b) Dietary ligands of the aryl hydrocarbon receptor induce anti-inflammatory and immunoregulatory effects on murine dendritic cells. Toxicological Sciences 124(2):327-338

Blackburn CC, Manley NR (2004) Developing a new paradigm for thymus organogenesis. Nature Reviews Immunology 4(4):278

Bozzuto G, Molinari A (2015) Liposomes as nanomedical devices. International journal of nanomedicine 10:975

Camacho IA, Singh N, Hegde VL, Nagarkatti M, Nagarkatti PS (2005b) Treatment of mice with 2, 3, 7, 8-tetrachlorodibenzo-p-dioxin leads to aryl hydrocarbon receptor-dependent nuclear translocation of NF-κB and expression of Fas ligand in thymic stromal cells and consequent apoptosis in T cells. The Journal of Immunology 175(1):90-103

Carlstedt-Duke JM (1979) Tissue distribution of the receptor for 2, 3, 7, 8-tetrachlorodibenzo-p-dioxin in the rat. Cancer research 39(8):3172-3176

Cepeda S, Griffith AV (2017) Thymic stromal cells: Roles in atrophy and age-associated dysfunction of the thymus. Experimental gerontology

Coder BD, Wang H, Ruan L, Su D-M (2015) Thymic involution perturbs negative selection leading to autoreactive T cells that induce chronic inflammation. The Journal of Immunology:1500082

Connor K, Finley B (2003) Naturally occurring ah-receptor agonists in foods: Implications regarding dietary dioxin exposure and health risk. Human and Ecological Risk Assessment 9(7):1747-1763
Denison MS, Nagy SR (2003) Activation of the aryl hydrocarbon receptor by structurally diverse exogenous and endogenous chemicals. Annual review of pharmacology and toxicology 43(1):309-334
Dolwick KM, Swanson HI, Bradfield CA (1993) In vitro analysis of Ah receptor domains involved in ligand-activated DNA recognition. Proceedings of the National Academy of Sciences 90(18):8566-8570
Ema M, Ohe N, Suzuki M, et al. (1994) Dioxin binding activities of polymorphic forms of mouse and human arylhydrocarbon receptors. Journal of Biological Chemistry 269(44):27337-27343
Esser C, Rannug A (2015) The aryl hydrocarbon receptor in barrier organ physiology, immunology, and toxicology. Pharmacological reviews 67(2):259-279
Esser C, Welzel M (1993) Ontogenic development of murine fetal thymocytes is accelerated by 3, 3′, 4, 4′-tetrachlorobiphenyl. International journal of immunopharmacology 15(8):841-852
Gagliani N, Vesely MC, Iseppon A, et al. (2015) Th17 cells transdifferentiate into regulatory T cells during resolution of inflammation. Nature 523(7559):221-5 doi:10.1038/nature14452
Goudot C, Coillard A, Villani A-C, et al. (2017) Aryl hydrocarbon receptor controls monocyte differentiation into dendritic cells versus macrophages. Immunity 47(3):582-596. e6
Hanieh H (2014) Toward understanding the role of aryl hydrocarbon receptor in the immune system: current progress and future trends. BioMed research international 2014:520763 doi:10.1155/2014/520763
Harper PA, Riddick DS, Okey AB (2006) Regulating the regulator: factors that control levels and activity of the aryl hydrocarbon receptor. Biochemical pharmacology 72(3):267-279
Harris M, Moore J, Vos J, Gupta B (1973) General biological effects of TCDD in laboratory animals. Environmental health perspectives 5:101
Haynes L, Swain SL (2006) Why aging T cells fail: implications for vaccination. Immunity 24(6):663-666
Holladay S, Lindstrom P, Blaylock B, et al. (1991) Perinatal thymocyte antigen expression and postnatal immune development altered by gestational exposure to tetrachlorodibenzo‐p‐dioxin (TCDD). Teratology 44(4):385-393
Hubbard TD, Murray IA, Bisson WH, et al. (2016) Divergent Ah Receptor Ligand Selectivity during Hominin Evolution. Mol Biol Evol 33(10):2648-58 doi:10.1093/molbev/msw143
Kamath AB, Nagarkatti PS, Nagarkatti M (1998) Characterization of Phenotypic Alterations Induced by 2, 3, 7, 8-Tetrachlorodibenzo-p-dioxin on Thymocytesin Vivoand Its Effect on Apoptosis. Toxicology and applied pharmacology 150(1):117-124

Kamath AB, Xu H, Nagarkatti PS, Nagarkatti M (1997) Evidence for the induction of apoptosis in thymocytes by 2, 3, 7, 8-tetrachlorodibenzo-p-dioxinin vivo. Toxicology and applied pharmacology 142(2):367-377
Kambayashi T, Laufer TM (2014) Atypical MHC class II-expressing antigen-presenting cells: can anything replace a dendritic cell? Nature reviews Immunology 14(11):719
Kerkvliet NI (2012) TCDD: an environmental immunotoxicant reveals a novel pathway of immunoregulation—a 30-year odyssey. Toxicologic pathology 40(2):138-142
Knight SC, Iqball S, Roberts MS, Macatonia S, Bedford PA (1998) Transfer of antigen between dendritic cells in the stimulation of primary T cell proliferation. European journal of immunology 28(5):1636-1644
Kouri RE, Ratrie H, Atlas SA, Niwa A, Nebert DW (1974) Aryl hydrocarbon hydroxylase induction in human lymphocyte cultures by 2, 3, 7, 8-tetrachlorodibenzo-p-dioxin. Life sciences 15(9):1585-1595
Kreitinger JM, Beamer CA, Shepherd DM (2016) Environmental immunology: lessons learned from exposure to a select panel of immunotoxicants. The Journal of Immunology 196(8):3217-3225
Lai ZW, Kremer J, Gleichmann E, Esser C (1994) 3, 3′, 4, 4′‐Tetrachlorobiphenyl Inhibits Proliferation of Immature Thymocytes in Fetal Thymus Organ Culture. Scandinavian journal of immunology 39(5):480-488
Lee YH, Lin CH, Hsu PC, et al. (2015b) Aryl hydrocarbon receptor mediates both proinflammatory and anti‐inflammatory effects in lipopolysaccharide‐activated microglia. Glia 63(7):1138-1154
Lepletier A, Chidgey AP, Savino W (2015) Perspectives for improvement of the thymic microenvironment through manipulation of thymic epithelial cells: a mini-review. Gerontology 61(6):504-514
Li S, Pei X, Zhang W, Xie HQ, Zhao B (2014) Functional analysis of the dioxin response elements (DREs) of the murine CYP1A1 gene promoter: beyond the core DRE sequence. International journal of molecular sciences 15(4):6475-6487
Lundberg K, Grönvik K-O, Goldschmidt TJ, Klareskog L, Dencker L (1990) 2, 3, 7, 8-Tetrachlorodibenzo-p-dioxin (TCDD) alters intrathymic T-cell development in mice. Chemico-biological interactions 74(1-2):179-193
Lutz CT, Browne G, Petzold CR (1998) Methylcholanthrene causes increased thymocyte apoptosis. Toxicology 128(2):151-167
Masters A, Haynes L, Su DM, Palmer D (2017) Immune senescence: significance of the stromal microenvironment. Clinical & Experimental Immunology 187(1):6-15
Merad M, Sathe P, Helft J, Miller J, Mortha A (2013) The dendritic cell lineage: ontogeny and function of dendritic cells and their subsets in the steady state and the inflamed setting. Annual review of immunology 31:563-604
Miniero R, De Felip E, Ferri F, Di Domenico A (2001) An overview of TCDD half-life in mammals and its correlation to body weight. Chemosphere 43(4-7):839-844

Mo R, Chen J, Han Y, et al. (2003) T cell chemokine receptor expression in aging. The Journal of Immunology 170(2):895-904
Murphy K, Weaver C (2016) Janeway's immunobiology. Garland Science
Murray JM, Kaufmann GR, Hodgkin PD, et al. (2003) Naive T cells are maintained by thymic output in early ages but by proliferation without phenotypic change after age twenty. Immunology and Cell Biology 81(6):487
Nikolaidis E, Brunström B, Dencker L (1988) Effects of the TCDD congeners 3, 3′, 4, 4′-tetrachlorobiphenyl and 3, 3′, 4, 4′-tetrachloroazoxybenzene on lymphoid development in the bursa of Fabricius of the chick embryo. Toxicology and applied pharmacology 92(2):315-323
Nukaya M, Bradfield CA (2009) Conserved genomic structure of the Cyp1a1 and Cyp1a2 loci and their dioxin responsive elements cluster. Biochemical pharmacology 77(4):654-659
Okey A, Bondy G, Mason M, et al. (1979) Regulatory gene product of the Ah locus. Characterization of the cytosolic inducer-receptor complex and evidence for its nuclear translocation. Journal of Biological Chemistry 254(22):11636-11648
Pearse G (2006) Normal structure, function and histology of the thymus. Toxicologic pathology 34(5):504-514
Platzer B, Richter S, Kneidinger D, Waltenberger D, Woisetschläger M, Strobl H (2009) Aryl hydrocarbon receptor activation inhibits in vitro differentiation of human monocytes and Langerhans dendritic cells. The Journal of Immunology:jimmunol. 0802997
Pohjanvirta R (2011) The AH receptor in Biology and Toxicology. John Wiley & Sons
Poland A, Glover E (1975) Genetic expression of aryl hydrocarbon hydroxylase by 2, 3, 7, 8-tetrachlorodibenzo-p-dioxin: evidence for a receptor mutation in genetically non-responsive mice. Molecular Pharmacology 11(4):389-398
Prelog M (2006) Aging of the immune system: a risk factor for autoimmunity? Autoimmunity reviews 5(2):136-139
Proietto AI, van Dommelen S, Zhou P, et al. (2008a) Dendritic cells in the thymus contribute to T-regulatory cell induction. Proceedings of the National Academy of Sciences 105(50):19869-19874
Qiu J, Heller JJ, Guo X, et al. (2012) The aryl hydrocarbon receptor regulates gut immunity through modulation of innate lymphoid cells. Immunity 36(1):92-104 doi:10.1016/j.immuni.2011.11.011
Quintana FJ, Murugaiyan G, Farez MF, et al. (2010a) An endogenous aryl hydrocarbon receptor ligand acts on dendritic cells and T cells to suppress experimental autoimmune encephalomyelitis. Proceedings of the National Academy of Sciences 107(48):20768-20773
Quintana FJ, Murugaiyan G, Farez MF, et al. (2010c) An endogenous aryl hydrocarbon receptor ligand acts on dendritic cells and T cells to suppress experimental autoimmune encephalomyelitis. Proc Natl Acad Sci U S A 107(48):20768-73 doi:10.1073/pnas.1009201107
Savino W (2006) The thymus is a common target organ in infectious diseases. PLoS pathogens 2(6):e62

Silverstone AE, Frazier DE, Jr., Gasiewicz TA (1994b) Alternate immune system targets for TCDD: lymphocyte stem cells and extrathymic T-cell development. Exp Clin Immunogenet 11(2-3):94-101
Simones T, Shepherd DM (2011) Consequences of AhR activation in steady-state dendritic cells. Toxicol Sci 119(2):293-307 doi:10.1093/toxsci/kfq354
Smith KJ, Murray IA, Boyer JA, Perdew GH (2018) Allelic variants of the aryl hydrocarbon receptor differentially influence UVB-mediated skin inflammatory responses in SKH1 mice. Toxicology 394:27-34
Song J, Clagett-Dame M, Peterson RE, et al. (2002) A ligand for the aryl hydrocarbon receptor isolated from lung. Proceedings of the National Academy of Sciences 99(23):14694-14699
Staples JE, Murante FG, Fiore NC, Gasiewicz TA, Silverstone AE (1998) Thymic alterations induced by 2,3,7,8-tetrachlorodibenzo-p-dioxin are strictly dependent on aryl hydrocarbon receptor activation in hemopoietic cells. J Immunol 160(8):3844-54
Stockinger B, Meglio PD, Gialitakis M, Duarte JH (2014) The aryl hydrocarbon receptor: multitasking in the immune system. Annual review of immunology 32:403-432
Surh CD, Sprent J (2000) Homeostatic T cell proliferation: how far can T cells be activated to self-ligands? Journal of Experimental Medicine 192(4):F9-F14
Swanson HI, Chan WK, Bradfield CA (1995) DNA binding specificities and pairing rules of the Ah receptor, ARNT, and SIM proteins. Journal of Biological Chemistry 270(44):26292-26302
Temchura VV, Frericks M, Nacken W, Esser C (2005) Role of the aryl hydrocarbon receptor in thymocyte emigration in vivo. European journal of immunology 35(9):2738-2747
Vogel CF, Goth SR, Dong B, Pessah IN, Matsumura F (2008) Aryl hydrocarbon receptor signaling mediates expression of indoleamine 2, 3-dioxygenase. Biochemical and biophysical research communications 375(3):331-335
Vorderstrasse BA, Kerkvliet NI (2001) 2, 3, 7, 8-Tetrachlorodibenzo-p-dioxin affects the number and function of murine splenic dendritic cells and their expression of accessory molecules. Toxicology and applied pharmacology 171(2):117-125
Wang C, Ye Z, Kijlstra A, Zhou Y, Yang P (2014) Activation of the aryl hydrocarbon receptor affects activation and function of human monocyte‐derived dendritic cells. Clinical & Experimental Immunology 177(2):521-530
Winans B, Nagari A, Chae M, et al. (2015) Linking the Aryl Hydrocarbon Receptor with Altered DNA Methylation Patterns and Developmentally Induced Aberrant Antiviral CD8+ T Cell Responses. The Journal of Immunology 194(9):4446-4457
Wright EJ, De Castro KP, Joshi AD, Elferink CJ (2017) Canonical and non-canonical aryl hydrocarbon receptor signaling pathways. Current Opinion in Toxicology 2:87-92

Yao EF, Denison MS (1992) DNA sequence determinants for binding of transformed Ah receptor to a dioxin-responsive enhancer. Biochemistry 31(21):5060-5067

CHAPTER 2: TARGETED DELETION OF THE ARYL HYDROCARBON RECEPTOR IN DENDRITIC CELLS PREVENTS THYMIC ATROPHY IN RESPONSE TO DIOXIN.

In Press in Archives of Toxicology

Authors

Celine A. Beamer, Joanna M. Kreitinger, Shelby L. Cole, David M. Shepherd

Corresponding Author

David M. Shepherd, Ph.D.

University of Montana

Department of Biomedical and Pharmaceutical Sciences

32 Campus Drive, Skaggs Building Room 284

Missoula, MT 59812

406-243-2224 (phone)

406-243-2807 (fax)

david.shepherd@umontana.edu

Keywords: involution, TCDD, ITE, I3C, AhR^d, apoptosis

Grant Funding: Research reported in this publication was supported by the National Institute of Environmental Health Sciences and the National Institute of General Medical Sciences of the National Institutes of Health under grant numbers R01-ES013784 (DMS), P30-GM103338, P20-GM103546. JMK was supported by The American Association of Immunologists through a Careers in Immunology Fellowship. The content is solely the responsibility of the authors and does not necessarily represent the official views of the National Institutes of Health.

Abstract

In nearly every species examined, administration of the persistent environmental pollutant, 2,3,7,8-tetrachlorodibenzo-*p*-dioxin (dioxin, TCDD) causes profound immune suppression and thymic atrophy in an aryl hydrocarbon receptor (AhR)-dependent manner. Moreover, TCDD alters the development and differentiation of thymocytes, resulting in decreases in the relative proportion and absolute number of double positive (DP, $CD4^+CD8^+$) thymocytes, as well as an enrichment in the relative proportion and absolute number of double negative (DN, $CD4^-CD8^-$) and single positive (SP) $CD4^+CD8^-$ and $CD4^-CD8^+$ thymocytes. Previous studies suggested that the target for TCDD-induced thymic atrophy resides within the hematopoietic compartment and implicated apoptosis, proliferation arrest of thymic progenitors, and emigration of DN thymocytes to the periphery as potential contributors to TCDD-induced thymic atrophy. However, the precise cellular and molecular mechanisms involved remain largely unknown. Our results show that administration of 10 μg/kg TCDD and 8 mg/kg 2-(1H-Indol-3-ylcarbonyl)-4-thiazolecarboxylic acid methyl ester (ITE) induced AhR-dependent thymic atrophy in mice on day 7 following exposure, whereas 100 mg/kg indole 3-carbinol (I3C) did not. Though our studies demonstrate that TCDD triggers a 2-fold increase in the frequency of apoptotic thymocytes, TCDD-induced thymic atrophy is not dependent on Fas-FasL interactions and thus, enhanced apoptosis is unlikely to be a major mechanistic contributor. Finally, our results show that activation of the AhR in $CD11c^+$ dendritic cells is directly responsible for TCDD-induced alterations in the development and differentiation of thymocytes, which results in thymic atrophy. Collectively, these results suggest that $CD11c^+$ dendritic cells play a critical role in mediating TCDD-induced

thymic atrophy and disruption of T lymphocyte development and differentiation in the thymus.

Introduction

The thymus is a complex, specialized organ that is responsible for the maturation and education of most peripheral T cells. Progenitor cells enter the thymus from the blood stream after originating in the bone marrow and/or fetal liver. Once in the thymus, these cells progress through multiple developmental stages that can be delineated by cell surface markers such as CD3, CD4, and CD8. In the earliest stage, classified as double negative (DN) thymocytes, cells do not express any of these markers. Subsequently, cell surface markers are up-regulated to give rise to $CD4^+CD8^+$ double positive (DP) cells, which then undergo a rigorous selection process eventually down-regulating either CD4 or CD8 expression to become $CD4^+$ or $CD8^+$ single-positive (SP) cells, which are released into the periphery. Self-reactive cells failing negative selection are removed via apoptotic pathways, and mature, self-tolerant SP thymocytes are released into the periphery as naïve Th cells (CD4) or cytotoxic T cells (CD8). Because ongoing thymopoiesis is essential for the development and maintenance of a healthy immune system, agents that trigger thymic atrophy may decrease host ability to reconstitute the peripheral T cell repertoire or respond to new antigens. Similarly, because the overall process of maturation and education of T cells is orchestrated, to a degree, by the supporting cells of the stromal network, which includes thymic epithelial cells, dendritic cells, and macrophages (Nowell et al. 2007), agents that induce thymic atrophy may be acting on a variety of cellular targets.

The aryl hydrocarbon receptor (AhR) is a ligand activated transcription factor belonging to the Per-ARNT-SIM-basic-helix-loop-helix (PAS/bHLH) protein family,

which mediates a wide range of biological responses resulting from exposures to both natural and synthetic ligands (Gu et al. 2000; Okey 2007; Pohjanvirta 2011). AhR was first identified in the early 1970s and has since been shown to have dual roles as an activator of xenobiotic metabolism and as a participant in normal homeostasis, organogenesis, and immune modulation (Nebert and Gelboin 1968; Nebert and Gelboin 1969; Okey 2007; Wright et al. 2017). Nevertheless, details of the cellular and molecular mechanisms underlying many AhR-dependent physiological and toxicological effects are currently unknown.

Halogenated dioxins, biphenyls, and polycyclic aromatic hydrocarbons represent the best-characterized high-affinity, planar, and hydrophobic ligands of the AhR. Although numerous high affinity AhR ligands have since been discovered, the potent and persistent environmental pollutant, 2,3,7,8-tetrachlorodibenzo-p-dioxin (TCDD, dioxin) remains the prototypic AhR ligand for mechanistic studies (Kerkvliet 2012; Poland et al. 1976). Exposure of laboratory rodents to TCDD and TCDD-like chemicals profoundly affects the immune system, causing immunosuppression typified by suppressed cellular immunity, inhibition of antibody production, and thymic atrophy in a variety of animal species (Faith and Luster 1979; Funatake et al. 2005; Harris et al. 1973; Kerkvliet 2002; Poland and Glover 1980; Van Loveren et al. 1991; Vecchi et al. 1980) via direct effects of AhR activation (Fernandez-Salguero et al. 1996; Harrill et al. 2016; Staples et al. 1998). C57Bl/6 mice, which harbor the AhR^b allele that codes for a receptor with a high binding affinity for agonists, exhibit a decrease in thymic weight and cellularity as early as three days after exposure to a single 30 μg/kg dose of TCDD (Laiosa et al. 2003a). Maximal decline in thymocyte cellularity emerges 10 days later, yet recovery to near

baseline levels does not occur until approximately 30 days after exposure (Laiosa et al. 2003a).

During TCDD-induced thymic atrophy, the thymus undergoes a marked reduction in the frequency of DP thymocytes, as well as a relative increase in the frequency of DN and SP thymocytes. Moreover, based upon the observed values for thymic cellularity, these shifts in thymocyte subset frequencies correspond to significant decreases in the absolute number of thymocytes in each of the four subpopulations (Kamath et al. 1998; Kamath et al. 1997; Lundberg et al. 1990). Although the precise cellular and molecular mechanisms involved remain largely unknown, previous studies demonstrated that the target for TCDD-induced thymic atrophy resides within the hematopoietic compartment and implicated reduced proliferation of DN precursor thymocytes (Lai et al. 1994), enhanced apoptosis via Fas:FasL interactions at the DP stage (Camacho et al. 2005b), and enhanced emigration of thymocytes (Temchura et al. 2005), or a combination of these possible mechanisms. Therefore, it was of great interest to evaluate TCDD-induced thymic atrophy in naïve wild-type mice (C57Bl/6), mice expressing the low affinity AhR (AhR^{d}), and AhR conditional knockout mice ($LyzM^{Cre}AhR^{fx}$, $CD11c^{Cre}AhR^{fx}$, $RORc^{Cre}AhR^{fx}$, and $FoxN1^{Cre}AhR^{fx}$). Furthermore, we assessed whether an endogenous, non-toxic AhR ligand 2-(1H-Indol-3-ylcarbonyl)-4-thiazolecarboxylic acid methyl ester (ITE) (Abron et al. 2018; Benson and Shepherd 2011b; Song et al. 2002) and a dietary AhR ligand, indole 3-carbinol (I3C) (Benson and Shepherd 2011b; Bjeldanes et al. 1991; Connor and Finley 2003) exhibited thymotoxic effects similar to TCDD. The findings presented here extend our understanding of how activation of the AhR contributes to thymic atrophy and mediates immune suppression.

Materials and Methods

Chemicals

2,3,7,8, tetrachlorodibenzo-p-dioxin (dioxin, TCDD) was obtained from Cambridge Isotopes (Cambridge, MA). A 1 mg/mL stock solution of TCDD in anisole/peanut oil was diluted to yield treatment solutions containing 1 or 10 μg/mL in peanut oil. 2-(1*H*-Indol-3-ylcarbonyl)-4-thiazolecarboxylic acid methyl ester (ITE) was obtained from Tocris (Bio-techne brand, Minneapolis, MN). A 20 mg/mL stock solution of ITE in DMSO was diluted to yield a treatment solution containing 0.8 mg/mL in peanut oil. Indole 3-carbinol (I3C), obtained from Sigma-Aldrich (St. Louis, MO), was suspended in peanut oil (10 mg/mL). The estimated half-life of TCDD is approximately 10 days in mice (Birnbaum 1986; Gasiewicz et al. 1983), whereas the *in vivo* absorption, metabolism, distribution, and excretion rates of ITE and I3C in mice remain largely undetermined. Therefore, we selected the dose and route of exposure based upon earlier reports, thus integrating our results with previous findings in other model systems (Abron et al. 2018; Benson and Shepherd 2011a; Boule et al. 2018b; Nugent et al. 2013; Quintana et al. 2010c; Singh et al. 2016).

Biohazard precaution

TCDD is highly toxic and a known human carcinogen. All personnel were instructed in safe handling procedures. Proper personal protective equipment (e.g. lab coats, gloves and masks) were worn at all times, and contaminated materials were

collected separately for hazardous waste disposal. TCDD-treated mice were housed separately, and their carcasses and bedding regarded as contaminated materials.

Mice

Breeding pairs of mice were originally purchased from The Jackson Laboratory (Bar Harbor, ME) and maintained as both individual colonies and crossed strains to yield AhR conditional knockouts (supplemental Table 1). Tails snips were digested in direct PCR lysis reagent according to the manufacturer's protocol (Viagen Biotech, Los Angeles, CA). Mice of the correct genotype were identified according to PCR conditions furnished by the Jackson Laboratory, and littermates were used as controls. All mice were maintained in microisolator cages in the University of Montana specific pathogen-free (SPF) laboratory animal facility, and provided breeder (Teklad 2019, Envigo, Denver, CO) or standard rodent chow (Teklad 2020x, Envigo) and tap water ad libitum. All animal use procedures were in accordance with NIH and University of Montana IACUC guidelines.

In Vivo Exposure

Naïve, adult (6-10-week-old) mice received 10 or 100 μg TCDD/kg, 1 to 8 mg/kg ITE, or 100 mg/kg I3C (Camacho et al. 2005b; Nguyen and Bradfield 2007; Quintana et al. 2010a; Singh et al. 2014) via oral gavage (p.o.) or intraperitoneal injection (i.p.) as described in the appropriate results sections. Control mice received solvent/peanut oil or a peanut oil only vehicle control. Each experiment was performed in duplicate or triplicate with age-matched littermates (±7 days), containing a minimum of three mice of

each sex for n=6 per treatment group. Mice were weighed daily, tissues collected 7 days later, and analyzed individually.

Cell Isolation

Following euthanasia by CO_2 asphyxiation, body weights were recorded and thymi removed free of lymph nodes and blood vessels. Individual thymi were weighed and pressed through a 70 μm sterile cell strainer with the flat end of a 1 mL syringe plunger to release the cells into cold complete RPMI (cRPMI) media supplemented with 10% FBS (Atlanta Biologicals, Atlanta, GA), 50 μM β-mercaptoethanol, 20 mM 4-(2-hydroxyethyl)-1-piperazineethanesulfonic acid, 10 mM sodium pyruvate, and 50 μg/ml gentamicin (Gibco, Grand Island, NY) (Corning, Manassas, VA). Thymocytes were pelleted by centrifugation at 1500 rpm for 5 minutes, re-suspended in fresh cRPMI, and maintained on ice.

Flow cytometry

Single cell suspensions of thymocytes were washed once with cRPMI and re-suspended in 100 μl of purified rat anti-mouse CD16/CD32 (2.4G2, Tonbo, San Diego, CA) diluted 1:100 in PBS containing 1% bovine serum albumin and 0.1% sodium azide (PAB) to block Fc receptors. 2 x 10^6 thymocytes were immunostained for 30 minutes on ice with titrated monoclonal antibodies specific to CD3ε PerCPCy5.5 (145-2C11, Tonbo), CD4 FITC or redfluor 710 (RM4-5, Tonbo), and CD8 PE-Cy7 (53-6.7, Tonbo) to identify live, propidium iodide (PI, Tonbo) negative singlet thymocytes. Another 2 x 10^6 thymocytes were immunostained for 30 minutes on ice with monoclonal antibodies

specific to CD45 v450 (30-F11, Tonbo), CD4 FITC (RM4-5, Tonbo), CD8α PE-Cy7 (53-6.7, Tonbo), CD11c PE (HL3, BD Pharmingen, San Diego, CA), Fas Alexa Fluor 647 (Jo2, BD Pharmingen), FasL PerCP Cy5.5 (MFL3, BD Pharmingen) to identify cell surface expression of Fas and FasL. Alternatively, 2 x 10^6 thymocytes were immunostained with monoclonal antibodies specific to CD4 FITC (RM4-5, Tonbo), CD8α PE-Cy7 (53-6.7, Tonbo), in addition to Annexin V and 7-AAD staining solution according to the manufacturer's instructions (Tonbo). Unstained, single stained, and fluorescence minus one controls were used to set positive/negative gating. Cells were washed twice with 1 mL PAB and re-suspended in 350 μL of PAB and acquisition was performed on a FACS Aria II flow cytometer using FACS Diva software (v 6.1.2, Becton Dickinson, Franklin Lakes, NJ). Compensation of the spectral overlap was performed using One Comp compensation control beads (BD Biosciences, San Diego, CA) in combination with single stained controls where appropriate. Data files were exported as FCS 3.1 files and analyzed by Flow Logic (v 4.0, Miltenyi, Auburn,CA).

RNA isolation and RT-qPCR

Total RNA was extracted from 5 x 10^6 thymocytes using TRIzol reagents (Invitrogen) or a RNeasy mini kit (Qiagen, Germantown, MD) according to the manufacturer protocols. Two-step qRT-PCR was performed by synthesizing cDNA using iScript Reverse Transcription Supermix (BioRad, Hercules, CA) followed by RT-qPCR relative quantification of 50 ng cDNA per reaction using CFX Connect, SSO Advanced Universal SYBR Green Master Mix, and PrimePCR validated primers for murine

GAPDH, Hprt, Tbp, Fas, and FasL (BioRad, Hercules, CA). The data were normalized to the reference genes Hprt, Tbp, and GAPDH.

Statistical Analysis

For each parameter, the values for individual experiments were averaged and the standard error calculated. Student t-tests, one-way or two-way ANOVA were performed using Prism 7 (GraphPad, La Jolla, CA). A p value of ≤ 0.05 was considered significant.

Results

ITE, but not I3C, induces thymic atrophy

Although AhR activation promotes immunoregulatory responses in a ligand-dependent manner (Ehrlich et al. 2018), little is known about the thymotoxic effects of other AhR ligand chemotypes. To test the hypothesis that activation of the AhR induces thymic atrophy in a ligand-dependent manner, C57Bl/6 mice were gavaged with an endogenous ligand (ITE) (Song et al. 2002) and a dietary ligand (I3C) (Connor and Finley 2003), with chemical structures that are distinct from TCDD (Figure 1A). The dose and route of exposure to each chemical were selected based on prior reports, thus simplifying integration of our results with previous findings (Benson et al. 2012b; Boule et al. 2018b; Quintana et al. 2010b). After daily administration of 8 mg/kg ITE, C57Bl/6 mice exhibited extensive thymic atrophy as evidenced by a significant loss in organ weight (52% decrease) and a dramatic reduction in thymic cellularity (73% decrease) relative to vehicle control on day 7. In contrast, administration of 100 mg/kg I3C to C57Bl/6 mice every other day resulted in a trend towards increased thymic weight and a

significant increase in cellularity (30% increase) relative to vehicle control on day 7 (Figure 1B and 1C). No sex-specific effects were observed at day 7 with ITE or I3C (data not shown). Because ITE and I3C differentially affected thymic weight and cellularity, we also compared effects on intra-thymic differentiation by assessing the surface expression of CD4 and CD8 on live thymocytes via flow cytometry (Figure 2). Although administration of ITE revealed a trend similar to TCDD with regards to a significant reduction in the frequency of DP and increase in the frequency of DN and $CD4^+$ SP thymocytes, no difference was observed in the frequency of $CD8^+$ SP thymocytes compared to vehicle control. Lastly, administration of I3C to C57Bl/6 mice resulted in no significant changes in the development and/or differentiation of any CD4/CD8 thymocyte subsets examined (Figure 2.1 and Figure 2.2). Together, these data show that activation of the AhR induces thymic atrophy in a ligand-dependent manner.

Figure 2. 1 ***ITE, but not I3C, induces thymic atrophy.***

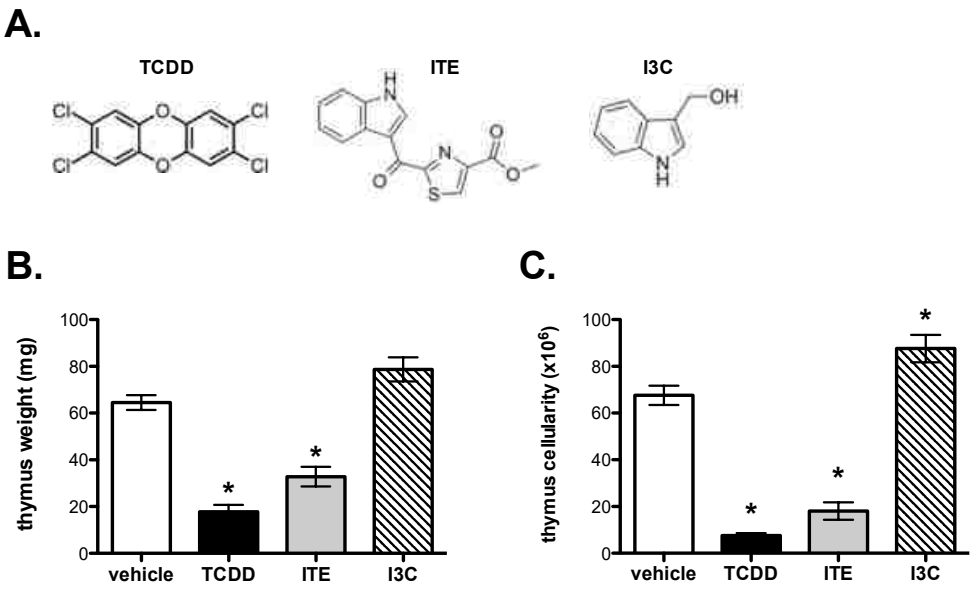

Figure 2.1 ITE, but not I3C, induces thymic atrophy.

Naïve wild-type mice (C57Bl/6) were gavaged with 3 chemically distinct AhR ligands (A): TCDD (10 µg/kg), ITE (8 mg/kg), or I3C (100 mg/kg). Three indicators of toxicity: body weight (data not shown), thymus weight (B), and thymus cell numbers (C) were measured on day 7 to evaluate toxicity and thymic atrophy after administration of TCDD, ITE, and I3C. Data represent one of two independent experiments, n=3-5 per treatment group, mean $\pm$ SEM; 1-way ANOVA, *$p < 0.05$ vehicle.

Figure 2. 2 ***Comparison of CD4/CD8 thymocyte subsets from vehicle, TCDD, ITE, and I3C exposed mice***

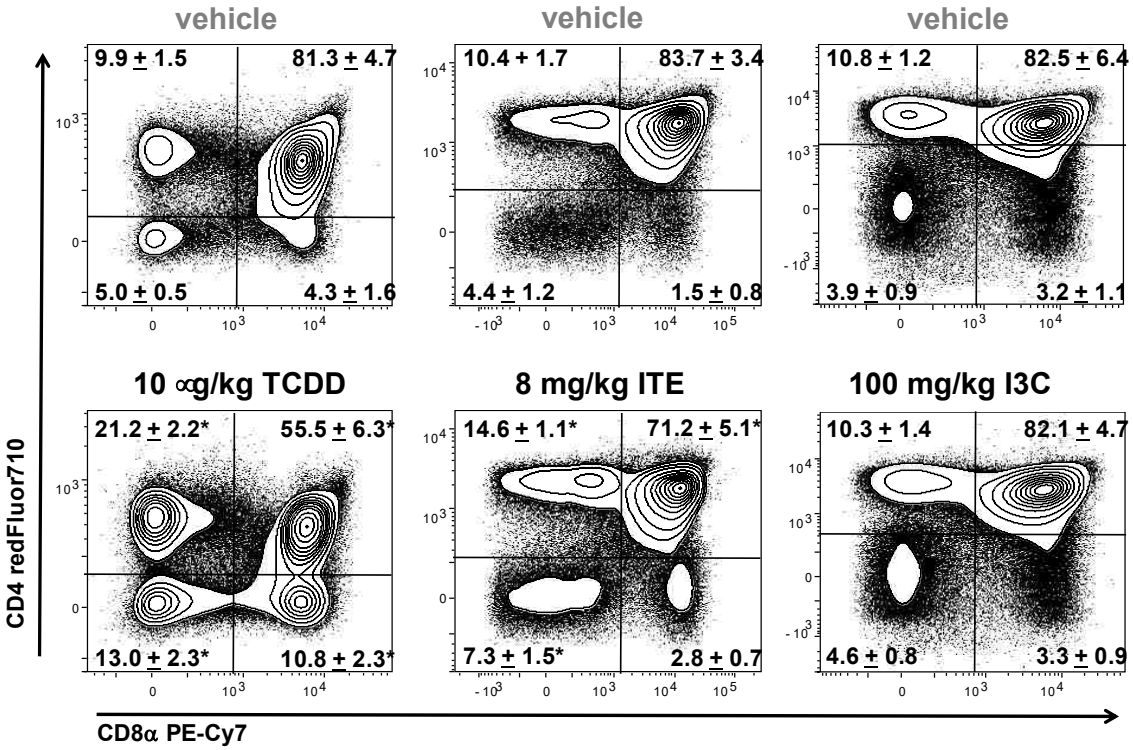

Figure 2. Comparison of CD4/CD8 thymocyte subsets from vehicle, TCDD, ITE, and I3C exposed mice.

C57Bl/6 mice were gavaged with the appropriate vehicle control, TCDD (10 μg/kg, once), ITE (8 mg/kg daily), or I3C (100 mg/kg every other day). Representative contour plots gating on live thymocytes revealed a significant decline in the frequency of $CD4^+CD8^+$ DP thymocytes, as well as a relative enrichment in the percent of $CD4^-CD8^-$ DN and $CD4^+CD8^-$ and $CD4^-CD8^+$ SP thymocytes in 10 μg/kg TCDD- and 8 mg/kg ITE-treated mice compared to vehicle controls on day 7. These shifts in CD4/CD8 thymocyte subsets were not observed in mice treated with 100 mg/kg I3C. The mean percentages of the CD4/CD8 thymocyte subsets ± SEM are indicated in the plots. Data represent one of two independent experiments, n=3-5 per treatment group; 1-way ANOVA, *$p < 0.05$ vehicle.

ITE induces thymic atrophy in a dose- and AhR-dependent manner

Although exposure to ITE *in vitro* caused dose-dependent alterations in thymocyte differentiation and maturation that paralleled those observed following *in vitro* exposure to TCDD, previous reports did not detect changes in thymus weight 12 days following a single delivery of 5.6 mg/kg ITE (i.v.) (Henry et al. 2006). To test the hypothesis that ITE induces thymic atrophy in an AhR-dependent manner, C57Bl/6 and low affinity AhR^d mice were gavaged daily with a previously described immunosuppressive dose of ITE (Abron et al. 2018; Henry et al. 2006; Nugent et al. 2013; Quintana et al. 2010b) and tissues analyzed at day 7. First, we confirmed that mice expressing the low affinity AhR^d allele do not exhibit thymic atrophy when exposed to 10 μg/kg TCDD and that a 10-fold higher dose of TCDD (e.g. 100 μg/kg) in AhR^d mice overcame the low-affinity receptor, resulting in thymic atrophy (Supp. Figure 2.1 and 2.2). This supplemental data support the use of AhR^d mice as a model to evaluate ligands for AhR-dependent effects. ITE exposure to naive C57Bl/6 mice resulted in thymic atrophy as evidenced by a significant decline in organ weight (49% decrease) and a reduction in thymic cellularity (73% decrease) relative to vehicle control. In contrast, AhR^d mice were refractory to the same 8 mg/kg dose of ITE with regards to thymic weight (Figure 2.3A) and cellularity (Figure 2.3B). Likewise, the dose-dependent effects of ITE were scrutinized in C57Bl/6 mice by assessing thymic weight and cellularity. Daily administration of 1, 2, 4, and 8 mg/kg ITE (p.o.) resulted in dose-dependent thymic atrophy as evidenced by a decline in organ weight of 13%, 25%, 30% and 35%, respectively (Figure 2.3C) and a dramatic decrease in thymic cellularity of 25%, 25%, 40% and 50% (Figure 2.3D) respectively, in C57Bl/6 mice relative to vehicle control on

day 7. Lastly, comparable levels of thymic atrophy were observed following daily administration of 1 mg/kg ITE i.p. and 4 mg/kg ITE p.o. (data not shown).

Figure 2. 3 ***ITE-induced thymic atrophy in an AhR- and dose-dependent manner.***

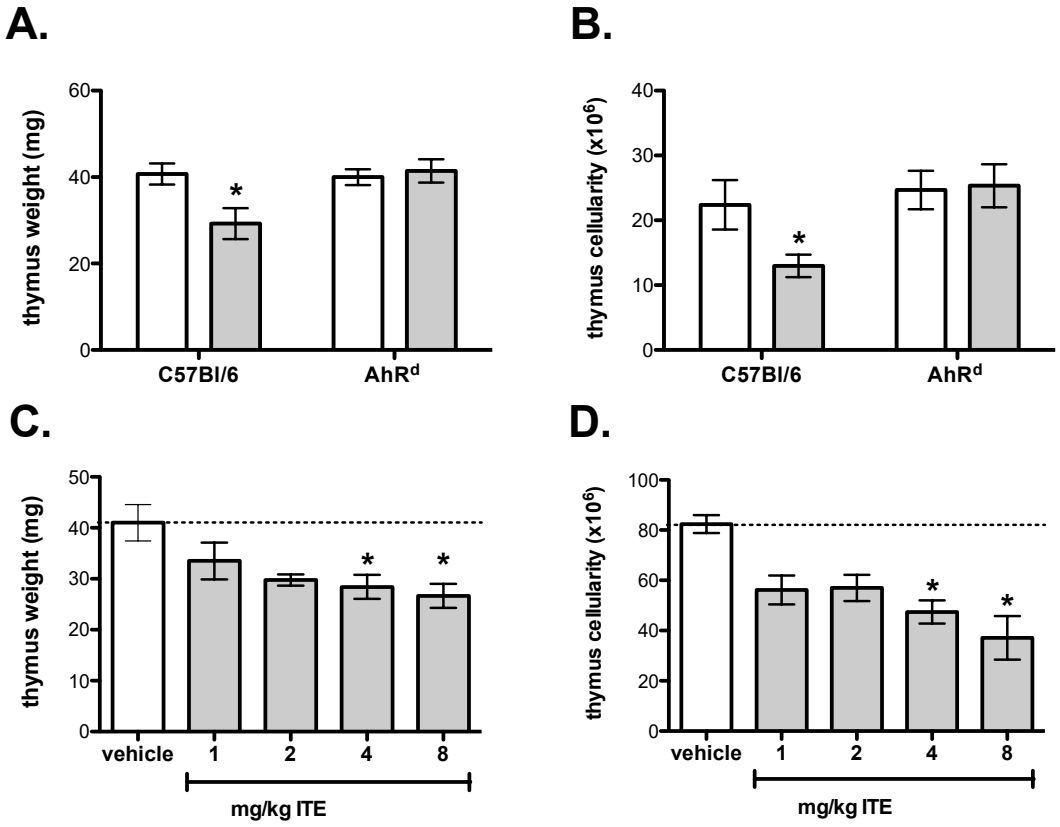

Figure 2.3. ITE-induced thymic atrophy in an AhR- and dose-dependent manner.

Naïve wild-type mice (C57Bl/6) and mice expressing the low affinity receptor (AhR^d mice) were gavaged with vehicle (anisole/peanut oil) or ITE (8 mg/kg). Three indicators of toxicity: body weight (data not shown), thymus weight (A), and thymus cell number (B) were measured on day 7 to evaluate toxicity and thymic atrophy. n=5-6 mice per treatment group, mean $\pm$ SEM; 1-way ANOVA, *$p < 0.05$ vehicle. An additional cohort of C57Bl/6 mice were gavaged with vehicle (anisole/peanut oil) or increasing doses of ITE (1, 2, 4, or 8 mg/kg). Three indicators of toxicity: body weight (data not shown), thymus weight (C), and thymus cell number (D) were measured on day 7 to evaluate

toxicity and thymic atrophy. n=5-6 mice per treatment group, mean ± SEM; 1-way ANOVA, *p < 0.05 vehicle.

Dioxin-mediated thymic atrophy is not dependent on apoptosis via Fas:FasL interactions

Since TCDD has been reported to initiate apoptosis in immature thymocytes (Fisher et al. 2004; Rhile et al. 1996) and Fas:FasL interactions have been implicated in this process (Dencker et al. 1985; Kamath et al. 1999a), C57Bl/6 mice were treated with 10 μg/kg TCDD and the degree of apoptosis measured by assessing the expression of 7AAD and Annexin V, as well as Fas and FasL on thymocytes via flow cytometry. Representative dot plots gating on singlet thymocytes revealed a slight, but statistically significant increase in the frequency of Annexin V^+7AAD^- apoptotic thymocytes in 10 μg/kg TCDD-treated mice (6.5% ± 0.8 of thymocytes) compared to vehicle (3.8% ± 0.6 of thymocytes) on day 7 (Figure 2.4A). However, this did not correspond to a significant increase in the absolute number of apoptotic cells—perhaps due to the massive decline in thymus cellularity (data not shown). Moreover, representative dot plots gating on Annexin V^+7AAD^- apoptotic thymocytes revealed that the majority of apoptotic cells were DP thymocytes, followed by DN and $CD4^+$ SP thymocytes, with very few apoptotic cells observed in the $CD8^+$ SP subset. In contrast, TCDD exposed animals exhibited a distribution shift at day 7—resulting in an increased frequency of Annexin V^+7AAD^- apoptotic thymocytes within the DN, $CD4^+$, and $CD8^+$ SP thymocytes and a decreased frequency of Annexin V^+7AAD^- apoptotic thymocytes being of the DP thymocyte subset (Figure 2.4A and 2.4B). Additionally, C57Bl/6 mice were treated with 10 μg/kg TCDD and Fas-FasL gene expression was analyzed in freshly isolated thymocytes on days 3, 7, and 14 post exposure. TCDD resulted in no change in either Fas or FasL gene expression as measured by quantitative RT-PCR (data not shown). Furthermore, 3 days after

administration of TCDD to C57Bl/6 mice, there were no observable effects on the frequency nor the MFI of Fas and FasL expression on live $CD45^+$ thymocytes relative to vehicle controls (Figure 2.5a). Because previous studies reported that dioxin induced FasL-dependent thymocyte cell death (Camacho et al. 2005a; Kamath et al. 1999b), we examined the role of Fas-FasL signaling in TCDD-induced thymic atrophy using FasL-deficient (*gld/gld*) mice. FasL deficient mice were exposed to 10 μg/kg TCDD (p.o.) and their thymic weight and cellularity measured on day 7. Contrary to a previous report (Kamath et al. 1999b), FasL-deficient mice in our experiments were not protected against TCDD-induced thymic atrophy and exhibited significant reductions in thymic weight (60% decrease) and cellularity (70% decrease) comparable to wild-type C57Bl/6 mice (Figure 2.5B). Similarly, representative dot plots (gating on live thymocytes) revealed a significant decline in the frequency of DP thymocytes, as well as a relative enrichment in the percent of DN and $CD4^+$ and $CD8^+$ SP thymocytes in 10 μg/kg TCDD-treated mice compared to vehicle control (Figure 2.5C).

Figure 2. 4 ***The effect of TCDD on apoptotic thymocytes.***

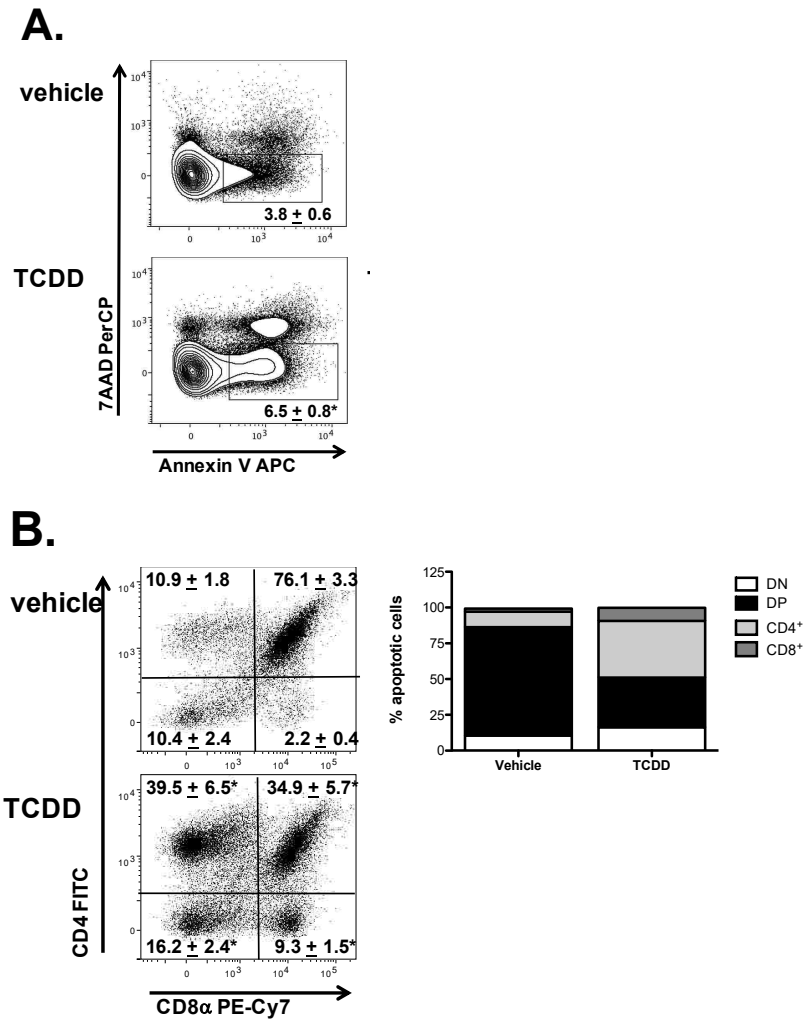

Figure 2.4. The effect of TCDD on apoptotic thymocytes.
Naïve wild-type mice (C57Bl/6) were gavaged with vehicle (anisole/peanut oil) or TCDD (10 μg/kg). Representative contour plots gating on 7-AAD$^+$Annexin V$^+$ thymocytes revealed a significant increase in the frequency of apoptotic thymocytes (A), as well as a dramatic shift in the distribution of thymocytes which were undergoing apoptosis 7 days following exposure to TCDD (B). Data represent one of two independent experiments, n=3-5 mice per treatment group, mean ± SEM; 1-way ANOVA, *$p < 0.05$ vehicle.

Figure 2. 5 ***TCDD-mediated thymic atrophy is not dependent on Fas-FasL interactions***

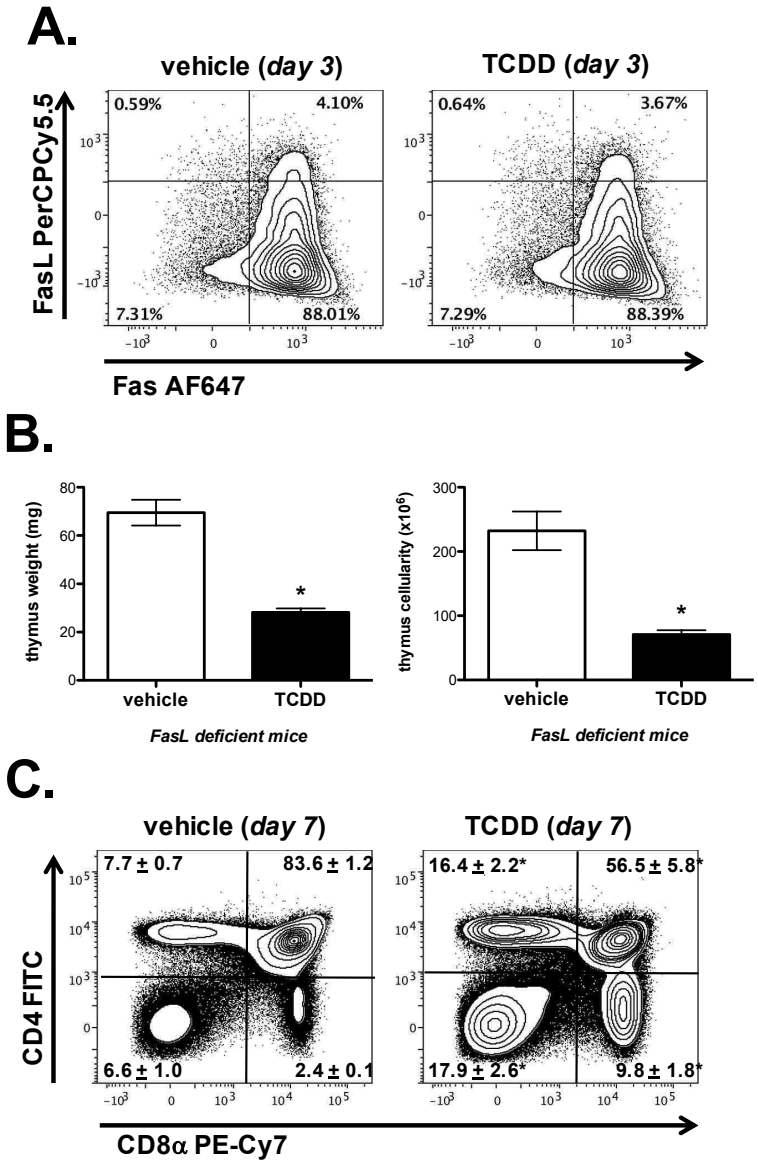

Figure 2.5. TCDD-mediated thymic atrophy is not dependent on Fas-FasL interactions. Naïve wild-type mice (C57Bl/6) were gavaged with vehicle (anisole/peanut oil) or TCDD (10 μg/kg). Representative contour plots gating on singlet thymocytes revealed that 3 days after administration of vehicle or 10 μg/kg TCDD to C57Bl/6 mice, there were no observable effects on the frequency of Fas and FasL expression on $CD45^+$ thymocytes relative to vehicle control (A). FasL deficient (*gld/gld*) mice were exposed to 10 μg/kg TCDD and their thymic weight and cellularity measured on day 7 (B). Similarly, representative dot plots (gating on live thymocytes) revealed a significant decline in the frequency of DP thymocytes, as well as a relative enrichment in the percent of DN and $CD4^+CD8^-$ and $CD4^-CD8^+$ SP thymocytes in 10 μg/kg TCDD-treated FasL deficient (*gld/gld*) mice compared to vehicle control (C). n=5 mice per treatment group, mean ± SEM; t-test, *$p < 0.05$ vehicle.

Targeted deletion of the AhR in CD11c^{+} dendritic cells protects against dioxin-induced thymic atrophy

Previous studies revealed that the target/s for TCDD-induced thymic atrophy reside within the hematopoietic cells and not stromal tissues (Staples et al. 1998); however, it is uncertain which hematopoietically derived cells contribute to TCDD-induced thymic atrophy. To determine how AhR signaling in specific immune cells mediates TCDD-induced thymic atrophy, we generated AhR conditional knockout mice for myeloid derived cells (LyzM^{Cre}AhR^{fx}), CD11c^{+} dendritic cells (CD11c^{Cre}AhR^{fx}), RORγt^{+} DP and SP thymocytes (RORc^{Cre}AhR^{fx}), and thymic epithelial cells (FoxN1^{Cre}AhR^{fx}). Mice were dosed with solvent/peanut oil vehicle or 100 μg/kg TCDD—a dose of dioxin necessary to elicit thymotoxic endpoints in conditional AhR$^{fx/fx}$ mice which carry the low affinity AhR^{d} allele (Poland and Glover 1980; Walisser et al. 2005). Seven days later, Cre^{-}AhR$^{fx/fx}$ and AhR^{d} mice, as well as LyzM^{Cre}AhR^{fx}, RORc^{Cre}AhR^{fx}, and FoxN1^{Cre}AhR^{fx} exhibited extensive thymic atrophy as evidenced by a decline in organ weight (68%, 63%, and 63% decrease, respectively) (Figure 2.6A) and a dramatic reduction in thymic cellularity (89%, 89%, and 82% decrease, respectively) (Figure 2.6B) relative to vehicle control. In contrast, CD11c^{Cre}AhR^{fx} mice were protected from TCDD-induced thymic atrophy and showed no significant difference from vehicle controls in either thymic weight (Figure 2.6A) or cellularity (Figure 2.6B). These findings led us to further investigate whether targeted deletion of the AhR in specific immune cell types also facilitates TCDD-induced effects on intra-thymic development and differentiation. Representative dot plots from AhR^{d}, LyzM^{Cre}AhR^{fx}, RORc^{Cre}AhR^{fx}, and FoxN1^{Cre}AhR^{fx} mice administered 100 μg/kg TCDD echoed the typical alterations in thymocyte subsets which can be observed in wild-type mice following exposure to

TCDD: decreases in the frequency of DP thymocytes and increases in the frequency of DN, $CD4^+$, and $CD8^+$ SP thymocytes compared to vehicle control (data not shown). Importantly, representative dot plots gating on live thymocytes from $CD11c^{Cre}AhR^{fx}$ mice treated with 100 μg/kg TCDD exhibited protection from TCDD-induced alterations in thymocyte subsets (Figure 2.7). Because conditional Cre negative x $AhR^{fx/fx}$ mice carry the low affinity AhR^d allele (Poland and Glover 1980; Walisser et al. 2005), this strain can be utilized interchangeably with Cre^-AhR^{fx} as controls for experiments involving AhR conditional knockout mice (supplemental Figure 2.3). Collectively these data show that targeted deletion of the AhR in $CD11c^+$ dendritic cells protects against TCDD-induced thymic atrophy.

Figure 2. 6 ***Deletion of the AhR in CD11c+ dendritic cells protects against dioxin-induced thymic atrophy.***

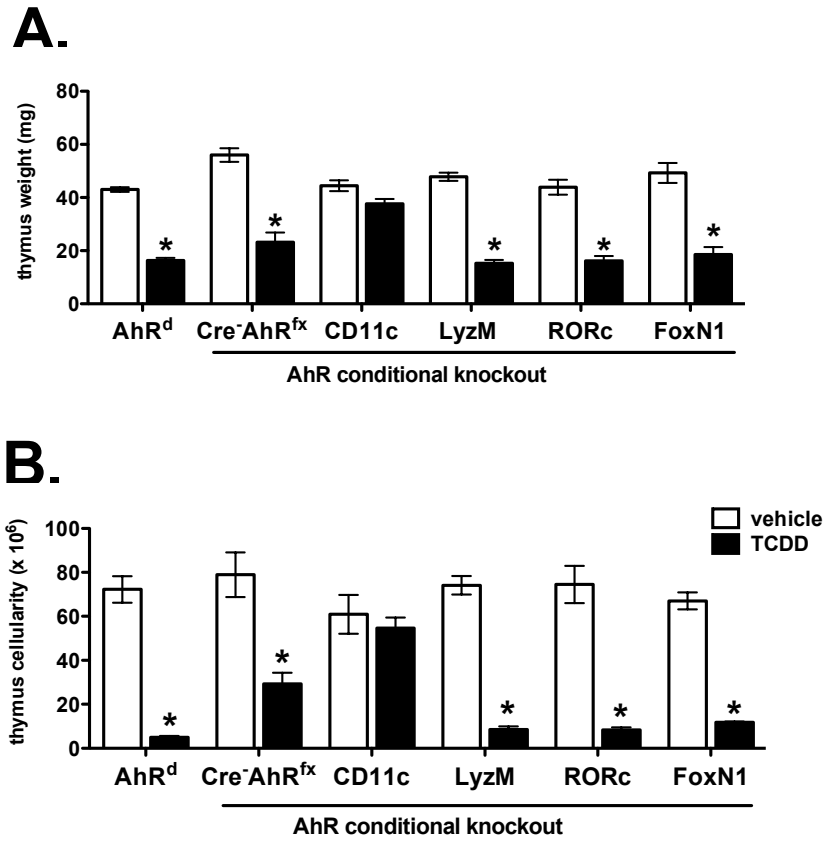

Figure 2.6. Deletion of the AhR in CD11c+ dendritic cells protects against dioxin-induced thymic atrophy.

AhR conditional knockout mice were generated for myeloid derived cells ($LyzM^{Cre}AhR^{fx}$), $CD11c^{+}$ dendritic cells ($CD11c^{Cre}AhR^{fx}$), $ROR\gamma t^{+}$ DP and SP thymocytes ($RORc^{Cre}AhR^{fx}$), and thymic epithelial cells ($FoxN1^{Cre}AhR^{fx}$). Mice were exposed to either solvent/peanut oil vehicle or 100 μg/kg TCDD. Three indicators of toxicity: body weight (data not shown), thymus weight (A), and thymus cell number (B) were measured on day 7. Data represent one of three independent experiments, n=3-4 mice per treatment group, mean ± SEM; 2-way ANOVA, *$p < 0.05$ vehicle.

Figure 2. 7 ***Comparison of CD4/CD8 thymocyte subsets from*** **CD11c^{Cre}AhR^{fx}** ***and AhR^{d} mice exposed to vehicle or TCDD.***

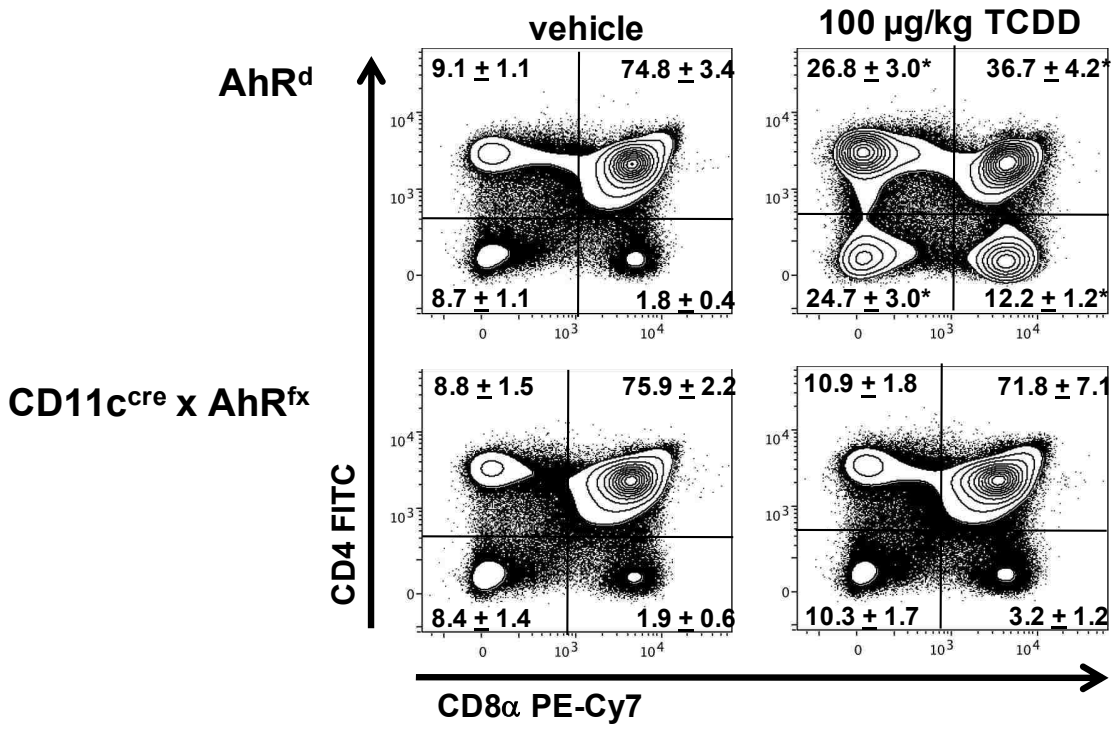

Figure 2.7. Comparison of CD4/CD8 thymocyte subsets from **CD11c^{Cre}AhR^{fx}** ***and AhR^{d} mice exposed to vehicle or TCDD.***

AhR conditional knockout and AhR^{d} control mice were exposed to either solvent/peanut oil vehicle or 100 µg/kg TCDD. Representative contour plots gating on live thymocytes revealed a significant decline in the frequency of CD4^{+}CD8^{+} DP thymocytes, as well as a relative enrichment in the percent of CD4^{-}CD8^{-} DN and CD4^{+}CD8^{-} and CD4^{-}CD8^{+} SP thymocytes in AhR^{d} mice exposed to 100 µg/kg TCDD compared to vehicle controls on day 7. These shifts in CD4/CD8 thymocyte subsets were not observed in CD11c^{Cre}AhR^{fx} mice treated with TCDD. The mean percentages of the CD4/CD8 thymocyte subsets ± SEM are indicated in the plots. Data represent one of three independent experiments, n=3-4 per treatment group; 2-way ANOVA, *p < 0.05 vehicle.

Discussion

Administration of dioxin (TCDD) and dioxin-like chemicals to laboratory rodents dramatically affects the immune system, triggering immunosuppression characterized by suppressed cellular immunity, inhibition of antibody production, and thymic atrophy (Silkworth and Antrim 1985; Silkworth et al. 1986)—effects which are dependent on the AhR (Fernandez-Salguero et al. 1996; Harrill et al. 2016; Staples et al. 1998). Unlike many nuclear receptors, the AhR is a highly promiscuous receptor, directly binding a wide variety of structurally diverse natural and synthetic compounds, thereby promoting the up- or down-regulation of a multitude of target genes in different tissues. The spectrum of biological effects produced by the ligand/AhR/ARNT signaling complex is dependent on the physicochemical characteristics and persistence of the ligand (Ehrlich et al. 2018). To date, most analyses exploring AhR-induced immune modulation have taken advantage of TCDD's specificity and high affinity for the AhR (6 pM – 2.4 nM), as well as its long half-life (~11 days in mice; 8-10 years in humans) (Miniero et al. 2001). However, the same properties that make TCDD an excellent tool also contribute to its profound toxicity. While other ligands such as ITE and indole-3-carbinol (I3C) can activate the AhR and have been evaluated as potential therapeutics (Abron et al. 2018; Quintana et al. 2010c; Yeste et al. 2012), little is known about their potential thymotoxic effects. Thus, the present study investigated the effects of an endogenous (ITE) and a dietary (I3C) ligand on thymic development and differentiation.

Administration of 8 mg/kg ITE to C57Bl/6 mice resulted in a dramatic reduction in organ weight and thymic cellularity on day 7. In contrast, administration of 100 mg/kg

I3C to C57Bl/6 mice resulted in a slight increase in thymic weight and a significant increase in cellularity. Because previous studies in a murine colitis model suggested that sex-specific effects existed with select AhR ligands (Benson et al. 2012a), we also tested the hypothesis that male vs. female mice would exhibit disparate thymic atrophy following activation of the AhR. Interestingly, no sex specific effects were observed with regards to thymic weight or cellularity following exposure to TCDD, ITE, or I3C. Likewise, because AhR activation by TCDD and TCDD-like compounds results in alterations in the frequency of thymocyte subsets, we investigated whether ITE and I3C similarly affected thymic development and differentiation. Our results demonstrate for the first time that ITE induced thymic atrophy, as well as reduced the frequency of DP thymocytes and increased the frequency of DN, $CD4^+$ and $CD8^+$ SP thymocytes—albeit to a slightly lesser degree than TCDD. These data are in contrast to a previous report (Henry et al. 2006), which did not detect changes in thymus weight 12 days following a single delivery of 5.6 mg/kg ITE (i.v.). It is likely that the discrepancy between our results and the study by Henry et al., 2006 reside in the differences between dose (acute vs sub-acute) and route of delivery (i.v. vs. p.o.) of the AhR ligand (Boule et al. 2018b; Ehrlich et al. 2018). Interestingly, I3C did not result in thymic atrophy with a slight increase in thymic cellularity being observed. This divergence in effects between two natural AhR ligands was surprising as the administered doses had both been shown to elicit immunosuppressive effects, and the thymus is known to be acutely sensitive to AhR ligands. Importantly, the previously reported immunosuppression observed with I3C occurred within the intestines, which given the oral route of administration as well as documented non-enzymatic cleavage of I3C into additional AhR ligands by gastric acid,

it is conceivable that higher concentrations of I3C and its newly formed metabolites are available within the gut (Benson et al. 2012a; Bjeldanes et al. 1991; Perdew et al. 2015). Recent advances in AhR biology further suggest that binding affinity and ligand metabolism may be better predictors of immunosuppressive outcome than ligand source (Boule et al. 2018a). Therefore, further analysis of I3C through a higher dose response as well as administration of purified metabolites would better evaluate I3C for effects on the thymus. Together, this is the first study to compare AhR activation by different types of compounds on thymocyte development and differentiation; thus, extending our knowledge of ligand-specific, AhR-mediated immunotoxic effects.

Because we observed gross thymic atrophy with ITE, we more extensively characterized the ability of ITE to induce thymic atrophy. Following previously published dosing regimens (Nugent et al. 2013; Quintana et al. 2010b), our data clearly demonstrate that daily administration of 8mg/kg ITE p.o. induced significant thymic atrophy in an AhR-dependent manner. In addition, ITE induced noticeable decreases in both thymic weight and cellularity at doses as low as 1 mg/kg. Moreover, 4m/kg ITE p.o. and 1mg/kg i.p. induced comparable levels of thymic atrophy in C57Bl/6 mice, demonstrating that ITE causes thymic atrophy regardless of the route of systemic exposure. This point is particularly important given the growing interest in AhR research on identifying novel classes of potent, non-toxic AhR ligands for use in various therapeutic settings (Stockinger 2009). Moreover, these observations raise concerns about potential off-target immune toxicities associated with the use of ITE based immune therapies (Abron et al. 2018; Dolciami et al. 2018; Hao and Whitelaw 2013; Nugent et al. 2013; Quintana et al. 2010c).

Multiple mechanisms for TCDD induced thymic hypocellularity have been suggested including reduced proliferation of DN precursor thymocytes (Lai et al. 1994), enhanced apoptosis at the DP stage (Camacho et al. 2005b), and enhanced emigration of thymocytes (Poland et al. 1994; Temchura et al. 2005), or a combination of these possible mechanisms. Apoptosis occurs normally during development and aging as a homeostatic mechanism to maintain cell populations in tissues, and as a defense mechanism when disease or noxious agents damage cells. Although apoptosis was reported to underlie TCDD-induced thymic atrophy (Kamath et al. 1998; Kamath et al. 1997), and thymic and peripheral T cells are highly sensitive to TCDD-induced apoptosis *in vitro* (Camacho et al. 2004), our work and that of others (Comment et al. 1992; De Heer et al. 1994; Silverstone et al. 1994a; Silverstone et al. 1994b; Staples et al. 1998) have failed to support this *in vivo*. In the current study, we investigated whether 10 μg/kg TCDD initiates apoptosis in C57Bl/6 mice by quantifying the frequency and absolute number of apoptotic thymocytes by flow cytometry on day 7 post-exposure. Although TCDD-induced thymic atrophy corresponded with an almost doubling of the frequency of Annexin V^+7-AAD^- apoptotic thymocytes compared to control animals, this did not correspond to a significant increase in the absolute number of apoptotic cells—likely due to the massive decline in overall thymus cellularity observed with exposure to TCDD. Earlier studies suggested that the timing and pathway of apoptosis was important to AhR-mediated thymic atrophy (Kamath et al. 1998) and implied Fas-FasL interactions regulated apoptosis during TCDD-induced thymic atrophy (Camacho et al. 2005a). This led us to assess the mRNA expression of Fas and FasL using qRT-PCR on days 3, 7 and 14 after administration of 10 μg/kg TCDD in naïve wild-type C57Bl/6 mice, which did

not support TCDD-mediated induction of Fas and/or FasL gene expression in the thymus. Analysis of Fas and FasL protein expression by flow cytometry 3 days after administration of 10 μg/kg TCDD to C57Bl/6 mice, further confirmed these results at the protein level.

Because apoptotic cells may be rapidly cleared by phagocytic cells *in vivo* (Platt et al. 1998), we also probed the role of Fas-FasL interactions in TCDD-induced thymic atrophy using FasL-deficient (*gld/gld*) mice. In our studies, FasL-deficient (*gld/gld*) mice exposed to 10 μg/kg TCDD experienced the same degree of thymic atrophy as Fas-FasL competent control mice and thymocyte subsets demonstrated no protection from TCDD-induced alterations. Interestingly, assessment of an apoptosis and survival RT-PCR array yielded four genes which showed a significant increase in expression: BAD (7-fold change vs vehicle), Akt1 (4-fold change vs vehicle), and Pik3cd (2.5-fold change vs vehicle), Ppp3ca (2.5-fold change vs vehicle) in thymocytes on day 7 and no genes which were significantly reduced in expression. These data are consistent with evidence that suggests that apoptosis and survival genes in thymocytes are in constant flux. Collectively, our results fail to support Fas-FasL-mediated apoptosis as a mechanism of TCDD-induced thymic atrophy. These findings are in direct contrast to previously published reports, which implicated Fas-FasL interactions as playing an important role in TCDD-mediated induction of apoptosis and immunotoxicity (Camacho et al. 2002; Kamath et al. 1999b; Rhile et al. 1996). In a majority of the previously reported *in vivo* studies, C57Bl/6 mice were exposed to 30-50 μg/kg TCDD intraperitoneally (i.p.), and evaluated shortly thereafter, 6-24hrs, whereas in our study C57Bl/6 mice were exposed to 10 ug/kg TCDD through oral gavage (p.o) and evaluated 3-14 days post-exposure.

Pharmacokinetics indicate that TCDD is more readily metabolized following p.o. than i.p. administration (Olson et al. 1980), thus we would expect that p.o. administration would yield lower bioavailability than i.p. delivery. These differences in dose and administration route may yield a substantially lower systemic TCDD concentration in our studies, and thus leads us to question whether exceedingly high concentrations of systemic TCDD initiate an immediate apoptotic response that does not last beyond the early time points tested by Camacho et al. (2005a). Supporting this, it was initially reported that thymocytes exhibit markers of apoptosis up until 24-hours post exposure (Camacho et al. 2005a); however, maximal thymic atrophy does not occur until 7-10 days post-exposure in adult mice (Silverstone et al. 1994a). Together, this may explain the difference in reports and suggests that apoptosis may be the most immediate, although not the most substantial mechanism, involved in thymic atrophy following exposure to lower concentrations of TCDD.

Previous studies identified the AhR signaling pathway as the pivotal event in TCDD-induced thymic atrophy (Laiosa et al. 2003b; Staples et al. 1998) and the hematopoietic compartment as the target for TCDD-induced thymic atrophy (Staples et al. 1998). However, until now, it was unclear which hematopoietically derived cell/s triggered TCDD-induced thymic atrophy. To investigate the importance of cell-specific AhR signaling in TCDD-induced thymic atrophy, mice expressing the AhR floxed allele (AhR^{fx}) were crossed to mice expressing Cre transgenes driven by LyzM (myeloid derived cells), CD11c (dendritic cells), RORγt (DP and SP thymocytes), and FoxN1 (thymic epithelial cells) specific promoters. Our results show for the first time that deletion of the AhR in $CD11c^{+}$ dendritic cells prevents TCDD-induced thymic atrophy, a

previously unreported phenomenon. Therefore, the immunotoxic responses of TCDD on the thymus are dependent on AhR activation in $CD11c^+$ dendritic cells. DCs make up a small percentage of the thymic stroma (Wu and Shortman 2005) and are located mainly in the medulla and corticomedullary region. Thymic DCs cross-present self-antigens to developing thymocytes, facilitate the generation of regulatory T cells, and act as gatekeepers of lymphocyte trafficking (Bonasio et al. 2006; Hubert et al. 2011; Lei et al. 2011; Proietto et al. 2008b). DCs are thus poised to exert control over thymic output in response to environmental conditions. Unfortunately, the solubility limitations of ITE (~30 mg/mL DMSO) and I3C (~10 mg/mL in ethanol) prevent the use of either of these ligands in AhR conditional knockout mice at doses that would be expected to induce thymic atrophy. Together, the current study significantly advances our understanding of how the AhR regulates immune responses and demonstrates for the first time that TCDD-induced thymic atrophy occurs as a result of activation of the AhR in $CD11c^+$ dendritic cells. Identification of $CD11c^+$ dendritic cells as the direct target of TCDD-induced thymic atrophy offers insights into novel pathways to further understand the mechanisms of AhR-mediated immune regulation. Collectively, this work emphasizes the importance of research examining the contribution of cell- and tissue-specific consequences of chemical exposures on immune responses.

References

Abron JD, Singh NP, Mishra MK, et al. (2018) An endogenous aryl hydrocarbon receptor (AhR) ligand, ITE induces regulatory T cells (Tregs) and ameliorates experimental colitis. Am J Physiol Gastrointest Liver Physiol doi:10.1152/ajpgi.00413.2017

Benson J, Beamer C, Seaver B, Shepherd D (2012a) Indole-3-Carbinol Exerts Sex-Specific Effects in Murine Colitis. European Journal of Inflammation 10(3):335-346

Benson JM, Beamer CA, Seaver BP, Shepherd DM (2012b) Indole-3-Carbinol Exerts Sex-Specific Effects in Murine Colitis. Eur J Inflamm 10(3):335-346 doi:Doi 10.1177/1721727x1201000309

Benson JM, Shepherd DM (2011a) Aryl hydrocarbon receptor activation by TCDD reduces inflammation associated with Crohn's disease. Toxicological sciences : an official journal of the Society of Toxicology 120(1):68-78 doi:10.1093/toxsci/kfq360

Benson JM, Shepherd DM (2011b) Dietary ligands of the aryl hydrocarbon receptor induce anti-inflammatory and immunoregulatory effects on murine dendritic cells. Toxicological Sciences 124(2):327-338

Birnbaum LS (1986) Distribution and excretion of 2,3,7,8-tetrachlorodibenzo-p-dioxin in congenic strains of mice which differ at the Ah locus. Drug metabolism and disposition: the biological fate of chemicals 14(1):34-40

Bjeldanes LF, Kim J-Y, Grose KR, Bartholomew JC, Bradfield CA (1991) Aromatic hydrocarbon responsiveness-receptor agonists generated from indole-3-carbinol in vitro and in vivo: comparisons with 2, 3, 7, 8-tetrachlorodibenzo-p-dioxin. Proceedings of the national academy of sciences 88(21):9543-9547

Bonasio R, Scimone ML, Schaerli P, Grabie N, Lichtman AH, von Andrian UH (2006) Clonal deletion of thymocytes by circulating dendritic cells homing to the thymus. Nat Immunol 7(10):1092-100 doi:10.1038/ni1385

Boule LA, Burke CG, Jin G-B, Lawrence BP (2018a) Aryl hydrocarbon receptor signaling modulates antiviral immune responses: ligand metabolism rather than chemical source is the stronger predictor of outcome. Scientific reports 8(1):1826

Boule LA, Burke CG, Jin GB, Lawrence BP (2018b) Aryl hydrocarbon receptor signaling modulates antiviral immune responses: ligand metabolism rather than chemical source is the stronger predictor of outcome. Sci Rep 8(1):1826 doi:10.1038/s41598-018-20197-4

Camacho IA, Nagarkatti M, Nagarkatti PS (2002) 2, 3, 7, 8-Tetrachlorodibenzo-p-dioxin (TCDD) induces Fas-dependent activation-induced cell death in superantigen-primed T cells. Archives of toxicology 76(10):570-580

Camacho IA, Nagarkatti M, Nagarkatti PS (2004) Evidence for induction of apoptosis in T cells from murine fetal thymus following perinatal exposure to 2, 3, 7, 8-tetrachlorodibenzo-p-dioxin (TCDD). Toxicological Sciences 78(1):96-106

Camacho IA, Singh N, Hegde VL, Nagarkatti M, Nagarkatti PS (2005a) Treatment of mice with 2,3,7,8-tetrachlorodibenzo-p-dioxin leads to aryl hydrocarbon receptor-dependent nuclear translocation of NF-kappaB and expression of

Fas ligand in thymic stromal cells and consequent apoptosis in T cells. J Immunol 175(1):90-103
Camacho IA, Singh N, Hegde VL, Nagarkatti M, Nagarkatti PS (2005b) Treatment of mice with 2, 3, 7, 8-tetrachlorodibenzo-p-dioxin leads to aryl hydrocarbon receptor-dependent nuclear translocation of NF-κB and expression of Fas ligand in thymic stromal cells and consequent apoptosis in T cells. The Journal of Immunology 175(1):90-103
Comment CE, Blaylock BL, Germolec DR, et al. (1992) Thymocyte injury after in vitro chemical exposure: potential mechanisms for thymic atrophy. J Pharmacol Exp Ther 262(3):1267-73
Connor K, Finley B (2003) Naturally occurring ah-receptor agonists in foods: Implications regarding dietary dioxin exposure and health risk. Human and Ecological Risk Assessment 9(7):1747-1763
De Heer C, Verlaan AP, Penninks AH, Vos JG, Schuurman HJ, Van Loveren H (1994) Time course of 2,3,7,8-tetrachlorodibenzo-p-dioxin (TCDD)-induced thymic atrophy in the Wistar rat. Toxicol Appl Pharmacol 128(1):97-104
Dencker L, Hassoun E, d'Argy R, Alm G (1985) Fetal thymus organ culture as an in vitro model for the toxicity of 2, 3, 7, 8-tetrachlorodibenzo-p-dioxin and its congeners. Molecular pharmacology 27(1):133-140
Dolciami D, Gargaro M, Cerra B, et al. (2018) Binding Mode and Structure-Activity Relationships of ITE as an Aryl Hydrocarbon Receptor (AhR) Agonist. ChemMedChem 13(3):270-279 doi:10.1002/cmdc.201700669
Ehrlich AK, Pennington JM, Bisson WH, Kolluri SK, Kerkvliet NI (2018) TCDD, FICZ, and Other High Affinity AhR Ligands Dose-Dependently Determine the Fate of CD4+ T Cell Differentiation. Toxicol Sci 161(2):310-320 doi:10.1093/toxsci/kfx215
Faith RE, Luster MI (1979) Investigations on the effects of 2, 3, 7, 8‐tetrachlorodibenzo‐p‐dioxin (TCDD) on parameters of various immune functions. Annals of the New York Academy of Sciences 320(1):564-571
Fernandez-Salguero PM, Hilbert DM, Rudikoff S, Ward JM, Gonzalez FJ (1996) Aryl-hydrocarbon receptor-deficient mice are resistant to 2,3,7,8-tetrachlorodibenzo-p-dioxin-induced toxicity. Toxicol Appl Pharmacol 140(1):173-9 doi:10.1006/taap.1996.0210
Fisher MT, Nagarkatti M, Nagarkatti PS (2004) Combined screening of thymocytes using apoptosis-specific cDNA array and promoter analysis yields novel gene targets mediating TCDD-induced toxicity. Toxicol Sci 78(1):116-24 doi:10.1093/toxsci/kfh058
Funatake CJ, Marshall NB, Steppan LB, Mourich DV, Kerkvliet NI (2005) Cutting edge: activation of the aryl hydrocarbon receptor by 2, 3, 7, 8-tetrachlorodibenzo-p-dioxin generates a population of CD4+ CD25+ cells with characteristics of regulatory T cells. The Journal of Immunology 175(7):4184-4188
Gasiewicz TA, Geiger LE, Rucci G, Neal RA (1983) Distribution, excretion, and metabolism of 2,3,7,8-tetrachlorodibenzo-p-dioxin in C57BL/6J, DBA/2J, and

B6D2F1/J mice. Drug metabolism and disposition: the biological fate of chemicals 11(5):397-403
Gu Y-Z, Hogenesch JB, Bradfield CA (2000) The PAS superfamily: sensors of environmental and developmental signals. Annual review of pharmacology and toxicology 40(1):519-561
Hao N, Whitelaw ML (2013) The emerging roles of AhR in physiology and immunity. Biochem Pharmacol 86(5):561-70 doi:10.1016/j.bcp.2013.07.004
Harrill JA, Layko D, Nyska A, et al. (2016) Aryl hydrocarbon receptor knockout rats are insensitive to the pathological effects of repeated oral exposure to 2,3,7,8-tetrachlorodibenzo-p-dioxin. J Appl Toxicol 36(6):802-14 doi:10.1002/jat.3211
Harris M, Moore J, Vos J, Gupta B (1973) General biological effects of TCDD in laboratory animals. Environmental health perspectives 5:101
Henry EC, Bemis JC, Henry O, Kende AS, Gasiewicz TA (2006) A potential endogenous ligand for the aryl hydrocarbon receptor has potent agonist activity in vitro and in vivo. Arch Biochem Biophys 450(1):67-77 doi:10.1016/j.abb.2006.02.008
Hubert FX, Kinkel SA, Davey GM, et al. (2011) Aire regulates the transfer of antigen from mTECs to dendritic cells for induction of thymic tolerance. Blood 118(9):2462-72 doi:10.1182/blood-2010-06-286393
Kamath AB, Camacho I, Nagarkatti PS, Nagarkatti M (1999a) Role of Fas-Fas ligand interactions in 2,3,7,8-tetrachlorodibenzo- p-dioxin (TCDD)-induced immunotoxicity: increased resistance of thymocytes from Fas-deficient (lpr) and Fas ligand-defective (gld) mice to TCDD-induced toxicity. Toxicol Appl Pharmacol 160(2):141-55 doi:10.1006/taap.1999.8753
Kamath AB, Camacho I, Nagarkatti PS, Nagarkatti M (1999b) Role of Fas–Fas ligand interactions in 2, 3, 7, 8-tetrachlorodibenzo-p-dioxin (TCDD)-induced immunotoxicity: increased resistance of thymocytes from Fas-deficient (lpr) and Fas ligand-defective (gld) mice to TCDD-induced toxicity. Toxicology and applied pharmacology 160(2):141-155
Kamath AB, Nagarkatti PS, Nagarkatti M (1998) Characterization of Phenotypic Alterations Induced by 2, 3, 7, 8-Tetrachlorodibenzo-p-dioxin on Thymocytesin Vivoand Its Effect on Apoptosis. Toxicology and applied pharmacology 150(1):117-124
Kamath AB, Xu H, Nagarkatti PS, Nagarkatti M (1997) Evidence for the induction of apoptosis in thymocytes by 2, 3, 7, 8-tetrachlorodibenzo-p-dioxinin vivo. Toxicology and applied pharmacology 142(2):367-377
Kerkvliet NI (2002) Recent advances in understanding the mechanisms of TCDD immunotoxicity. International immunopharmacology 2(2-3):277-291
Kerkvliet NI (2012) TCDD: an environmental immunotoxicant reveals a novel pathway of immunoregulation—a 30-year odyssey. Toxicologic pathology 40(2):138-142
Lai ZW, Kremer J, Gleichmann E, Esser C (1994) 3, 3′, 4, 4′‐Tetrachlorobiphenyl Inhibits Proliferation of Immature Thymocytes in Fetal Thymus Organ Culture. Scandinavian journal of immunology 39(5):480-488

Laiosa MD, Wyman A, Murante FG, et al. (2003a) Cell proliferation arrest within intrathymic lymphocyte progenitor cells causes thymic atrophy mediated by the aryl hydrocarbon receptor. The Journal of Immunology 171(9):4582-4591
Laiosa MD, Wyman A, Murante FG, et al. (2003b) Cell proliferation arrest within intrathymic lymphocyte progenitor cells causes thymic atrophy mediated by the aryl hydrocarbon receptor. J Immunol 171(9):4582-91
Lei Y, Ripen AM, Ishimaru N, et al. (2011) Aire-dependent production of XCL1 mediates medullary accumulation of thymic dendritic cells and contributes to regulatory T cell development. J Exp Med 208(2):383-94 doi:10.1084/jem.20102327
Lundberg K, Grönvik K-O, Goldschmidt TJ, Klareskog L, Dencker L (1990) 2, 3, 7, 8-Tetrachlorodibenzo-p-dioxin (TCDD) alters intrathymic T-cell development in mice. Chemico-biological interactions 74(1-2):179-193
Miniero R, De Felip E, Ferri F, Di Domenico A (2001) An overview of TCDD half-life in mammals and its correlation to body weight. Chemosphere 43(4-7):839-844
Nebert D, Gelboin H (1968) Substrate-inducible microsomal aryl hydroxylase in mammalian cell culture I. Assay and properties of induced enzyme. Journal of Biological Chemistry 243(23):6242-6249
Nebert D, Gelboin H (1969) The in vivo and in vitro induction of aryl hydrocarbon hydroxylase in mammalian cells of different species, tissues, strains, and developmental and hormonal states. Archives of biochemistry and biophysics 134(1):76-89
Nguyen LP, Bradfield CA (2007) The search for endogenous activators of the aryl hydrocarbon receptor. Chemical research in toxicology 21(1):102-116
Nowell CS, Farley AM, Blackburn CC (2007) Thymus organogenesis and development of the thymic stroma Immunological Tolerance. Springer, p 125-162
Nugent LF, Shi G, Vistica BP, Ogbeifun O, Hinshaw SJ, Gery I (2013) ITE, a novel endogenous nontoxic aryl hydrocarbon receptor ligand, efficiently suppresses EAU and T-cell-mediated immunity. Invest Ophthalmol Vis Sci 54(12):7463-9 doi:10.1167/iovs.12-11479
Okey AB (2007) An aryl hydrocarbon receptor odyssey to the shores of toxicology: the Deichmann Lecture, International Congress of Toxicology-XI. Toxicol Sci 98(1):5-38 doi:10.1093/toxsci/kfm096
Olson JR, Holscher MA, Neal RA (1980) Toxicity of 2,3,7,8-tetrachlorodibenzo-p-dioxin in the golden Syrian hamster. Toxicol Appl Pharmacol 55(1):67-78
Perdew GH, Murray IA, Hubbard TD (2015) Indole and tryptophan metabolism: endogenous and dietary routes to Ah receptor activation. Drug Metabolism and Disposition:dmd. 115.064246
Platt N, da Silva RP, Gordon S (1998) Recognizing death: the phagocytosis of apoptotic cells. Trends in cell biology 8(9):365-372
Pohjanvirta R (2011) The AH receptor in Biology and Toxicology. John Wiley & Sons
Poland A, Glover E (1980) 2, 3, 7, 8-Tetrachlorodibenzo-p-dioxin: segregation of toxicity with the Ah locus. Molecular Pharmacology 17(1):86-94

Poland A, Glover E, Kende A (1976) Stereospecific, high affinity binding of 2, 3, 7, 8-tetrachlorodibenzo-p-dioxin by hepatic cytosol. Evidence that the binding species is receptor for induction of aryl hydrocarbon hydroxylase. Journal of Biological Chemistry 251(16):4936-4946

Poland A, Palen D, Glover E (1994) Analysis of the four alleles of the murine aryl hydrocarbon receptor. Molecular pharmacology 46(5):915-921

Proietto AI, van Dommelen S, Zhou P, et al. (2008b) Dendritic cells in the thymus contribute to T-regulatory cell induction. Proc Natl Acad Sci U S A 105(50):19869-74 doi:10.1073/pnas.0810268105

Quintana FJ, Murugaiyan G, Farez MF, et al. (2010a) An endogenous aryl hydrocarbon receptor ligand acts on dendritic cells and T cells to suppress experimental autoimmune encephalomyelitis. Proceedings of the National Academy of Sciences 107(48):20768-20773

Quintana FJ, Murugaiyan G, Farez MF, et al. (2010b) An endogenous aryl hydrocarbon receptor ligand acts on dendritic cells and T cells to suppress experimental autoimmune encephalomyelitis. Proceedings of the National Academy of Sciences of the United States of America 107(48):20768-73 doi:10.1073/pnas.1009201107

Quintana FJ, Murugaiyan G, Farez MF, et al. (2010c) An endogenous aryl hydrocarbon receptor ligand acts on dendritic cells and T cells to suppress experimental autoimmune encephalomyelitis. Proc Natl Acad Sci U S A 107(48):20768-73 doi:10.1073/pnas.1009201107

Rhile MJ, Nagarkatti M, Nagarkatti PS (1996) Role of Fas apoptosis and MHC genes in 2, 3, 7, 8-tetrachlorodibenzo-p-dioxin (TCDD)-induced immunotoxicity of T cells. Toxicology 110(1-3):153-167

Silkworth J, Antrim L (1985) Relationship between Ah receptor-mediated polychlorinated biphenyl (PCB)-induced humoral immunosuppression and thymic atrophy. Journal of Pharmacology and Experimental Therapeutics 235(3):606-611

Silkworth JB, Antrim L, Sack G (1986) Ah receptor mediated suppression of the antibody response in mice is primarily dependent on the Ah phenotype of lymphoid tissue. Toxicology and applied pharmacology 86(3):380-390

Silverstone AE, Frazier DE, Jr., Fiore NC, Soults JA, Gasiewicz TA (1994a) Dexamethasone, beta-estradiol, and 2,3,7,8-tetrachlorodibenzo-p-dioxin elicit thymic atrophy through different cellular targets. Toxicol Appl Pharmacol 126(2):248-59 doi:10.1006/taap.1994.1114

Silverstone AE, Frazier DE, Jr., Gasiewicz TA (1994b) Alternate immune system targets for TCDD: lymphocyte stem cells and extrathymic T-cell development. Exp Clin Immunogenet 11(2-3):94-101

Singh NP, Singh UP, Rouse M, et al. (2016) Dietary Indoles Suppress Delayed-Type Hypersensitivity by Inducing a Switch from Proinflammatory Th17 Cells to Anti-Inflammatory Regulatory T Cells through Regulation of MicroRNA. J Immunol 196(3):1108-22 doi:10.4049/jimmunol.1501727

Singh U, Abron J, Singh N, et al. (2014) An endogenous aryl hydrocarbon receptor (AhR) ligand, ITE induces regulatory T cells (Tregs) and ameliorates experimental colitis (IRC4P. 490). Am Assoc Immnol

Song J, Clagett-Dame M, Peterson RE, et al. (2002) A ligand for the aryl hydrocarbon receptor isolated from lung. Proceedings of the National Academy of Sciences 99(23):14694-14699
Staples JE, Murante FG, Fiore NC, Gasiewicz TA, Silverstone AE (1998) Thymic alterations induced by 2,3,7,8-tetrachlorodibenzo-p-dioxin are strictly dependent on aryl hydrocarbon receptor activation in hemopoietic cells. J Immunol 160(8):3844-54
Stockinger B (2009) Beyond toxicity: aryl hydrocarbon receptor-mediated functions in the immune system. J Biol 8(7):61 doi:10.1186/jbiol170
Temchura VV, Frericks M, Nacken W, Esser C (2005) Role of the aryl hydrocarbon receptor in thymocyte emigration in vivo. European journal of immunology 35(9):2738-2747
Van Loveren H, Schuurman H-J, Kampinga J, Vos JG (1991) Reversibility of thymic atrophy induced by 2, 3, 7, 8-tetrachlorodibenzo-p-dioxin (TCDD) and bis (tri-n-butyltin) oxide (TBTO). International journal of immunopharmacology 13(4):369-377
Vecchi A, Mantovani A, Sironi M, Luini W, Cairo M, Garattini S (1980) Effect of acute exposure to 2, 3, 7, 8-tetrachlorodibenzo-p-dioxin on humoral antibody production in mice. Chemico-biological interactions 30(3):337-342
Walisser JA, Glover E, Pande K, Liss AL, Bradfield CA (2005) Aryl hydrocarbon receptor-dependent liver development and hepatotoxicity are mediated by different cell types. Proceedings of the National Academy of Sciences of the United States of America 102(49):17858-17863
Wright EJ, De Castro KP, Joshi AD, Elferink CJ (2017) Canonical and non-canonical aryl hydrocarbon receptor signaling pathways. Current Opinion in Toxicology 2:87-92
Wu L, Shortman K (2005) Heterogeneity of thymic dendritic cells. Seminars in immunology 17(4):304-12 doi:10.1016/j.smim.2005.05.001
Yeste A, Nadeau M, Burns EJ, Weiner HL, Quintana FJ (2012) Nanoparticle-mediated codelivery of myelin antigen and a tolerogenic small molecule suppresses experimental autoimmune encephalomyelitis. Proc Natl Acad Sci U S A 109(28):11270-5 doi:10.1073/pnas.1120611109

Chapter 2 Supplemental Figures

Table 2. 1 ***Supplemental Mouse strains examined in this study***

Strain	**Common name**	**Stock #**	**Relevant Phenotype(s)**
C57BL/6J	C57BL/6	000664	Express the AhR^b allele and are sensitive to TCDD-induced toxicity at 10 μg/kg
B6.D2N-Ahrd/J	AhR^d	002921	Express the AhR^d allele and are sensitive to TCDD-induced toxicity at 100 μg/kg
B6Smn.C3-Faslgld/J	Gld	0010210	Unable to express functional Fas Ligand
B6.129P2-Lyz2tm1(cre)Ifo/J	$LyzM^{Cre}$	004781	Allow for targeted deletion of the AhR in cells of the myeloid lineage: monocytes, mature macrophages, and granulocytes
B6.Cg-Tg(Itgax-cre)1-1Reiz/J	$CD11c^{Cre}$	008068	Allow for targeted deletion of the AhR in cells of the dendritic lineage: conventional and plasmacytoid dendritic cells
B6(Cg)-Foxn1tm3(cre)Nrm/J	$Foxn1^{Cre}$	018448	Allow for targeted deletion of the AhR in thymic epithelial cells and keratinocytes.
B6.FVB-Tg(Rorc-cre)1Litt/J	$ROR\gamma t^{Cre}$	022791	Allow for targeted deletion of the AhR in DP thymocytes and their SP progeny.
Ahrtm3.1Bra/J	AhR^{flox}	006203	Use to generate cell/tissue-specific mutants of the aryl-hydrocarbon receptor (AhR)

Figure 2. 8 ***Supplemental Figure 1. AhR^d mice are unresponsive to TCDD-induced thymic atrophy at 10 μg/kg.***

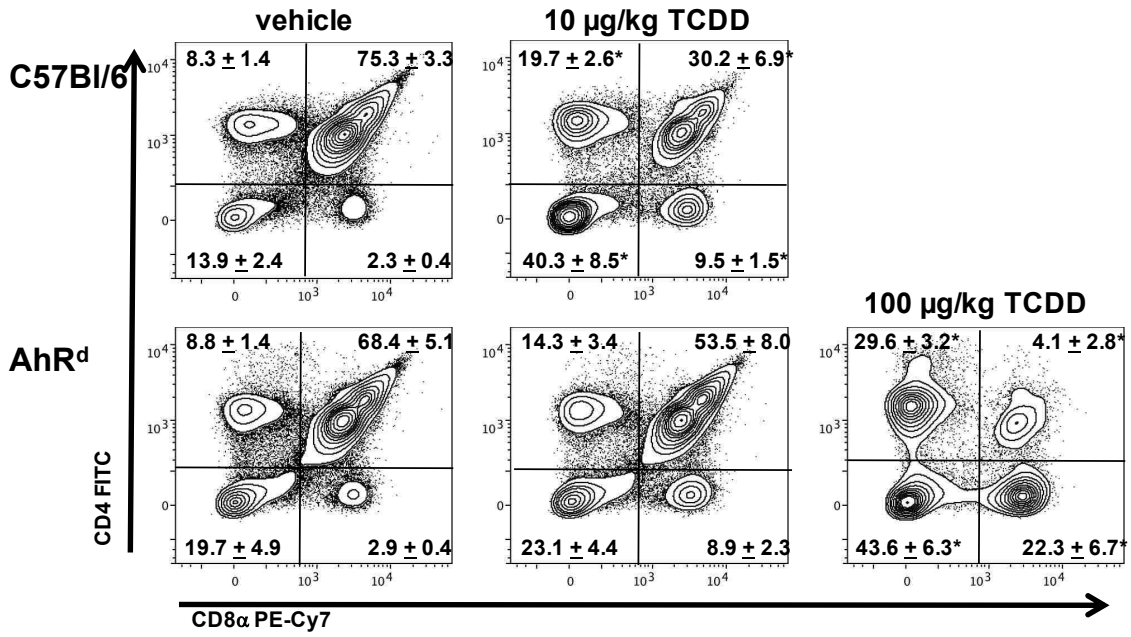

Supplemental Figure 1. AhR^d mice are unresponsive to TCDD-induced thymic atrophy at 10 μg/kg. Naïve wild-type mice (C57Bl/6) and mice expressing the low affinity receptor (AhR^d mice) were gavaged with vehicle (anisole/peanut oil) or TCDD (10 or 100 μg/kg). Three indicators of toxicity: body weight (data not shown), thymus weight (A), and thymus cell number (B) were measured on day 7 to evaluate toxicity and thymic atrophy after low dose (10 μg/kg) and high dose (100 μg/kg) of TCDD. Data represent one of two independent experiments, n=4-6 per treatment group, mean ± SEM; 2-way ANOVA, *$p < 0.05$ vehicle.

Figure 2. 9 ***Supplemental Figure 2. Comparison of CD4/CD8 thymocyte subsets from vehicle and TCDD-exposed mice.***

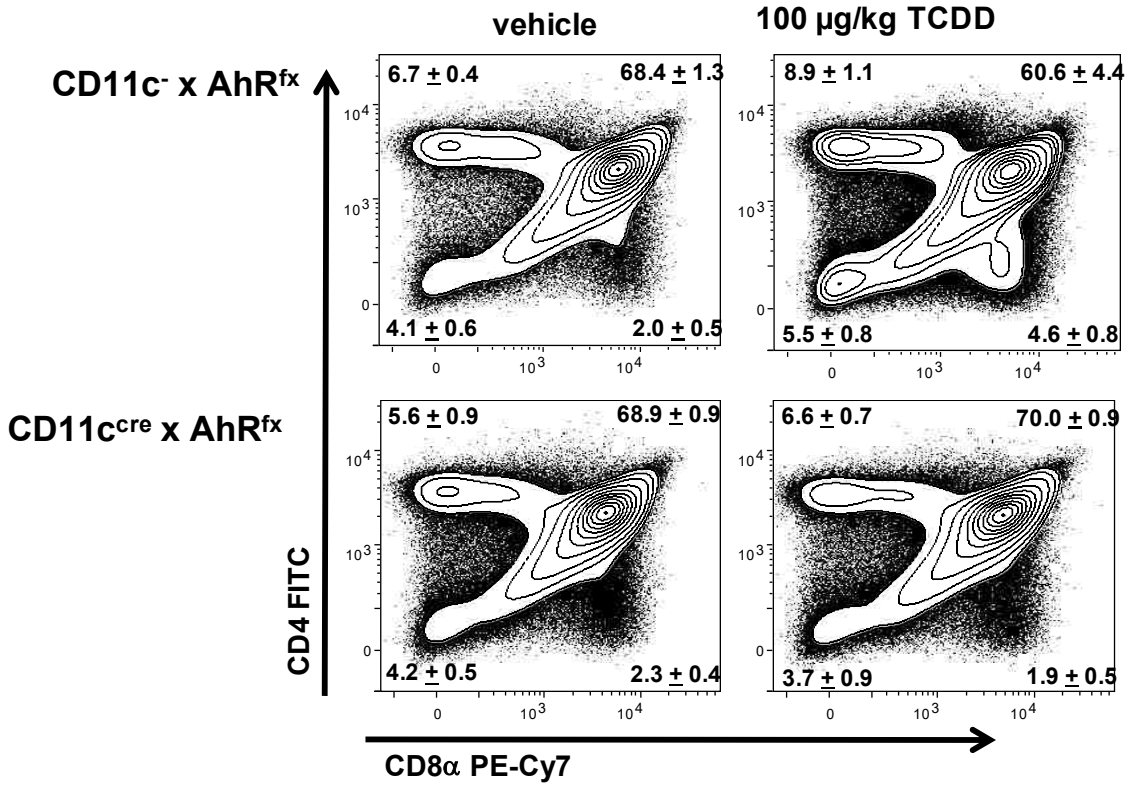

Supplemental Figure 2. Comparison of CD4/CD8 thymocyte subsets from vehicle and TCDD-exposed mice. C57Bl/6 and AhR^d mice were gavaged with vehicle (anisole/peanut oil) or TCDD (10 or 100 µg/kg). Representative contour plots gating on live thymocytes from wild-type C57Bl/6 mice revealed a significant decline in the frequency of CD4$^+$CD8$^+$ DP thymocytes, as well as a relative enrichment in the percent of CD4$^-$CD8$^-$ DN and CD4$^+$CD8$^-$ and CD4$^-$CD8$^+$ SP thymocytes in 10 µg/kg TCDD-treated mice compared to vehicle control on day 7. These shifts in CD4/CD8 thymocyte subsets were not observed in AhR^d mice treated with 10 µg/kg TCDD but were observed following administration of 100 µg/kg TCDD. The mean percentages of the CD4/CD8 thymocyte subsets ± SEM are indicated in the plots. Data represent one of two independent experiments, n=4-6 per treatment group; 2-way ANOVA, *$p < 0.05$ vehicle

CHAPTER 3: DEVELOPMENT OF PEGYLATED LIPOSOMAL NANOPARTICLES FOR THE DELIVERY OF THE AHR AGONIST, 2-(1′ H-INDOLO-3′ -CARBONYL)-THIAZOLE-4-CARBOXYLIC ACID METHYL ESTER (ITE), TO DENDRITIC CELLS.

Authors

Fanny Astruc-Diaz[*1], Joanna Kreitinger[*2], Shelby Cole[2], Philippe Diaz[1], Celine Beamer[1], Izola Ramalho[1], David Shepherd[1]

[*] Denotes First Authorship

Corresponding Author

David M Shepherd, Ph.D.

University of Montana

Department of Biomedical and Pharmaceutical Sciences

32 Campus Drive, Skaggs Building Room 284

Missoula, MT 59812

406-243-2224 (phone)

406-243-2807 (fax)

david.shepherd@umontana.edu

Keywords: ITE, AhR agonist, liposomal nanoparticle, dendritic cell, immunosuppression

Grant Funding: Research reported in this publication was supported by the National Institute of Environmental Health Sciences and the National Institute of General Medical Sciences of the National Institutes of Health under grant numbers R01-ES013784 (DMS), P30-GM103338, P20-GM103546. JMK was supported by The American Association of Immunologists through a Careers in Immunology Fellowship. The content is solely the responsibility of the authors and does not necessarily represent the official views of the National Institutes of Health.

Abstract

The AhR is a critical regulator of both innate and adaptive immune responses with potent immunomodulatory effects that make the AhR an attractive molecular target for novel therapeutics. Harnessing the immunosuppressive effects of AhR activation holds immense promise; however, the prototypical AhR ligand 2,3,78,8 tetracholoro-p-dioxin, is highly toxic and not compatible for use in humans. Natural AhR ligands offer a safer alternative to TCDD, but barriers exist due to their rapid degradation, poor solubility, and high-dosing schemes. Packaging AhR agonists in liposomal nanoparticles, a biodegradable and biocompatible drug delivery system, offers an intriguing solution. Here, the thin film hydration method was used to develop Cy5-labelled PEGylated liposomal nanoparticles (LNP) loaded with the natural AhR ligand, 2-(1′H-indole-3′-carbonyl)-thiazole-4-carboxylic acid methyl ester (ITE). ITE entrapment efficiency was >90%, and LNP demonstrated long-term chemical and physical stability. LNP enabled steady release of ITE under physiological parameters with minimal drug escape or burst effect being observed. Murine bone marrow derived dendritic cells (BMDCs) cultured with LNP exhibit >85% cellular interaction efficiency with LNPs as measured by fluorescent cytometry and laser scanning cytometry. LNP exposure does not reduce cell viability *in vitro*, and ITE-loaded LNP induce AhR responsive genes, including *CYP1a1*, *TGFβ3*, and *IDO1/2*. Furthermore, LNP administered intraperitoneally accumulated in the spleen with highest uptake occurring by splenic APCs. Collectively, these results demonstrate LNP delivery of AhR agonists as a promising mechanism for targeted, cell-specific AhR activation.

Introduction

The Aryl hydrocarbon Receptor (AhR) is a potent immune-modulator and promising target for the treatment of autoimmune diseases, allergies, and chronic inflammatory disorders (Kerkvliet et al. 2009; Quintana et al. 2010a; Zhang et al. 2010). AhR activation by the high affinity ligand, 2,3,7,8 tetrachlorodibenzo-p-dioxin (TCDD), results in pronounced immune suppression through the induction of suppressive immune cells including regulatory T cells (Tregs) and tolerogenic dendritic cells (DCs) (REF). However, TCDD is a highly toxic and persistent compound, which effectively eliminates its therapeutic use in humans (Needham et al. 1999). Numerous natural compounds generated endogenously and derived from plants, such as 2-(1*H*-Indol-3-ylcarbonyl)-4-thiazolecarboxylic acid methyl ester (ITE), indirubin-3'-oxime (IO), and indole-3-carbinol (I3C) can activate the AhR and can promote tolerogenic DCs and Tregs, providing favorable alternatives to TCDD for therapeutic AhR activation (Abron et al. 2018; Benson et al. 2012a; Benson and Shepherd 2011b; Boule et al. 2018a; Ehrlich et al. 2018; Singh et al. 2014). However, as AhR activation and natural agonists gain traction for pharmaceutical use, solutions are needed to overcome current barriers that reduce efficacy and practicality of natural ligands including poor solubility, rapid metabolism in vivo, and the requirement of frequent administration of high doses.

Numerous nanoparticle formulations are gaining traction as drug delivery systems. Liposomal nanoparticles (LNPs) are optimal biodegradable and biocompatible delivery systems to enhance therapeutic benefits, both *in vitro* and *in vivo*, and are considered to be the most successful drug-carrier system to date (Bozzuto and Molinari 2015; Kraft et al. 2014). LNPs have been shown to improve drug solubility and potency,

reduce off-target effects, protect drugs against metabolic degradation, and enable controlled drug release, which together, result in an increased therapeutic index (Akbarzadeh et al. 2013; Singh et al. 2014). Therefore, development of an ITE-loaded LNP could mitigate current obstacles associated with natural AhR agonist-based therapies and enable sustained, concentrated drug delivery to target tissues, while reducing adverse outcomes of systemic exposure and off-target effects.

Within the immune system, AhR expression varies significantly by cell type, maturation state, and activation status (Kreitinger et al. 2016). It is well documented that the effects of AhR activation during an immune response vary based on the target cell (Esser and Rannug 2015; Kreitinger et al. 2016; Stockinger et al. 2014) and that AhR activation can result in drastically different outcomes, from increasing inflammatory responses to promoting immune regulation or tolerance (Lee et al. 2015b). DCs, professional antigen-presenting cells that bridge the innate and adaptive immune system, constitutively express AhR at high levels and are keenly sensitive to AhR activation by multiple ligands (Bankoti et al. 2010a; Bankoti et al. 2010b; Kreitinger et al. 2016). AhR activation within DCs has been shown to induce a potent regulatory phenotype that promotes peripheral immune tolerance via induction of indoleamine-2,3-dioxygenase (IDO) and transforming growth factor beta (TGFβ) isoforms, and generation of Tregs (Mezrich et al. 2010; Nguyen and Bradfield 2007; Simones and Shepherd 2011; Vogel et al. 2008). Together, DCs are an attractive focus for delivery of concentrated AhR agonists (Quintana et al. 2010c; Simones and Shepherd 2011).

In the present study, we aimed to develop fluorescently labeled, PEGylated ITE-loaded LNPs using the thin film hydration method for delivery to dendritic cells. LNPs

were characterized for average particle size, long-term physical and chemical stability, and ITE entrapment efficiency. LNP uptake and drug delivery were evaluated *in vitro* through cultures with bone marrow derived dendritic cells (BMDCs), and *in vivo* biodistribution was assessed within lymphoid tissues following intraperitoneal administration. Together, the results from this study support PEGylated LNPs as an effective ITE delivery system.

Materials and Methods

Chemicals

1,2-dipalmitoyl-sn-glycero-3-phosphoethanolamine (DPPE), 1,2-distearoyl-sn-glycero-3-phosphocholine (DSPC), and 1,2-distearoyl-sn-glycero-3-phosphoethanolamine-N-[methoxy(polyethylene glycol)-2000] (ammonium salt) (DSPE-mPEG2000) were purchased from Avanti Polar Lipids, Inc (Alabaster, AL, USA). Cyanine5 NHS ester (Cy5) was obtained from Lumiprobe Corp., Hallandale Beach, FL, USA). Cholesterol, chloroform ($CHCl_3$), methanol (MeOH), triethylamine HPLC grade, and ethyl ether anhydrous ACS grade were purchased from Fisher scientific (Pittsburgh, PA, USA). 0.1M Phosphate Buffered Saline (PBS) pH 7.4, was purchased from EMD Millipore (Billerica, MA, USA). 2-(1H-Indol-3-ylcarbonyl)-4-thiazolecarboxylic acid methyl ester (ITE) was purchased from Tocris (St Louis, MO, USA). Thin-layer chromatographic analyses were performed on Sigma-Aldrich 60 F254 thin-layer chromatographic plates. Column chromatography was performed with silica gel 230-400 mesh. ^{1}H NMR spectra were recorded on a Bruker Avance III^{TM} spectrometer at 400MHz and are reported in parts per million (ppm) on the δ scale relative to tetramethylsilane as

an internal standard. ^{13}C NMR spectra were recorded at 100 or 125 MHz and are reported in parts per million (ppm) on the δ scale relative to $CDCl_3$.Signals were abbreviated as follows: s = singlet, br s = broad singlet, d = doublet, t = triplet, q =quadruplet, m = multiplet. Coupling constants (J) are expressed in hertz. All solvents and chemicals used were reagent or analytical grade when not specified, and used as received.

Procedure for the Preparation of Cy5-labelled DPPE

A previously published procedure was adapted to synthesize Cy5-NHS (Mizrahy et al. 2014). Cy5-NHS (12 mg, 0.019 mmol) was dissolved in 2 ml of DMF and 1 ml of $CHCl_3$. Then, 1,2-dipalmitoyl-sn-glycero-3-phosphoethanolamine (DPPE) (13.2 mg, 0.019 mmol) was added followed by the addition of Et_3N (2.6 μL, 0.019 mmol) (Figure 1). The reaction mixture was heated to 70°C and stirred overnight. Upon completion, the solvent was removed under reduced pressure and the crude product was purified by column chromatography (length 15.5 cm; diameter 15 cm) on silica gel (gradient 100, 5:95, 10:90, 15:85 MeOH:DCM) to afford the Cy5–DPPE conjugate as a blue solid. Mass spectrometry spectra were obtained on a Waters/Micromass LCT-TOF instrument in methanol: $M + H)^+$ 1156, purity>95%. ^1H NMR (400 MHz, $CDCl_3/CD_3OD$: 2/1) δ 8.13 (s, 1H), 8.06 – 7.86 (m, 1H), 7.43 (d, J = 7.2 Hz, 1H), 7.35 – 7.13 (m, 3H), 6.64 (t, J =12.5 Hz, 1H), 6.23 (dd, J = 18.4, 13.8 Hz, 2H), 5.37 (s, 1H), 5.24 (s, 1H), 4.43 (d, J = 11.9 Hz, 1H), 4.20 (dd, J = 12.0, 6.7 Hz, 1H), 4.14 – 3.90 (m, 8H), 3.62 (s, 3H), 3.44 (s, 4H), 2.42 – 2.23 (m, 4H), 1.83 (d, J = 6.8 Hz, 2H), 1.74 (s, 8H), 1.52 (d, J = 7.3 Hz, 2H), 1.26 (s,48H), 0.88 (t, J = 6.1 Hz, 6H). Rf of Cy5-DPPE: 0.6 in 10/90 methanol:dichloromethane.

Figure 3. 1 Preparation of Cy5-labelled DPPE

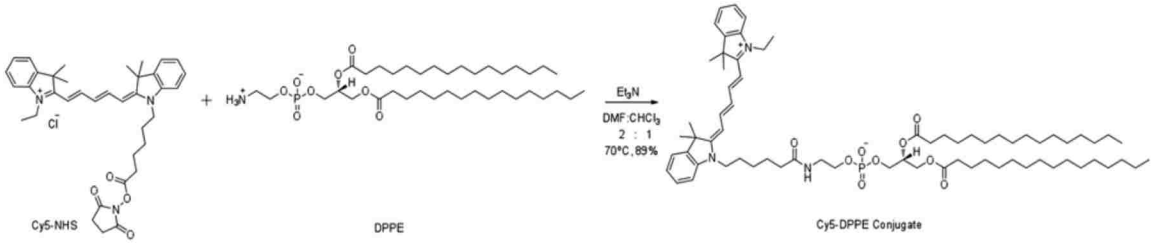

Figure 3.1 Preparation of Cy5-labelled DPPE
Schematic of fluorescent molecule, Cy5-NHS, added to 1,2-dipalmitoyl-sn-glycero-3-phosphoethanolamine (DPPE) for incorporation into, and tracking of, liposomal nanoparticles.

Preparation of Liposomal nanoparticles (LNPs) by lipid film hydration

The lipid mixture (0.85 mM) composed of DSPC: cholesterol: DSPE-mPEG2000: Cy5-DPPE at a molar ratio of 59:34:5:2 was dissolved in a chloroform:methanol mixture (2:1, vol/vol) in a round bottom flask. 1 μM ITE stock solution in DMSO was added to the lipid mixture and the resulting solution was dried to a thin and transparent film using a rotary evaporator (Buchi Rotavapor R-215, Switzerland) under reduced pressure (Bangham et al. 1974). Multilamellar vesicles (MLVs) were obtained by hydration of the film with PBS (pH 7.4). After five cycles of freezing and thawing, the liposome diameter was reduced by ultrasonication with a probe sonicator (MISONIX Microson™r XL2000, Farmingdale, NY, USA) and samples filtered through PFTE syringe filter, 0.2 μm, to remove the titanium fragments. ITE-loaded liposomal nanoparticles (ITE-LNPs), non-fluorescent and fluorescent empty liposomal nanoparticles were prepared following the steps described above. All the LNPs were stored at 4°C prior to analysis and experiments.

MLVs lyophilization and rehydration

The MLVs were prepared as above. Polysorbate 20 (5% of total lipids weight) or trehalose (4:1 lipids ratio) was added to the MLVs suspension and stirred at 65°C immediately after the freezing and thawing cycles. The MLVs suspension was frozen at -80°C and then lyophilized using a Labconco Dry Ice Benchtop Freeze Drying System (Kansas City, MO, USA). The resulting powder was stored at 4°C and rehydrated at different time points with PBS (pH 7.4) to its original volume. The liposome diameter was reduced by ultrasonication with a probe sonicator (MISONIX Microson™r XL2000, Farmingdale, NY, USA) and filtered through PFTE syringe filter, 0.2 μm, to remove the titanium fragment. The SUVs were stored at 4°C prior to analysis.

Morphological studies

Transmission electron microscopy (TEM) and scanning electron microscopy (SEM) were used to characterize the surface and structure of ITE-loaded LNP samples, respectively. Samples prepared for TEM were placed on single slot formvar-coated 400 mesh copper grids. Excess sample was blotted off with filter paper, and the grid was then stained with 1% phosphotungstic acid solution for 1 minute. Stain was blotted dry from the grids with filter paper and air-dried. Samples were imaged with a Hitachi H-7100 TEM (Hitachi, Tarrytown, NY, USA) at 75kV. ITE-loaded LNP samples prepared for SEM were placed on a 0.1 um pore PVDF filter and allowed to air dry. Dried LNP samples were placed on a non-conductive carbon adhesive tape applied on aluminum stub and coated with gold using a Denton Desk V sputter coater (Denton Vacuum LLV, Moorestown, NJ). Samples were imaged using a Hitachi S-4700 Field Emission scanning electron microscope

Size distribution and surface potential measurements

Mean diameter, size- distribution, polydispersity index (PDI) and zeta potential of the LNPs were determined at 25°C by dynamic light scattering (DLS) using a Zetasizer nano ZS (Malvern Intruments Ltd, Malvern, UK). Samples were analyzed 24H after preparation and three measurements were taken on each sample.

Determination of ITE entrapment efficiency

The entrapment efficiency for ITE was determined using a Waters HPLC Alliance system on an e2695 separations module with a Waters 2998 photo-diode array (PDA) detector (Milford, MA, USA). Samples were injected using a Waters auto injector and the instrument was controlled by use of MassLynx™ software (Milford, MA, USA). Components were separated on a Waters Phenomenex ™ C18 reversed-phase column (Milford, MA, USA) with 50 x 4.6 mm dimensions and 3 μm particle size. The column was kept thermostatic at 30°C in a Waters column oven (Milford, MA, USA). HPLC baseline resolution was obtained by employing a gradient elution at a flow rate of 0.3 ml/min with a gradient mobile phase composed of methanol (0.1% formic acid) (B) and water (0.1% formic acid)(A) ramped over a 12 minute period using the following conditions: and monitored at 360 nm as follows: The binary linear gradient began from a mixture of 10% A and 90% B and ended at 2% A and 98% B at 6.60min. After the 1.40 min. plateau at 2% A and 98% B, the mobile phase composition changed back to its initial composition starting at 8 min. in 4 min. The ITE entrapment efficiency in LNPs was expressed as entrapment percentage (EE%) and calculated through the following relationship: EE% = $(C_{total} - C_{free})/ C_{total}] X 100$. The free drug ($C_{free}$) was separated by

pressure ultrafiltration method using an Amicon 8010 (Millipore Corporation, bedford, USA) at 50psi and determined by the LC/MS method described above. The total content of ITE (C_{total})in the suspensions was determined after the ITE-loaded LNPs suspensions were frozen at -80°C and then lyophilized using a Labconco Dry Ice Benchtop Freeze Drying System (Kansas City, MO, USA). The ITE-loaded LNP powders were then diluted with methanol to disrupt the LNPs, release the entrapped drug into the solvent and to afford the LC/MS injectate solution. Peaks of products were monitored using the LC/MS method described above. The concentrations of ITE were determined using a calibration curve of the pure drugs in methanol solutions at the wavelength where it showed maximum absorbance (360 nm). The area under the curve was converted into percentage using a standard curve, and experiments were performed in triplicate in order to ensure accuracy.

Stability study of ITE-loaded LNPs

The stability of the ITE-loaded LNPs in suspension and lyophilized form was evaluated initially and after storage at +4°C for three months. The particle size distribution, the polydispersity index and the total drug content of the samples were determined as a function of the storage time.

In vitro release kinetics

ITE release from LNPs was studied using a dialysis method. Dialysis cassettes (Slide-A-Lyzer Dialysis Cassettes 10K MWCO, Thermo Fisher Scientific, Waltham, MA, USA) were immersed before use in ultrapure water overnight at 4°C to remove the preservative, followed by rinsing in PBS (pH 7.4) solution. 1 mL of ITE-loaded LNPs suspension (0.3µg ITE) was injected into the dialysis cassette and dialyzed at 37°C

against 100 mL of PBS (pH 7.4). The sink conditions may permit the free ITE released from the LNPs to migrate through the dialysis membrane without precipitating as the solubility of ITE has been calculated to be 0.05mg/mL (ChemAxon Aqueous Solubility Predictor - Version 16.3.14.0) in PBS (pH 7.4). At various time points (0-120H), 20 mL aliquots of the release buffer were withdrawn for analysis and replaced by 20 mL of fresh release medium. The samples were lyophilized and stored at 4°C until analysis. The amount of drug released was quantified using the LC/MS method described above. Drug release profile from LNPs was expressed as release percentage (RP%) and calculated through the following relationship: %RP= [$C_{releasel}$ / C_{total}] X 100. Where $C_{release}$ is the amount of ITE released at a specific time and C_{total} is the total amount of ITE in LNPs.

Thermal analysis

DSC analysis of the lyophilized empty and ITE-loaded LNPs was performed using a TA instruments Q10 model (TA Instruments, New Castle, DE, USA). Calibration of the instrument was done using Indium for the best heat capacity at constant pressure (Cp) estimate and high signal-to-noise ratio. Two mg of lyophilized LNPs samples were loaded in hermetically sealed aluminum pans along with the standard reference aluminum in the differential scanning calorimeter. The DSC was recorded between 10°C and 90°C at a scan rate of 1°C/min for three cycles and the last reproducible heating cycle was considered for analysis.

Mice

C57Bl/6 mice were originally obtained from The Jackson Laboratories (Bar Harbor, ME) and were bred and maintained in the animal research facilities at the

University of Montana. Mice were housed under specific pathogen-free conditions and maintained on 12 h dark/light cycles. Standard laboratory food and water were provided ad libitum. All protocols for the use of animals were approved by the University of Montana Institutional Animal Care and Use Committee and adhered to the current National Institutes of Health (NIH) guidelines for animal usage.

Bone Marrow Derived Dendritic Cell (BMDC) Cultures

Cellular uptake assays were performed using Bone Marrow Derived Dendritic Cells (BMDCs). BMDCs were generated from 7-day cultures of bone marrow-derived progenitor cells from femurs and tibias of C57Bl/6 mice (Bankoti et al., 2010). Briefly, hematopoietic progenitor cells were collected by flushing murine femurs and tibias with complete RMPI media (cRPMI) (Gibco, Grand Island, NY) supplemented with 10% fetal bovine serum (Atlanta Biologicals, Atlanta, GA), 50μM 2-mercaptoethanol, 20mM 4-(2-hydroxyethyl)-1-piperazineethanesulfonic acid, 10mM sodium pyruvate, and 50 μg/ml gentamicin (Gibco, Grand Island, NY) (Corning, Manassas, VA). Red blood cells were removed through density gradient centrifugation using Lympholyte-M reagent (Cedarlane Laboratories Limited, Ontario, Canada). Isolated hematopoietic precursors were then cultured at a density of $1x10^6$ cells/ml in T75 tissue culture flasks for 7 days at 37°C and 5% CO_2 in the presence of 30 ng/ml murine granulocyte macrophage-colony stimulating factor (GM-CSF) (PeproTech, Rocky Hill, NJ). cRPMI and GM-CSF growth factor were refreshed on days 3 and 5. On day 7, nonadherent cells were harvested and BMDC purity was verified via fluorescence cytometry. BMDCs were then re-cultured in 6-well plates with LNPs at 10^{-1},10^{-2},10^{-3} to yield ITE-loaded LNP concentrations [100nM, 10nM, 1nM

respectively] for 24-96 hours or with 10nM 2,3,7,8, tetrachlorodibenzo-p-dioxin (dioxin, TCDD) in DMSO (Cambridge, MA).

Dye exclusion viability assays

To assess effects of LNP uptake on cell viability, cultured cells were treated with optimum titrations of propidium iodide (PI) nucleic acid stain (Sigma-Aldrich) as a membrane exclusion assay via fluorescence cytometry. As a control for dead or dying cells, $1x10^6$ BMDCs were incubated at 55°C for >10-minutes and then stained with PI as described above.

In vivo LNP exposure

Naïve, adult (8-14 week-old) C57Bl/6 mice received 10uL LNP/gram body weight or PBS control via intraperitoneal injection (i.p.) daily for three consecutive days. Mice were weighed daily and tissues were collected 24 hours after the last injection. Following CO_2 euthanasia, blood was collected through cardiac puncture in EDTA (0.5 M) coated syringes. Tissues were collected and processed through 70μM cell strainers in cRPMI and maintained on ice prior to downstream assays.

Fluorescence cytometry

Fluorescence cytometry to assess cellular uptake of Cy5-labeled LNPs was performed using a FACS Aria II flow cytometer (v 6.1.2, Becton Dickinson, Franklin Lakes, NJ) or Attune NxT Acoustic Focusing Flow Cytometer (Thermo Fisher Scientific, Waltham, MA). Cells were harvested and washed with PAB (1% bovine serum albumin and 0.1% sodium azide in PBS), followed by a 10-minute incubation with anti-

CD16/CD32 Fc Block (BioLegend, San Diego, CA) to eliminate non-specific staining (Shepherd et al., 2001). Antibodies used in these experiments included CD11c-PE (HL3 and N418), F4/80-BV421 (BM8), CD11b-PE-Dazzle594 (M1/70), CD3-Percp/Cy5.5 (145-2C11), CD19-FITC (MB19-1), MHCII-FITC (M5/114.15.2), and CD86-BV510 (GL-1), and were obtained from Biolegend (San Diego, CA), Tonbo (San Diego, CA), and BD Biosciences (San Jose, CA). All staining was performed at optimized titrations for 20 minutes, on ice, and protected from light. To control for spectral spreading and autofluorescence by the LNPs, control samples were treated with empty liposomes lacking Cy5. Fluorescence Minus One (FMO) controls were used for gating controls. BDCompBeads (BD Biosciences, San Jose, CA) compensation beads were used for compensation controls.

Fluorescence microscopy

Laser scanning cytometry (LSC/iCys, CompuCyte, Cambridge, MA) was used to corroborate cellular interaction with Cy5+ LNPs. Cells were adhered to glass slides using the Cytospin 3 (Thermo Fisher Scientific, Waltham, MA) at a concentration of $1x10^5$ cells/slide. Cells were stained with diamidino-2-phenylindole (DAPI) nuclear stain (Thermo Fisher Scientific, Waltham, MA) and treated with Prolong Gold Antifade Mountant (Thermo Fisher Scientific, Waltham, MA) prior to cover slide placement. iCys CompuCyte software (Cambridge, MA) was used for obtaining images and calculating fluorescence intensity of samples. Cells exposed to unlabeled (Cy5-), empty LNPs were used as controls for autofluorescence.

RNA isolation and RT-qPCR

Total RNA was extracted from 5 x 10^6 BMDCs using a RNeasy mini kit (Qiagen, Germantown, MD) according to the manufacturer protocols. Two-step RT-qPCR was performed by synthesizing cDNA using iScript Reverse Transcription Supermix (BioRad, Hercules, CA) followed by RT-qPCR relative quantification of 50 ng cDNA per reaction using CFX Connect, SSO Advanced Universal SYBR Green Master Mix, and PrimePCR validated primers for murine CYP1A1, IDO1, IDO2, TGFB3 (BioRad, Hercules, CA). The data were normalized to the reference genes, GAPDH and HPRT, and displayed relative to control.

Statistical analyses

Data sets with multiple comparisons were evaluated by one-way analysis of variance (ANOVA) followed by post-hoc analysis using student's t-test. Values of $p<0.05$ were considered significant.

Results

LNPs are optimally sized, demonstrate high ITE entrapment efficiency, and maintain long-term stability.

Nanocarrier size has been established as a crucial determinant for optimal cellular delivery and should not exceed 500 nm (Olsen et al. 2011). Studies by Foged et al. demonstrated that limiting NP size to 100 nm resulted in twice the cellular uptake compared to larger NP (Foged et al. 2004); however, further reduction in size to 40nm did not increase cellular uptake. Particle size analysis established that the average size of

both freshly prepared and lyophilized PEGylated ITE-loaded LNPs was within the optimal range, ~100 nm, with a unimodal size distribution, and a low polydispersity index ≤0.2 (Figure 3.2a). The addition of Polysorbate 20 enabled median particle size of lyophilized LNP to be comparable to fresh LNP through a shortened rehydration step (< 5min). To evaluate LNP morphology, SEM and TEM of ITE-loaded LNP were performed. As modeled in Figure 3.2b, the ITE-loaded LNP should be composed of two lipid layers with an aqueous core. Representative SEM and TEM images, shown in Figure 3.2c and 3.2d, confirmed that ITE-loaded LNPs were spherical in shape, maintained an aqueous core, and were in the same nanosize range as observed from DLS measurements.

Previous studies have shown that high encapsulation efficiency of lipophilic drugs and almost no drug loss can be achieved using the lipid film hydration method (Çağdaş et al. 2014; Jesorka and Orwar 2008) ITE entrapment efficiency was greater than 70% for freshly prepared and lyophilized PEGylated LNPs at both 1nM (data not shown) and 1μM ITE loading (Figure 3.3a). Compared to lyophilized LNPs, dramatically higher entrapment efficiency was observed for the non-lyophilized LNPs, 72% and 94% respectively. As expected, a reciprocal relationship occurred between LNP ITE loading and free ITE concentrations with a higher level of free ITE detected in lyophilized LNP

Figure 3. 2 Morphology and Characterization of ITE-loaded LNPs.

A.

1μM ITE-loaded PEGylated LNPs	Hydrodynamic diameter (nm)	Polydispersity	z –Potential (mV)
Freshly prepared	104.7 ± 0.67	0.21 ± 0.02	-3.9 ± 0.1
Lyophilized	108.6 ± 1.11	0.15 ± 0.01	---

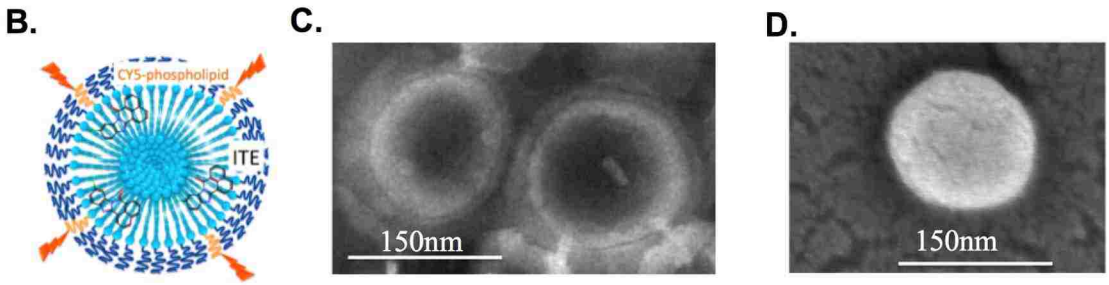

Figure 3.2 Morphology and Characterization of ITE-loaded LNPs.
Freshly prepared and lyophilized 1μM ITE-loaded PEGylated LNP were evaluated for hydrodynamic diameter (nm), polydispersity, and z-Potential (mV) (A). LNP morphology diagram depicting round morphology and ITE interaction with the lipid bilayer (B). Representative images of morphology studies of ITE-loaded LNP through Transmission Electron Microscopy micrograph (magnification X150000) (C) and Scanning Electron Microscopy micrograph (magnification X150000) (D).

(15.7%±2.1) compared to fresh LNP (2.2%±1.2); however, minimal ITE remained free in either preparation. Together, these results confirm that freshly formulated and lyophilized LNPs can be efficiently loaded with ITE and adopt an optimal size and morphology for cellular uptake.

The effects of storage conditions on LNPs were evaluated because chemical and physical stability over longer time periods is desirable for pharmaceutical applications. Following synthesis, ITE-loaded LNPs were stored at 4°C for three months to assess long-term chemical stability. As shown in Figure 3.3b, at 15 days and two months post-synthesis, there was no significant decrease in total drug loading in either fresh or lyophilized LNP; however by three months a slight, statistically significant, decrease in drug loading was observed in the lyophilized LNP (79%) compared to fresh LNP (85%). Despite the slight decrease observed in total drug loading by month three, no degradation product was identified, and stored LNPs elicited the same level of gene expression (CYP1A1) as fresh LNP when tested in vitro (data not shown). Additionally, LNPs showed high physical stability over three months whether stored at 4°C as an aqueous colloidal suspension or rehydrated in PBS (pH 7.4) from the lyophilized cake. As shown in Figure 3.3c, long-term storage did not significantly alter polydispersity of fresh LNP (0.22 ± 0.02) or lyophilized LNP (0.15 ± 0.01) and mean diameters were equally maintained in both fresh LNP (115.7nm ± 1.9) and lyophilized LNP (97.9nm ± 0.3). Thus, both freshly prepared and lyophilized LNP demonstrate physical and chemical stability over three months at 4°C.

Figure 3. 3 Chemical and physical stability of ITE-loaded LNP

A.

1μM ITE-loaded PEGylated LNPs	Total ITE content (%)	Free ITE content (%)	ITE Entrapment Efficiency (%)
Freshly prepared	96.1 ± 1.4	2.2 ± 1.2	93.9 ± 0.3
Lyophilized	87.9 ± 0.4*	15.7 ± 2.1*	72.2 ± 1.7*

B.

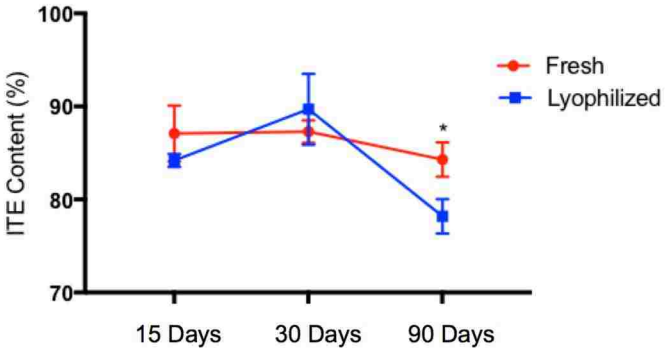

C.

1μM ITE-loaded PEGylated LNPs	3 months	
	Hydrodynamic diameter (nm)	Polydispersity
Freshly prepared	115.7 ± 1.9	0.22 ± 0.02
Lyophilized	97.9 ± 0.3	0.15 ± 0.004

Figure 3.3 Chemical and physical stability of ITE-loaded LNP

Total ITE content and free ITE of LNP was determined using HPLC and calculated as EE% = (C_{total} – C_{free})/ C_{total}] X 100 (A). Long term ITE entrapment was evaluated in LNP stored at 4°C for 15 days, 30 days, and 90 days prior to HPLC analysis (n=3) (B). Physical stability of LNP was assessed for both fresh and lyophilized LNP at 90 days (C).

ITE interacts with lipid bilayers of the LNP following drug loading and is released within 24-hours in vitro

ITE is a highly lipophilic compound due to its planar, aromatic structure, and LNPs were observed to contain an aqueous core, together suggesting ITE containment is occurring by the LNP lipid bilayer. To confirm this, differential scanning calorimetry (DSC) thermograms of empty and ITE-loaded LNPs were performed. As shown in Figure 3.4, endothermic peaks of the phase transitions from a gel phase to a liquid crystalline (T_m) phase were observed for both empty and ITE-loaded LNPs. The empty LNP thermogram showed a broad endotherm at 34.09°C corresponding to lipid bilayer components. The melting endotherm of the lipid bilayer components was found to be shifted to 43.32°C, suggesting interaction of ITE with lipid bilayers (Hathout et al. 2007) and successful drug encapsulation. In addition, enthalpy changes (δH_{cal}) reflect the differences in the packing properties of the acyl chains(Sade et al. 2010; Serro et al. 2014). As seen in Figure 3.4., δH_{cal} increased from 0.06 J/g for the empty LNPs to 0.19 J/g for the ITE-loaded LNPs, which may indicate a more densly packed LNP membrane following ITE loading.(Maswadeh et al. 2002; Sade et al. 2010).

Figure 3. 4 Differential scanning calorimetry (DSC) thermograms of empty and ITE-loaded LNPs

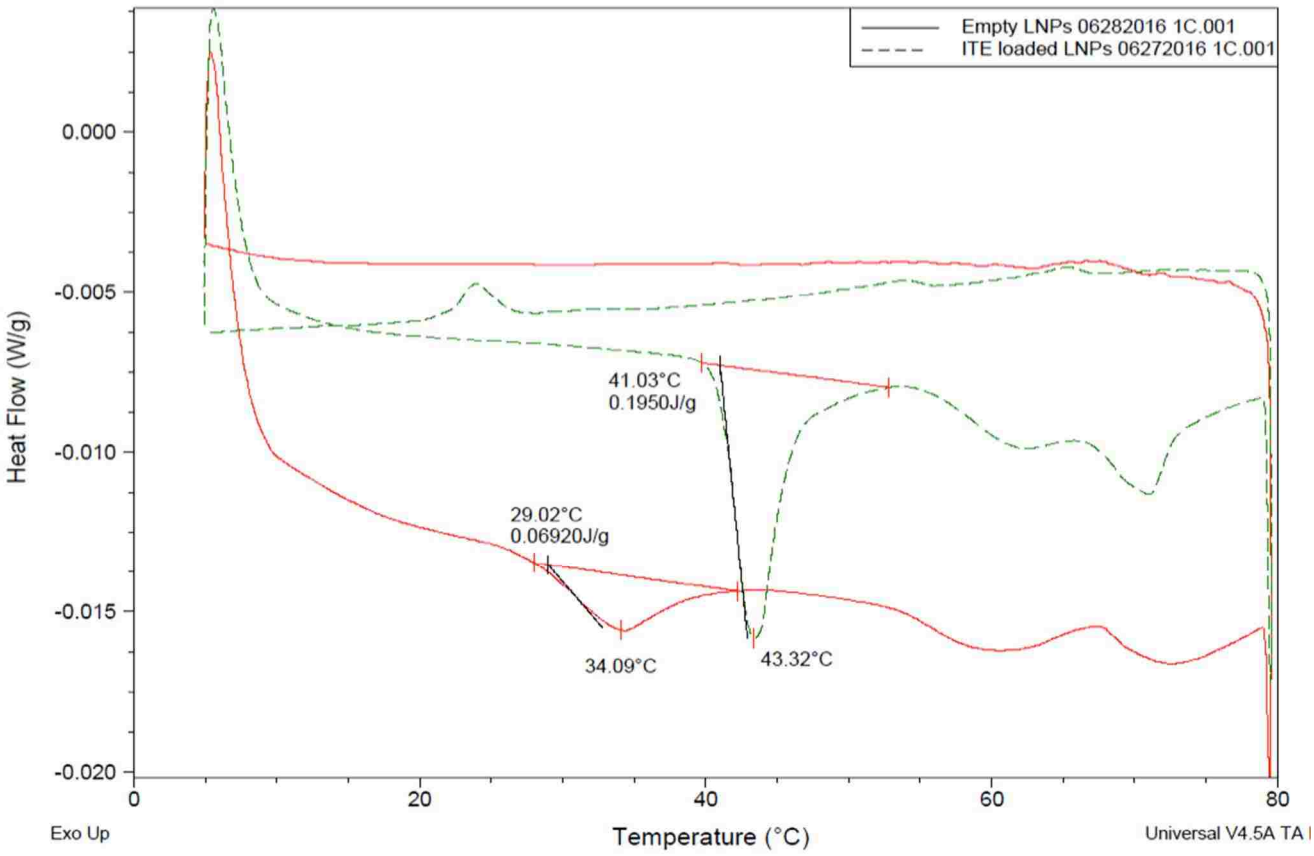

Figure 3.4 Differential scanning calorimetry (DSC) thermograms of empty and ITE-loaded LNPs. The DSC was recorded between 10°C and 90°C at a scan rate of 1°C/min for three cycles and the last reproducible heating cycle was considered for analysis. Endorthermic peaks of empty LNP (solid) and ITE-loaded LNP (dashed) are shown.

Previous studies have shown that uptake of nanoparticles in the size range of 100-200 nm by dendritic cells can occur at a relatively fast rate, within 1 to 2 hours of *in vitro* exposure at 37°C (Kochiadakis et al. 2001; Tacken et al. 2011; Tran et al. 2018). To evaluate the rapidity of ITE release from LNPs *in vitro*, LNPs were incubated at 37°C against 100-fold excess PBS (pH 7.4) under dialysis conditions for 120 hours (5 days) and the cumulative percentage of ITE release was plotted versus time (Figure 3.5). A sustained-release effect was observed for ITE as only 14% of the drug was released from the LNPs in the first thirty minutes. The drug release profile fit a first kinetic order release phase in the first 4 hours and then approached a plateau at 24 hours. Approximately 50% of the total ITE dose was released within two hours *in vitro* and 90% release observed by 24 hours. The plateau value represented ~95% release of total incorporated drug and only ~3 % of the drug was still associated with the LNPs by day 5. Thus, LNPs release ITE rapidly and completely *in vitro*.

Figure 3. 5 *In vitro* ITE release curve from ITE-loaded LNPs under physiological conditions.

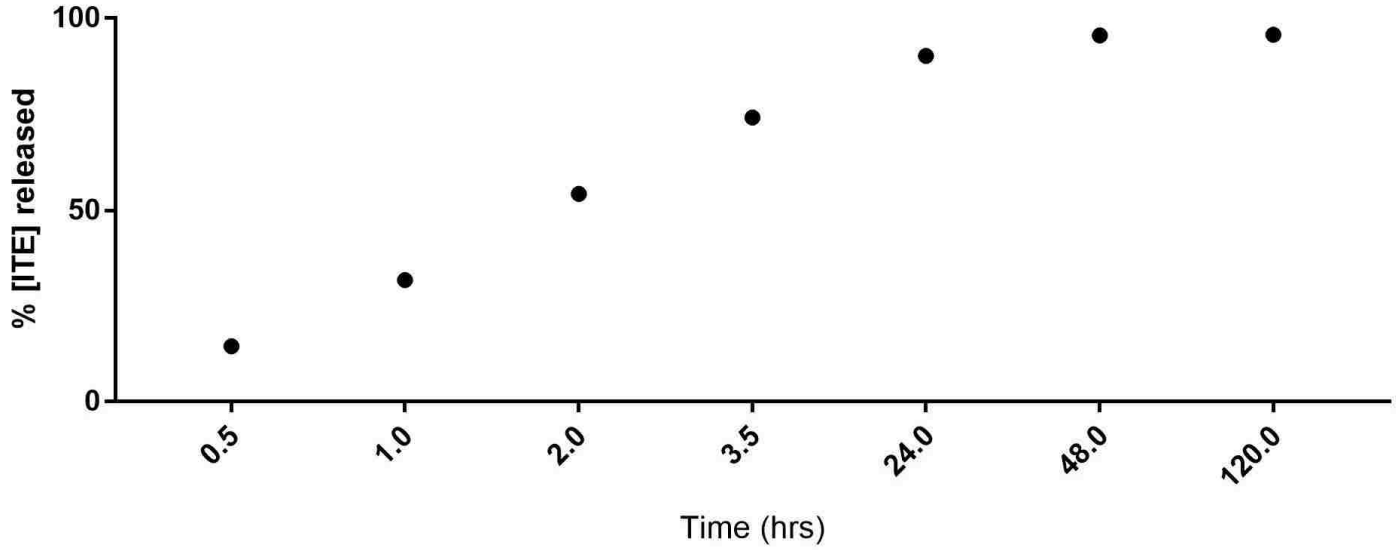

Figure 3.5 *In vitro* ITE release curve from ITE-loaded LNPs under physiological condition
Dialysis of LNP at pH7.4 and 37°C to represent physiological conditions. Cumulative ITE drug release was quantified by LC/MS over 100 hours where %= [$C_{releasel}$ / C_{total}] X 100.

Drug-loaded LNPs demonstrate increased uptake by BMDCs without affecting cell viability.

Liposomal formulations are highly promising therapeutic delivery systems as studies have demonstrated that LNPs are both biodegradable and biocompatible. To test potential cytotoxicity of LNPs on target cells, murine BMDCs were generated and exposed to three doses of empty LNP (ten-fold serial dilution of LNP:media 10^{-1},10^{-2},10^{-3}) for 24 or 96 hours. BMDC LNP uptake efficiency was evaluated for dose and time-dependent effects by measuring Cy5+ CD11c+ BMDCs via fluorescent cytometry. As shown in Figure 3.6a, dose-dependent effects were observed at both time points as BMDCs exposed to 10^{-1} LNP exhibited the highest frequency of Cy5+ (24H-85.2%±0.78) compared to 10^{-2} LNP (24H-73%± 1.0) and 10^{-3} LNP (24H-44%±1.3). LNP uptake occurred most rapidly and completely at high LNP concentrations with greater time required for LNP uptake at lower concentrations. BMDCs were then stained with propidium iodide (PI), a DNA intercalating agent that is unable to permeate healthy cell membranes, for analysis of cell viability by fluorescence cytometry. As shown in Figure 3.6b, compared to untreated cells, LNP exposure did not reduce BMDC viability at any concentration following either 24-hour exposure (~86% viable) or 96-hour exposure (~75% viable). Thus, LNPs interact with BMDCs rapidly and do not reduce cell viability.

Figure 3. 6 LNP interaction is dose and time dependent and does not reduce BMDC viability.

A.

LNP dose & Exposure duration	LNP+ BMDC Interaction Efficiency %±SD (n=3)
24hr LNP 10^{-1}	85.2%±0.78
24hr LNP 10^{-2}	73%± 1.0*
24hr LNP 10^{-3}	44%±1.3*
96hr LNP 10^{-1}	93.3% ±1.0#
96hr LNP 10^{-2}	81.9% ±1.0*#
96hr LNP 10^{-3}	63.17% ±1.8*#

B.

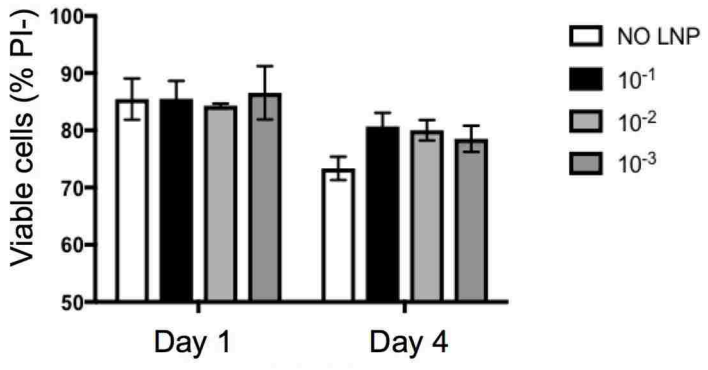

Figure 3.6 LNP interaction is dose and time dependent and does not reduce BMDC viability. Day 7 BMDCs were cultured with three concentration of LNP and interaction efficiency was calculated as IE=[%LNP+CD11c+ cells/Total CD11c+ cells]x100 (A). Cell viability was evaluated by propidium iodide nuclear staining and measured via fluorescence cytometry. n=3 with SD. *p<0.05 comparing LNP concentration within a single time point. # p<0.05 comparing time points with same LNP concentrations.

Because differences in LNP stability were observed following drug loading, BMDCs were cultured with 10^{-1} empty or ITE-loaded LNP for 24 hours and cells were imaged using iCys laser-scanning cytometry. Representative iCys images, Figure 3.7a, show that BMDCs cultured with ITE-loaded LNP exhibited higher LNP density per cell (MFI = 1.52 x 10^6) than BMDCs cultured with empty LNP (MFI = 1.43 x 10^6). Fluorescence cytometry corroborated iCys imaging as BMDCs cultured with ITE-loaded LNP, compared to empty LNP, displayed significantly greater LNP+ frequency (ITE-loaded 91.0%±0.2, empty LNP 85%± 1.0) and density (ITE-loaded 4,159.0 ± 80.0, empty LNP 3,676.3 ± 107.7), as shown in Figure 3.7b. Empty LNP exposure in the presence of ITE that was added directly to culturing medium did not lead to increased LNP uptake (data not shown). Interestingly, mature BMDCs (CD11c+ MHCII high) exhibited greater uptake of ITE-loaded LNP compared to immature BMDCS (CD11c+ MHCII low), and non-BMDC (CD11c-MHCII-), as shown in Figure 3.8. Together, ITE-loading of LNP resulted in increased LNP uptake by BMDCs with preferential acquisition by mature BMDCs.

Figure 3. 7 ITE-loaded LNP display increased uptake by BMDCs

A.

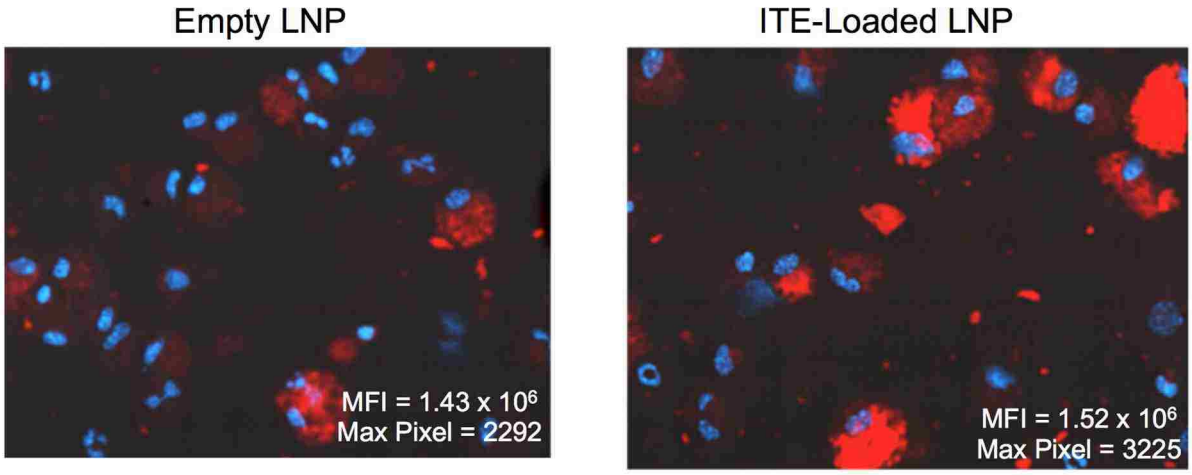

B.

LNP with (+) or without (-) ITE	LNP+ BMDC Uptake Efficiency (%)±SD (n=3)	Mean Fluorescence Intensity (MFI) ±SD (n=3)
ITE+ LNP 1:10	91.0%±0.2	4,159.0 ± 80.0
ITE- LNP 1:10	85%± 1.0*	3,676.3 ± 107.7*

Figure 3.7 ITE-loaded LNP display increased uptake by BMDCs.
Day 7 BMDCs were cultured with ITE-loaded and empty LNP for 24 hours and LNP uptake was assessed by laser scanning cytometry (A) and fluorescence cytometry (B). Nuclei are labeled with DAPI (blue) and LNP with Cy5 (red) in representative iCys images. n=3 per treatment
* $p<0.05$ between ITE loaded and empty LNP.

Figure 3. 8 LNP uptake is BMDC maturation state-dependent.

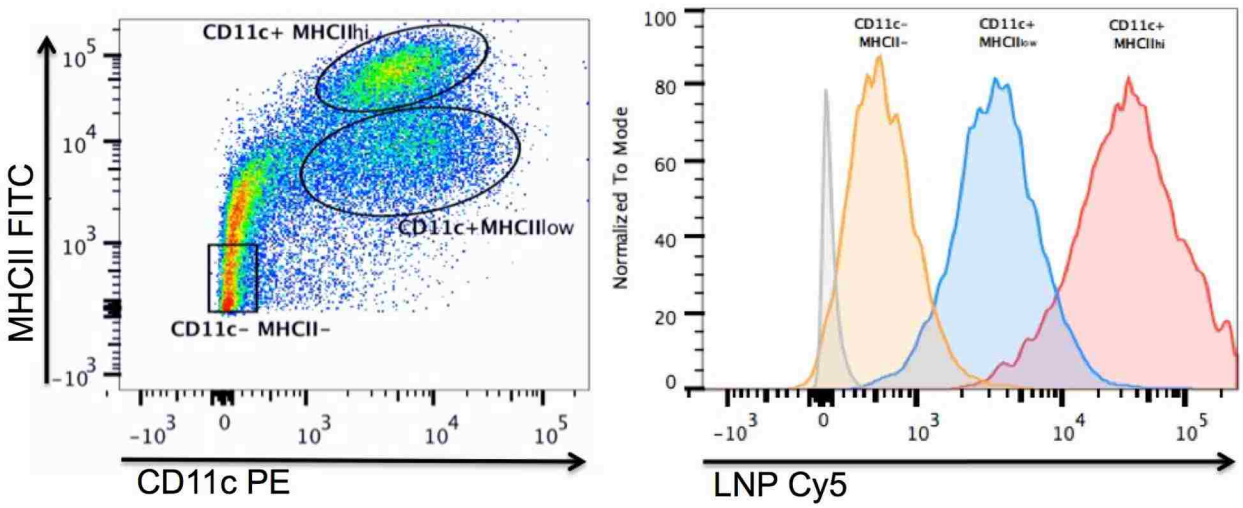

Figure 3.8 LNP uptake is BMDC maturation state-dependent.
BMDCs were exposed to ITE-loaded LNP (10^{-1}) for 24hrs and analyzed by fluorescence cytometry. LNP uptake after 24hrs was evaluated by BMDC maturation state where CD11c+MCHII^{high} denote mature BMDCs (Red), CD11c+MHCII^{Low} denote immature BMDCs (Blue), and CD11c-MHCII- denote non-DCs (orange) and cell only control (Gray).

ITE-loaded LNPs induce expression of AhR-responsive genes in BMDCs.

Dendritic cells display altered gene expression following TCDD-induced AhR activation that is associated with tolerogenic or regulatory DC function (Bankoti et al. 2010a; Bankoti et al. 2010b; Jin et al. 2010; Quintana et al. 2010a; Simones and Shepherd 2011; Takenaka and Quintana 2017; Vorderstrasse and Kerkvliet 2001). Therefore, to evaluate whether ITE-loaded LNP delivered the drug cargo to BMDCs and activated the AhR resulting in gene expression similar to TCDD, BMDCs were exposed to 10^{-1} ITE-loaded LNP [100nM ITE], to 10^{-1} empty LNP with ITE [100nM] added directly to culturing medium, or to TCDD [10nM]. Following 24-hour exposure, gene expression was measured by RT-qPCR. As shown in Figure 9, compared to untreated BMDC controls, the prototypical target gene induced by AhR activation, CYP1a1, was induced equally in BMDCs exposed to TCDD (25-fold) and ITE-loaded LNPs (25-fold induction vs control, respectively) while empty LNPs with ITE added exogenously to culture media resulted in significantly less CYP1a1 induction (10-fold vs control). While IDO1 transcription was not significantly altered by any treatment group, IDO2 was substantially upregulated in all treatments groups with greatest induction observed following treatment with ITE-loaded LNP (TCDD: 7-fold; Empty LNP+ ITE: 8-fold; ITE Loaded LNP: 36-fold). TGFβ3 was not significantly upregulated by any treatment other than ITE-loaded LNP (9-fold). Together, these data support that ITE-loaded LNP delivered ITE cargo to dendritic cells resulting in the upregulation of previously defined AhR-inducible immunoregulatory genes.

Figure 3. 9 ITE-Loaded LNP exposure leads to increased gene expression consistent with AhR activation

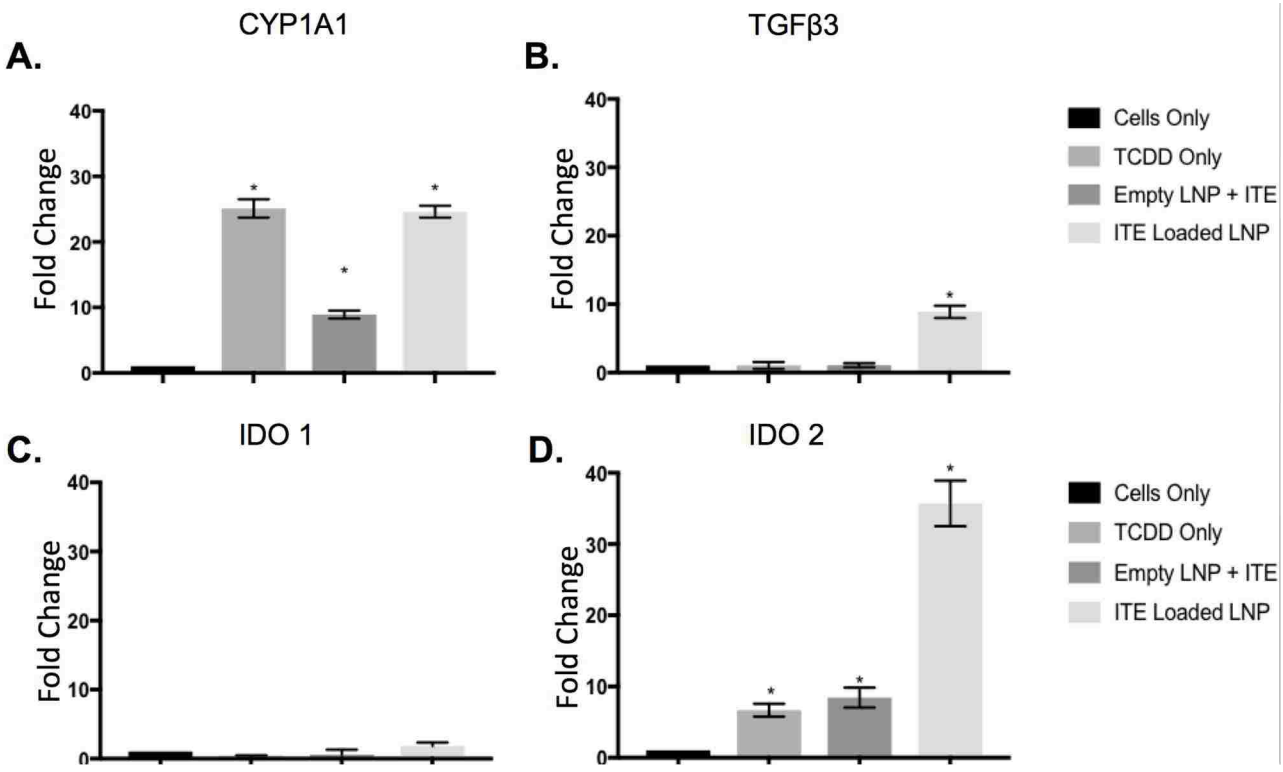

Figure 3.9 ITE-Loaded LNP exposure leads to increased gene expression consistent with AhR activation. Day 7 BMDCs were exposed to TCDD, Empty LNP with externally added ITE (100nM), and ITE-loaded LNPs (10^{-1}) or left untreated for 24hrs. mRNA expression was assessed via RT-qPCR analysis. Fold change is relative to cell only control and all genes are normalized to β-actin reference gene. Genes analyzed include: cytochrome P450, family 1, subfamily a, polypeptide 1 (Cyp1a1), indoleamine-2,3-dioxygenase 1 (IDO1), indoleamine-2,3-dioxygenase 2 (IDO2), transforming growth factor, beta 2 (Tgfb2). Data shown are representative of two experiments (n=3). Asterisks indicate significance of $p \leq 0.05$.

In vivo administration of ITE-loaded LNP results in their preferential deposition in the spleen and acquisition by APCs.

To assess biodistribution of ITE-loaded LNP within lymphoid tissues *in vivo*, C57Bl/6 mice received daily intraperitoneal injections (10uL/g/bw) for three consecutive days. Single cell suspensions of spleen, mesenteric and popliteal lymph nodes, as well as PBMCs were evaluated for LNP deposition by fluorescence cytometry. As shown in Figure 10, LNP were not detected in blood or lymph nodes, however, LNP were present in the spleen with twenty percent of live splenocytes having acquired LNP. Immune cell populations of the spleen were then evaluated individually to determine subset-specific LNP uptake. Antigen presenting cells, including macrophages and dendritic cells, exhibited the highest LNP interaction with 43% of macrophage and 48% of DCs being LNP+, while B cells and T cells had lower uptake frequencies at 22% and 15%, respectively. Additionally, the evaluation of LNP density per cell, measured by mean fluorescence intensity (MFI), established that DCs and macrophage acquired 1.5 times more LNP (1500 MFI) than B cells (1000 MFI) and 3 times more LNP than T cells (500 MFI). Together, splenic APCs preferentially, but not exclusively, acquire LNPs following *in vivo* intraperitoneal administration.

Figure 3. 10 Splenic APCs preferentially take up LNPs *in vivo following i.p. administration*

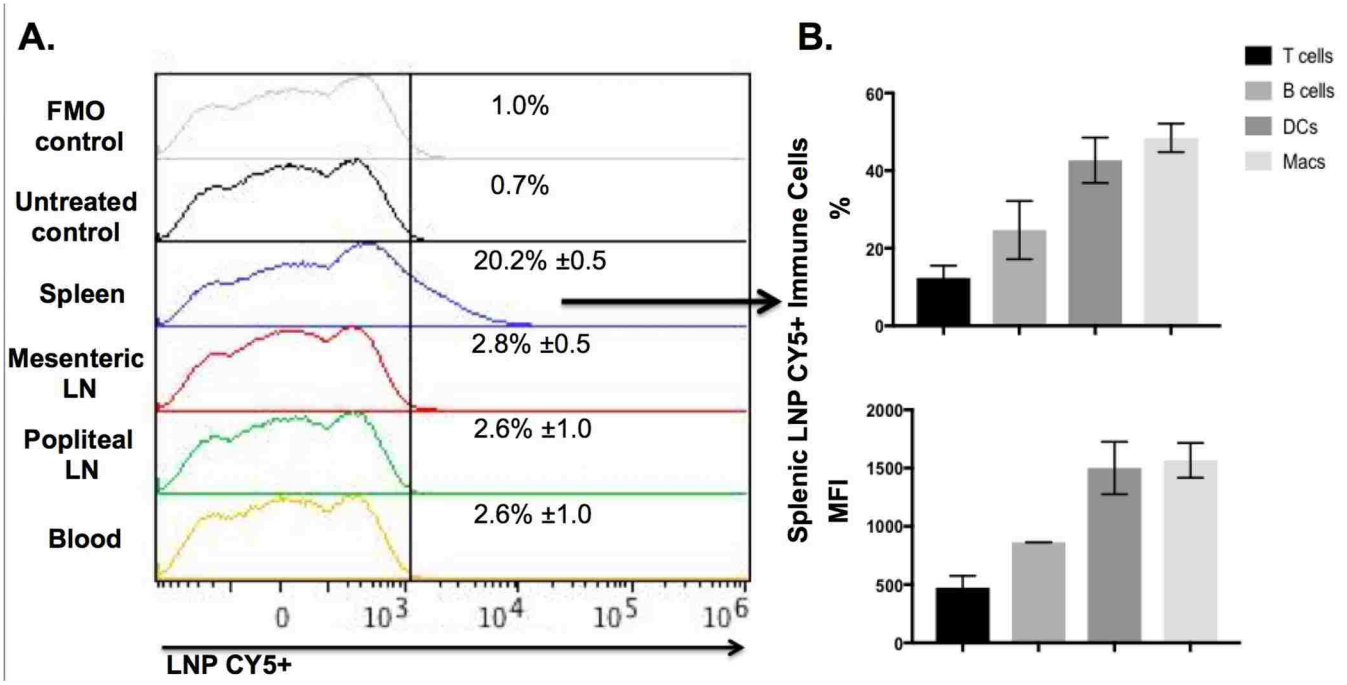

Figure 3.10 Splenic APCs preferentially take up LNPs in vivo following i.p. administration. C57Bl/6 mice were treated i.p. with LNP at 10µl/kg/bw daily for three days and tissues were analyzed for Cy5+ expression via fluorescence cytometry (A). The percent of LNP+ splenic immune cells was evaluated as frequency and mean fluorescence intensity (MFI).

Discussion

Activation of the AhR signaling pathway results in potent immunomodulatory outcomes and is a highly promising target for treatment of immune-mediated inflammatory diseases. Given that the prototypical AhR agonist, TCDD, is highly toxic, non-toxic AhR ligands are of keen interest for therapeutic activation of the AhR. Non-toxic compounds, such as ITE, can be potent AhR activators; however, barriers currently exist in the rapid metabolism and high dosing requirements necessary for biological effects. Therefore, this study investigated the potential for ITE as a proxy for natural AhR ligands, to be packaged and delivered using a PEGylated LNP carrier.

Numerous factors must be considered when determining drug delivery systems for biological use. Importantly, the size of particle can substantially affect toxicity and pharmacokinetics. Small particles are more reactive and toxic due to greater surface area and are more likely to undergo renal clearance than larger particles (Albanese et al. 2012). Conversely, if particles are too large, they are quickly opsonized and cleared by the mononuclear phagocyte system (Albanese et al. 2012). A combination of PEGylation and maintaining a hydrodynamic diameter <100nm should provide optimal pharmacokinetic properties with minimal toxicity. We demonstrated that both lyophilized and fresh PEGylated LNP maintained hydrodynamic ranges within the optimal size of 100nm and were of spherical shape. While freeze-drying can result in increased particle size compared to fresh LNP, the addition of Polysorbate 20 enabled comparable size retention, likely by preventing vesicle aggregation that can occur following lyophilization (Nohara et al. 2009). Maintaining optimal size of LNP following freeze-drying is important because lyophilization is considered a highly relevant method

to extend the shelf life of LNPs and drugs. Overall, the size and morphology of fresh and lyophilized LNP suggests that these nanoparticles are highly suitable for biological applications.

ITE is a very effective AhR activator; however, lower binding affinity and increased metabolism require higher concentrations and more frequent administration for effects similar to TCDD, the prototypical AhR ligand (Abron et al. 2018; Ehrlich et al. 2018; Henry et al. 2010; Quintana et al. 2010a). Therefore, we determined the efficiency of ITE entrapment and release from LNP. Both fresh and lyophilized LNP exhibited high entrapment efficiencies with a slight reduction observed following lyophilization. This was to be expected as freezing and drying can result in structural LNP changes leading to leakage of the drug during the hydration step (Desai et al. 2002; Yang et al. 2011). Despite a small amount of ITE leakage after the freeze and dry process, a high percentage of total ITE was retrieved in the final ITE-loaded LNPs using both preparation methods. ITE also appeared to be contained within the lipid bilayer, which was supported by thermogram analysis and lack of a burst effect in drug release studies. A burst effect, or an initial, rapid release of drug within the first thirty minutes, is commonly attributed to drug desorption from liposomal surfaces due to weak binding forces between the drug and surface lipids. In the present study, ITE release peaked by 24 hours *in vitro* with no burst effect present. This release pattern is in accordance with what has been observed for other lipophilic molecules packaged within liposomal nanoparticles (Ramana et al. 2010) and supports the likelihood of a steady diffusion of ITE across the lipid bilayer under physiological conditions. Importantly, negligible release occurred before analysis, suggesting that biological conditions, such as temperature and pH, initiated drug release.

Together, the efficient entrapment and steady release of ITE with minimal metabolites present suggests that LNPs formulated in the present study could deliver natural ligands for continual, more concentrated release within target cells, and thus, more sustained AhR activation.

AhR activation in DCs has potent immunomodulatory outcomes with demonstrated ability to suppress inflammatory diseases (Benson et al. 2012a; Benson and Shepherd 2010; Goettel et al. 2016; Quintana et al. 2010a; Yeste et al. 2012). It has been reported that non-targeted LNP preferentially interact with antigen presenting cells, including DCs and macrophage, and that LNP lipid composition can induce DC maturation (Watson et al. 2012, Foged, 2004 #1119). Interestingly, in the present study, mature BMDCs exhibited higher LNP density than both immature BMDCs and non-BMDCs. The LNP formulation did not appear to induce DC maturation as no changes in frequencies of mature and immature BMDCs were observed compared to untreated controls, suggesting that BMDC maturation state is an important factor in LNP uptake efficiency. This outcome was unexpected as immature DCs are highly phagocytic while DC maturation corresponds with reduced phagocytic activity (Mellman and Steinman 2001, Garrett, 2000 #1122), suggesting that phagocytosis is not the primary route for LNP uptake by BMDCs. The neutralization of liposomal surface charge by PEGylation and the use of phosphatidylcholine, which confers less charge than other phospholipids, are highly effective at increasing *in vivo* stability, but can lead to poor cellular interactions (Lee et al. 1993, Watson, 2012 #1111). However, the LNP in this study maintained high interaction efficiency with BMDCs. Microscopy and fluorescence cytometry confirmed that LNP and BMDCs were directly interacting in a manner

suggestive of uptake, and not accumulation on the plasma membrane; however it is noteworthy that this study did not definitively establish LNP internalization. To date, multiple studies have reported that LNP are internalized by DCs, supporting the likelihood of internalization accompanying the DC-LNP interactions observed in the present studies (Watson et al. 2012,Soema, 2015 #1112). Interestingly, ITE-loaded LNP showed greater cellular interaction than empty LNP, which may be explained by the increased LNP rigidity observed following ITE entrapment. Previous reports have shown that more rigid LNP are better internalized and result in more potent immune responses (Watson et al. 2012, Foged, 2004 #1114). Together, LNP readily interact with BMDCs in a maturation dependent manner and ITE-loaded LNP show greater uptake, suggesting that AhR agonists will be delivered directly to BMDCs.

To further explore the effects of ITE-loaded LNP on DCs, gene transcription was evaluated in BMDCs treated with ITE-loaded LNP, empty LNP, and empty LNP with ITE-supplemented media compared to TCDD. Both TCDD and ITE-loaded LNP resulted in equal induction of the prototypical AhR gene target, *CYP1a1*, supporting that ITE is being delivered and activating the AhR. The lower *CYP1a1* induction observed with ITE added directly to culture media suggests that ITE-loaded LNP elicit more AhR activity than free ITE. This is likely due to LNP enabling higher concentrations of ITE to accumulate within cells and/or LNP packaging acting to protect against ITE degradation. Strikingly, ITE-loaded LNP were more effective than TCDD in inducing both *IDO2* and *TGFβ3*, two genes tightly associated with TCDD-induced tolerogenic DCs (Simones and Shepherd 2011, Bankoti, 2010 #683). This suggests that ITE-loaded LNP may provide a route for greater induction of an immunoregulatory DC phenotype. Together,

immunoregulatory gene expression profiles support that ITE-loaded LNP delivered high concentrations of ITE to BMDCs and are potent AhR activators.

Nanoparticle composition, size, and surface modifications can alter biodistribution and lead to tissue-specific accumulation (Albanese et al. 2012, Love, 1990 #1115). Thus, LNP were evaluated for murine immune tissue deposition following intraperitoneal injection. Interestingly, minimal accumulation was observed in all tissues evaluated except the spleen. Substantial accumulation in the spleen was expected with intraperitoneal administration of LNP as nanoparticles with hydrodynamic diameters of ~100nm are associated with splenic deposition and rigid, cholesterol-rich liposomes have been shown to preferentially accumulate within the spleen (Capini et al. 2009, Love, 1990 #1115). Cell-specific uptake was also observed as splenic macrophage and DCs showed higher LNP density than T cells or B cells, which was to be expected as APCs have been shown to preferentially take up nanoparticles (Liu et al. 2013). This finding may also be, in part, due to the organization of splenic tissue, where antigen presenting cells are positioned closer to afferent lymphatics than both T cells and B cells, and likely provides greater opportunity for LNP interaction with APCs (Calabro et al. 2016). The future addition of targeting proteins such as anti-CD11c antibodies, a comprehensive DC lineage marker, to the surface of LNP may reduce macrophage uptake and enable greater cell specificity *in vivo*. Together, APCs acquire LNP at higher density than non-APCs with preferential splenic accumulation observed following intraperitoneal administration.

Seminal work by Yeste et al. (Yeste et al. 2012) has provided promising proof of principle for AhR agonist delivery *in vivo* using gold nanoparticles (auNP). However, key concerns have surrounded auNP therapies within the biomedical field (Alkilany and

Murphy 2010; Lewinski et al. 2008). At the cellular level, auNP exhibited significant cytotoxicity with greater cellular uptake corresponding to increased disruption of mitochondrial function, particularly within phagocytes (Liu et al. 2013). Recent studies have also identified size and time-dependent toxicity of auNP where substantial accumulation and low clearance rates were observed for three months in both the liver and spleen (Li et al. 2018). Therefore, alternative, non-toxic nanoparticle carriers are more desirable for pharmaceutical use. Additionally, while the present studies used nanoparticles loaded with ITE as a proxy for natural AhR agonists, a broad range of agonists exist and ligand-dependent effects are well documented (Boule et al. 2018a, Ehrlich, 2018 #522, Benson, 2011 #1071). AhR ligands have a common theme of hydrophobicity and planarity, suggesting that additional natural agonists could be incorporated into the LNP platform similarly to ITE (Pohjanvirta 2011). It is thus highly conceivable that this LNP platform could be tailored with ligands that elicit an AhR response most efficacious for treatment of specific pathologies. Collectively, the present study demonstrates that an alternative non-toxic, biodegradable LNP is an effective carrier for AhR agonist delivery and may provide for a more biologically compatible delivery system without sacrificing potency of AhR activation.

Conclusion

Liposomal nanoparticles exhibit high ITE entrapment efficiency, long-term stability, and sustained ITE release under physiological conditions. LNP are preferentially acquired by antigen presenting cells both *in vivo* and *in vitro,* with mature DCs exhibiting greater LNP uptake *in vitro.* LNP are capable of delivering AhR agonists

in order to activate the AhR and yield gene transcription equivalent to or surpassing, the prototypical, but highly toxic AHR ligand, TCDD. In conclusion, the agonist-loaded LNP developed in this study is a highly promising new route of therapeutic AhR activation.

Abron JD, Singh NP, Mishra MK, et al. (2018) An endogenous aryl hydrocarbon receptor (AhR) ligand, ITE induces regulatory T cells (Tregs) and ameliorates experimental colitis. Am J Physiol Gastrointest Liver Physiol doi:10.1152/ajpgi.00413.2017

Akbarzadeh A, Rezaei-Sadabady R, Davaran S, et al. (2013) Liposome: classification, preparation, and applications. Nanoscale research letters 8(1):102

Albanese A, Tang PS, Chan WC (2012) The effect of nanoparticle size, shape, and surface chemistry on biological systems. Annual review of biomedical engineering 14:1-16

Alkilany AM, Murphy CJ (2010) Toxicity and cellular uptake of gold nanoparticles: what we have learned so far? Journal of nanoparticle research 12(7):2313-2333

Bangham A, Hill M, Miller N (1974) Preparation and use of liposomes as models of biological membranes Methods in membrane biology. Springer, p 1-68

Bankoti J, Burnett A, Navarro S, Miller AK, Rase B, Shepherd DM (2010a) Effects of TCDD on the fate of naive dendritic cells. Toxicol Sci 115(2):422-34 doi:10.1093/toxsci/kfq063

Bankoti J, Rase B, Simones T, Shepherd DM (2010b) Functional and phenotypic effects of AhR activation in inflammatory dendritic cells. Toxicol Appl Pharmacol 246(1-2):18-28 doi:10.1016/j.taap.2010.03.013

Benson J, Beamer C, Seaver B, Shepherd D (2012a) Indole-3-Carbinol Exerts Sex-Specific Effects in Murine Colitis. European Journal of Inflammation 10(3):335-346

Benson JM, Shepherd DM (2010) Aryl hydrocarbon receptor activation by TCDD reduces inflammation associated with Crohn's disease. Toxicological Sciences 120(1):68-78

Benson JM, Shepherd DM (2011b) Dietary ligands of the aryl hydrocarbon receptor induce anti-inflammatory and immunoregulatory effects on murine dendritic cells. Toxicological Sciences 124(2):327-338

Boule LA, Burke CG, Jin G-B, Lawrence BP (2018a) Aryl hydrocarbon receptor signaling modulates antiviral immune responses: ligand metabolism rather than chemical source is the stronger predictor of outcome. Scientific reports 8(1):1826

Bozzuto G, Molinari A (2015) Liposomes as nanomedical devices. International journal of nanomedicine 10:975

Çağdaş M, Sezer AD, Bucak S (2014) Liposomes as potential drug carrier systems for drug delivery Application of nanotechnology in drug delivery. InTech

Calabro S, Liu D, Gallman A, et al. (2016) Differential intrasplenic migration of dendritic cell subsets tailors adaptive immunity. Cell reports 16(9):2472-2485

Capini C, Jaturanpinyo M, Chang H-I, et al. (2009) Antigen-specific suppression of inflammatory arthritis using liposomes. The Journal of Immunology 182(6):3556-3565

Desai TR, Wong JP, Hancock RE, Finlay WH (2002) A novel approach to the pulmonary delivery of liposomes in dry powder form to eliminate the deleterious effects of milling. Journal of pharmaceutical sciences 91(2):482-491

Ehrlich AK, Pennington JM, Bisson WH, Kolluri SK, Kerkvliet NI (2018) TCDD, FICZ, and Other High Affinity AhR Ligands Dose-Dependently Determine the Fate of CD4+ T Cell Differentiation. Toxicol Sci 161(2):310-320 doi:10.1093/toxsci/kfx215

Esser C, Rannug A (2015) The aryl hydrocarbon receptor in barrier organ physiology, immunology, and toxicology. Pharmacological reviews 67(2):259-279

Foged C, Arigita C, Sundblad A, Jiskoot W, Storm G, Frokjaer S (2004) Interaction of dendritic cells with antigen-containing liposomes: effect of bilayer composition. Vaccine 22(15-16):1903-1913

Goettel JA, Gandhi R, Kenison JE, et al. (2016) AHR Activation Is Protective against Colitis Driven by T Cells in Humanized Mice. Cell Rep 17(5):1318-1329 doi:10.1016/j.celrep.2016.09.082

Hathout RM, Mansour S, Mortada ND, Guinedi AS (2007) Liposomes as an ocular delivery system for acetazolamide: in vitro and in vivo studies. AAPS pharmscitech 8(1):E1-E12

Henry EC, Welle SL, Gasiewicz TA (2010) TCDD and a putative endogenous AhR ligand, ITE, elicit the same immediate changes in gene expression in mouse lung fibroblasts. Toxicol Sci 114(1):90-100 doi:10.1093/toxsci/kfp285

Jesorka A, Orwar O (2008) Liposomes: technologies and analytical applications. Annu Rev Anal Chem 1:801-832

Jin G-B, Moore AJ, Head JL, Neumiller JJ, Lawrence BP (2010) Aryl hydrocarbon receptor activation reduces dendritic cell function during influenza virus infection. Toxicological sciences 116(2):514-522

Kerkvliet NI, Steppan LB, Vorachek W, et al. (2009) Activation of aryl hydrocarbon receptor by TCDD prevents diabetes in NOD mice and increases Foxp3+ T cells in pancreatic lymph nodes. Immunotherapy 1(4):539-547

Kochiadakis GE, Kanoupakis EM, Kalebubas MD, et al. (2001) Sotalol vs metoprolol for ventricular rate control in patients with chronic atrial fibrillation who have undergone digitalization: a single-blinded crossover study. Europace 3(1):73-9 doi:10.1053/eupc.2000.0140

Kraft JC, Freeling JP, Wang Z, Ho RJ (2014) Emerging research and clinical development trends of liposome and lipid nanoparticle drug delivery systems. Journal of pharmaceutical sciences 103(1):29-52

Kreitinger JM, Beamer CA, Shepherd DM (2016) Environmental immunology: lessons learned from exposure to a select panel of immunotoxicants. The Journal of Immunology 196(8):3217-3225

Lee KD, Nir S, Papahadjopoulos D (1993) Quantitative analysis of liposome-cell interactions in vitro: rate constants of binding and endocytosis with suspension and adherent J774 cells and human monocytes. Biochemistry 32(3):889-899

Lee YH, Lin CH, Hsu PC, et al. (2015b) Aryl hydrocarbon receptor mediates both proinflammatory and anti‐inflammatory effects in lipopolysaccharide‐activated microglia. Glia 63(7):1138-1154
Lewinski N, Colvin V, Drezek R (2008) Cytotoxicity of nanoparticles. small 4(1):26-49
Li X, Hu Z, Ma J, et al. (2018) The systematic evaluation of size-dependent toxicity and multi-time biodistribution of gold nanoparticles. Colloids and Surfaces B: Biointerfaces 167:260-266
Liu X, Huang N, Li H, Jin Q, Ji J (2013) Surface and size effects on cell interaction of gold nanoparticles with both phagocytic and nonphagocytic cells. Langmuir 29(29):9138-9148
Maswadeh H, Demetzos C, Daliani I, et al. (2002) A molecular basis explanation of the dynamic and thermal effects of vinblastine sulfate upon dipalmitoylphosphatidylcholine bilayer membranes. Biochimica et Biophysica Acta (BBA)-Biomembranes 1567:49-55
Mellman I, Steinman RM (2001) Dendritic cells: specialized and regulated antigen processing machines. Cell 106(3):255-258
Mezrich JD, Fechner JH, Zhang X, Johnson BP, Burlingham WJ, Bradfield CA (2010) An interaction between kynurenine and the aryl hydrocarbon receptor can generate regulatory T cells. The Journal of Immunology:0903670
Mizrahy S, Goldsmith M, Leviatan-Ben-Arye S, et al. (2014) Tumor targeting profiling of hyaluronan-coated lipid based-nanoparticles. Nanoscale 6(7):3742-3752
Needham L, Gerthoux P, Patterson Jr D, et al. (1999) Exposure assessment: serum levels of TCDD in Seveso, Italy. Environmental research 80(2):S200-S206
Nguyen LP, Bradfield CA (2007) The search for endogenous activators of the aryl hydrocarbon receptor. Chemical research in toxicology 21(1):102-116
Nohara K, Suzuki T, Ao K, et al. (2009) Constitutively active aryl hydrocarbon receptor expressed in T cells increases immunization-induced IFN-gamma production in mice but does not suppress T(h)2-cytokine production or antibody production. Int Immunol 21(7):769-77 doi:10.1093/intimm/dxp045
Olsen PC, Ferreira TP, Serra MF, et al. (2011) Lidocaine-derivative JMF2-1 prevents ovalbumin-induced airway inflammation by regulating the function and survival of T cells. Clin Exp Allergy 41(2):250-9 doi:10.1111/j.1365-2222.2010.03580.x
Pohjanvirta R (2011) The AH receptor in Biology and Toxicology. John Wiley & Sons
Quintana FJ, Murugaiyan G, Farez MF, et al. (2010a) An endogenous aryl hydrocarbon receptor ligand acts on dendritic cells and T cells to suppress experimental autoimmune encephalomyelitis. Proceedings of the National Academy of Sciences 107(48):20768-20773
Quintana FJ, Murugaiyan G, Farez MF, et al. (2010c) An endogenous aryl hydrocarbon receptor ligand acts on dendritic cells and T cells to suppress experimental autoimmune encephalomyelitis. Proc Natl Acad Sci U S A 107(48):20768-73 doi:10.1073/pnas.1009201107

Ramana LN, Sethuraman S, Ranga U, Krishnan UM (2010) Development of a liposomal nanodelivery system for nevirapine. Journal of biomedical science 17(1):57
Sade A, Banerjee S, Severcan F (2010) Concentration-dependent differing actions of the nonsteroidal anti-inflammatory drug, celecoxib, in distearoyl phosphatidylcholine multilamellar vesicles. Journal of liposome research 20(2):168-177
Serro A, Galante R, Kozica A, et al. (2014) Effect of tetracaine on DMPC and DMPC+ cholesterol biomembrane models: Liposomes and monolayers. Colloids and Surfaces B: Biointerfaces 116:63-71
Simones T, Shepherd DM (2011) Consequences of AhR activation in steady-state dendritic cells. Toxicol Sci 119(2):293-307 doi:10.1093/toxsci/kfq354
Singh U, Abron J, Singh N, et al. (2014) An endogenous aryl hydrocarbon receptor (AhR) ligand, ITE induces regulatory T cells (Tregs) and ameliorates experimental colitis (IRC4P. 490). Am Assoc Immnol
Stockinger B, Meglio PD, Gialitakis M, Duarte JH (2014) The aryl hydrocarbon receptor: multitasking in the immune system. Annual review of immunology 32:403-432
Tacken PJ, Zeelenberg IS, Cruz LJ, et al. (2011) Targeted delivery of Toll-like receptor ligands to human and mouse dendritic cells strongly enhances adjuvanticity. Blood:blood-2011-07-367615
Takenaka MC, Quintana FJ Tolerogenic dendritic cells. In: Seminars in immunopathology, 2017. vol 39. Springer, p 113-120
Tran TH, Tran TTP, Nguyen HT, et al. (2018) Nanoparticles for dendritic cell-based immunotherapy. International journal of pharmaceutics
Vogel CF, Goth SR, Dong B, Pessah IN, Matsumura F (2008) Aryl hydrocarbon receptor signaling mediates expression of indoleamine 2, 3-dioxygenase. Biochemical and biophysical research communications 375(3):331-335
Vorderstrasse BA, Kerkvliet NI (2001) 2, 3, 7, 8-Tetrachlorodibenzo-p-dioxin affects the number and function of murine splenic dendritic cells and their expression of accessory molecules. Toxicology and applied pharmacology 171(2):117-125
Watson DS, Endsley AN, Huang L (2012) Design considerations for liposomal vaccines: influence of formulation parameters on antibody and cell-mediated immune responses to liposome associated antigens. Vaccine 30(13):2256-2272
Yang YY, Lee FY, Hsu HC, et al. (2011) Assessment of first-year post-graduate residents: usefulness of multiple tools. J Chin Med Assoc 74(12):531-8 doi:10.1016/j.jcma.2011.10.002
Yeste A, Nadeau M, Burns EJ, Weiner HL, Quintana FJ (2012) Nanoparticle-mediated codelivery of myelin antigen and a tolerogenic small molecule suppresses experimental autoimmune encephalomyelitis. Proc Natl Acad Sci U S A 109(28):11270-5 doi:10.1073/pnas.1120611109
Zhang L, Ma J, Takeuchi M, et al. (2010) Suppression of experimental autoimmune uveoretinitis by inducing differentiation of regulatory T cells via activation of

aryl hydrocarbon receptor. Investigative ophthalmology & visual science 51(4):2109-2117

CHAPTER 4: CONCLUSIONS

Soon after the discovery of the AhR by Conney, Okey, and Nebert, a curious link between the AhR and the immune system was identified when rodents exposed to a known AhR agonist *in vivo* displayed severe thymic atrophy. Since this initial observation, AhR-mediated thymic atrophy has been seen in every animal species tested to date. Numerous questions surround AhR-mediated thymic atrophy. Specifically, early studies showed that AhR activation within the hematopoietic compartment was necessary for AhR-mediated atrophy; however, the hematopoietic compartment is highly heterogeneous and a key question that has remained since these early studies is whether AhR expression within specific cell types of the hematopoietic compartment are responsible for thymic atrophy. Additionally, as classes of AhR agonists expand beyond exogenous compounds to include endogenous- and dietary-sourced ligands, some of which have high therapeutic potential, important questions emerge regarding ligand-specific effects on the thymus. Therefore, the studies in this dissertation (1) show that AhR activation within CD11c+ cells is necessary for TCDD-mediated thymic atrophy, and identify ligand-specific effects within the context of thymic atrophy.

As our understanding of AhR-mediated immunomodulation expands, the AhR is becoming a highly intriguing and promising target for novel therapeutics. Harnessing the immunosuppressive potential of AhR activation, particularly within dendritic cells as they are high AhR expressers and adopt a tolerogenic phenotype, could lead to regulation of inflammation and autoimmune diseases. Proof of principle comes from seminal research by the Quintana Laboratory at Harvard that showed systemic ITE exposure

could significantly lower disease scores in experimental autoimmune encephalomyelitis (EAE), the mouse model of multiple sclerosis. Additionally, ITE loaded onto gold nanoparticles in combination with a myelin peptide (MOG_{35-55}) resulted in tolerogenic DCs and T cells that significantly reduced the disease pathology. However, the use of gold nanoparticles in therapeutic applications is entrenched with concerns regarding safety and toxicity. Therefore, the studies in this dissertation (2) develop PEGylated liposomal nanoparticles for delivery of AhR agonists, test ITE-loaded liposomal nanoparticle interaction and AhR activation in murine bone marrow derived dendritic cells, and evaluate liposomal biodistribution in mice.

Thymic atrophy is ligand-specific and TCDD-mediated thymic atrophy requires AhR expression in CD11c+ cells.

The first goal of this study was to evaluate thymic atrophy by a select panel of ligands and determine the role of AhR activation in CD11c+ DCs during TCDD-mediated thymic atrophy. We demonstrated for the first time that administration of endogenous ligand, ITE, p.o. or i.p., resulted in thymic atrophy characteristically similar to TCDD albeit at higher doses, as indicated by reduced thymic weight and cellularity due to substantial loss of the DP thymocyte population. Conversely, exposure to dietary ligand, I3C, had an opposite effect with increased thymic cellularity observed by day 7. The effects observed with I3C are quite surprising, and with interest growing in cancer biology to promote or augment thymic function following severe immunosuppression from chemotherapeutics and radiation, especially in children who do not have such expansive T cell repertoires as adults, I3C may hold promise as a natural route to do so

(Chung et al. 2014).

As the AhR signaling pathway is becoming an increasingly promising clinical target with therapeutic immunomodulatory potential, alternatives to TCDD, which is not considered suitable for therapeutic applications due to adverse toxicity, are of keen interest within the field. ITE has shown extraordinarily promising therapeutic potential in treatment of autoimmune diseases such as experimental autoimmune encephalomyelitis (EAE) (Quintana et al. 2010c; Yeste et al. 2012); however, the severe thymic atrophy reported here following systemic exposure to ITE is an adverse effect that needs to be further considered when evaluating its therapeutic potential. One avenue to potentially harness the therapeutic potential of ITE while bypassing this adverse effect on the thymus is to contain ITE within a targeted delivery system. The use of a delivery system may reduce the dosing regimen, the concentration of systemic ITE exposure, and the adverse effects on the thymus.

Identification of the key cell type(s) mediating thymic atrophy following AhR activation has been an unanswered question in AhR research for multiple decades. While seminal work by Staples et al. (1998) showed that AhR activation within the hematopoietic compartment is required for TCDD-induced thymic atrophy, work in this dissertation has definitively established that AhR expression within CD11c+ cells, a comprehensive, but not exclusive, lineage marker for DCs, is necessary for thymic atrophy. Complete protection from TCDD-induced atrophy when mice lacked the AhR in CD11c+ cells was an unexpected result. DCs in the thymus are a rare population, comprising only ~1-2% of cells, while DP thymocytes, the population most affected by TCDD, compose ~80% of cells; however, DCs constitutively express high levels of AhR

with further inducible expression, while most T cell subsets and developing thymocytes are low AhR expressers (Kreitinger et al. 2016). To ensure that CD11c in the thymus is exclusive to DCs, we thoroughly performed CD11c staining on non-DC populations, and did not detect CD11c expression outside of the DC lineage. We also used a broad panel of conditional knock out mice to verify that AhR expression in thymic epithelial cells, monocytes and macrophages, as well as thymocytes and mature T cells, did not result in protection from thymic atrophy. Together, these results support that DCs are the key cell type mediating the rapid, severe loss of thymocytes following exposure to TCDD. It is necessary to mention that while CD11c is a comprehensive lineage marker for DCs, and it could not be detected on non-DC populations within the thymus, CD11c can be expressed by non-DC populations outside of the thymus, such as alveolar macrophages, and the studies presented here did not conclusively establish that AhR expression in CD11c+ cells specifically located within the thymus are sufficient for thymic atrophy. Taken together, to the best of our knowledge, these in vivo studies are the first to identify ligand-specific effects on thymic atrophy and to establish a requisite role for AhR expression within CD11c+ cells for TCDD-mediated thymic atrophy.

ITE-loaded liposomal nanoparticles for therapeutic AhR activation

The second goal of this study was to develop and test a PEGylated liposomal nanocarrier for delivery of natural AhR agonists. We demonstrated that liposomal nanoparticles entrap the natural AhR agonist, ITE, within the lipid bilayer with high efficiency. While natural AhR agonists provide a promising alternative to the highly toxic prototypical ligand, TCDD, substantial barriers currently exist in the rapid metabolism

and degradation of natural AhR ligands. The entrapment of ITE within the lipid bilayer resulted in little degradation product and provides a promising form of protection for AhR agonists that are less stable than TCDD. Notably, studies presented here demonstrate that natural ligands can have adverse consequences similar to TCDD, as ITE induced severe thymic atrophy following systemic administration. This reinforces the need for a delivery system that reduces systemic exposure for therapeutic AhR activation, but also may suggest that ITE is not the most suitable natural compound. Importantly, the platform developed within this study is well suited for incorporation of lipophilic compounds and indolic compounds, such as indole-3-carbinol, may be optimal candidates given their combination of AhR activating potential and absence of thymic atrophy. Shelf life is another factor to consider for clinical utility of novel therapeutics. LNPs within this study demonstrated release of ITE under physiological conditions with no leakage of ITE being observed under storage conditions and the storage of ITE-loaded LNP for three months did not reduce efficacy or interaction with BMDCs. Together, supporting that LNP could be highly compatible with pharmaceutical use.

TCDD is considered the prototypical AhR ligand for its high binding affinity and induction of dioxin-responsive genes, most notably *CYP1a1 (Bankoti et al. 2010a; Bankoti et al. 2010b; Simones and Shepherd 2011).* ITE delivered by LNP were able to induce *CYP1a1* at the same levels as TCDD, while ITE added directly to culture media resulted in lower induction. While the causes for this were not investigated in these studies, reasons could include higher ITE concentrations accumulating within BMDCs, reduced ITE degradation, or more sustained AhR activation by continual diffusion of ITE from LNP. Overall, LNP may circumvent key issues with natural AhR agonists.

In vivo experiments established that LNP accumulated within the spleen. This was to be expected given the route of administration and the size of particle, as both factors are optimal for splenic accumulation. While APCs of the spleen showed preferential LNP interactions, it is important to note that the successful delivery of ITE *in vivo* was not evaluated within these studies. However, *in vitro* studies indicate that ITE is maintained within LNP and then slowly released with a majority of release occurring within the first 24 hours, a timeframe that should accommodate LNP trafficking to splenic APCs. Notably, LNP of 100nm can accumulate in the liver and the liver is a high expresser of both AhR and CYP1a1 (Bozzuto and Molinari 2015; Çağdaş et al. 2014); however, LNP trafficking to the liver was not evaluated in the present study. If substantial LNP accumulation occurs within the liver, it has the potential to greatly reduce LNP efficacy through substantial induction of xenobiotic metabolism. Moreover, if a high concentration of ITE is being delivered to the liver, it may result in deleterious effects on liver tissue similar to TCDD, such as congestive hepatophathy, or nutmeg liver. While this was not evaluated in the present studies, the addition of PEG to LNPs has been reported to reduce liver accumulation (Desai et al. 2002) and therefore may reduce effects on the liver.

Future directions

The AhR provides a promising therapeutic target for treatment of immune-mediated diseases. Compounds such as ITE have been highlighted as non-toxic alternatives to TCDD for therapeutically activating the AhR; however, work here suggests that the thymus is adversely affected by systemic ITE exposure. It remains of

key interest to further assess the effects of natural ligands, including but not limited to ITE and I3C, on the thymus, especially in light of our findings that I3C appeared to have an opposite effect on the thymus by increasing, not decreasing, cellularity. While I3C is a well-established AhR ligand, we did not evaluate the effects of I3C on the thymus for AhR, or CD11c-AhR, dependence. To this end, it is necessary to develop higher concentration formulations of lower-affinity agonists, such as ITE and I3C, which would enable further testing in mouse strains on the AhR^d allele background. Additionally, while intraperitoneal injection of ITE-loaded LNP resulted in minimal thymic accumulation, the three-day time point of these in vivo LNP exposures is not sufficient to gauge thymic atrophy as peak atrophy occurs between 7-10 days post-exposure. Thus, future studies with ITE-loaded LNP should consider longer time points for evaluation of deleterious effects on the thymus.

Sex-dependent effects of AhR activation have been observed throughout my doctoral training, are reported in previous publications, and remain of keen interest and importance when evaluating AhR activation for therapeutic applications (Benson et al. 2012a; Nault et al. 2017). Key questions around sex-dependent effects include potential differences in AhR expression levels, increased or reduced drug metabolism rates or storage, and interactions with non-canonical proteins/pathways. AhR ligands are highly lipophilic with bioaccumulation occurring in fatty tissues and non-targeted liposomal nanoparticles have also been shown to accumulate within the liver (Lee et al. 2015a). Interestingly, in murine livers, females express higher levels of AhR transcripts than males; however, this has not yet been evaluated in immune cells or in the thymus. Notably, hepatic transcriptomic studies in rodents show that TCDD exposure results in

greater transcriptional variation in AhR-related genes within livers of males than females (Lee et al. 2015a). The authors of this report suggest that the narrowed response in females may be an adaptive function that enables females to better handle toxic metabolites and to limit adverse toxicity. Interestingly, male rodents show increased transcripts involved in oxidative stress and fatty acid biosynthesis after AhR activation. This could conceivably impact the efficacy and adverse side effects of LNP-delivered ligands in a sex-dependent manner; however, these possibilities remain to be evaluated. Taken together, AhR immune responsiveness and toxicity differ between male and female animals, which reinforces the importance of controlling for sex differences in both mechanistic and therapeutic AhR studies.

Collectively this work provides novel discoveries that contribute significantly to further our understanding of how the Aryl hydrocarbon receptor signaling pathway regulates the immune system. The data presented in this dissertation provide the foundation to direct future research studies that are expected to advance the basic, biological function of the AhR in the immune system, while also promoting the exciting potential of AhR ligand-loaded liposomal nanoparticles to become highly effective therapeutics for the treatment of immune-mediated diseases.

References

Bankoti J, Burnett A, Navarro S, Miller AK, Rase B, Shepherd DM (2010a) Effects of TCDD on the fate of naive dendritic cells. Toxicol Sci 115(2):422-34 doi:10.1093/toxsci/kfq063

Bankoti J, Rase B, Simones T, Shepherd DM (2010b) Functional and phenotypic effects of AhR activation in inflammatory dendritic cells. Toxicol Appl Pharmacol 246(1-2):18-28 doi:10.1016/j.taap.2010.03.013

Benson J, Beamer C, Seaver B, Shepherd D (2012a) Indole-3-Carbinol Exerts Sex-Specific Effects in Murine Colitis. European Journal of Inflammation 10(3):335-346

Bozzuto G, Molinari A (2015) Liposomes as nanomedical devices. International journal of nanomedicine 10:975

Çağdaş M, Sezer AD, Bucak S (2014) Liposomes as potential drug carrier systems for drug delivery Application of nanotechnology in drug delivery. InTech

Chung B, Montel‐Hagen A, Ge S, et al. (2014) Engineering the human thymic microenvironment to support thymopoiesis in vivo. Stem cells 32(9):2386-2396

Desai TR, Wong JP, Hancock RE, Finlay WH (2002) A novel approach to the pulmonary delivery of liposomes in dry powder form to eliminate the deleterious effects of milling. Journal of pharmaceutical sciences 91(2):482-491

Kreitinger JM, Beamer CA, Shepherd DM (2016) Environmental immunology: lessons learned from exposure to a select panel of immunotoxicants. The Journal of Immunology 196(8):3217-3225

Lee J, Prokopec SD, Watson JD, Sun RX, Pohjanvirta R, Boutros PC (2015a) Male and female mice show significant differences in hepatic transcriptomic response to 2, 3, 7, 8-tetrachlorodibenzo-p-dioxin. BMC genomics 16(1):625

Nault R, Fader KA, Harkema JR, Zacharewski T (2017) Loss of liver-specific and sexually dimorphic gene expression by aryl hydrocarbon receptor activation in C57BL/6 mice. PloS one 12(9):e0184842

Quintana FJ, Murugaiyan G, Farez MF, et al. (2010c) An endogenous aryl hydrocarbon receptor ligand acts on dendritic cells and T cells to suppress experimental autoimmune encephalomyelitis. Proc Natl Acad Sci U S A 107(48):20768-73 doi:10.1073/pnas.1009201107

Simones T, Shepherd DM (2011) Consequences of AhR activation in steady-state dendritic cells. Toxicol Sci 119(2):293-307 doi:10.1093/toxsci/kfq354

Yeste A, Nadeau M, Burns EJ, Weiner HL, Quintana FJ (2012) Nanoparticle-mediated codelivery of myelin antigen and a tolerogenic small molecule suppresses experimental autoimmune encephalomyelitis. Proc Natl Acad Sci U S A 109(28):11270-5 doi:10.1073/pnas.1120611109

Combined References

Abron JD, Singh NP, Mishra MK, et al. (2018) An endogenous aryl hydrocarbon receptor (AhR) ligand, ITE induces regulatory T cells (Tregs) and ameliorates experimental colitis. Am J Physiol Gastrointest Liver Physiol doi:10.1152/ajpgi.00413.2017

Akbarzadeh A, Rezaei-Sadabady R, Davaran S, et al. (2013) Liposome: classification, preparation, and applications. Nanoscale research letters 8(1):102

Albanese A, Tang PS, Chan WC (2012) The effect of nanoparticle size, shape, and surface chemistry on biological systems. Annual review of biomedical engineering 14:1-16

Alkilany AM, Murphy CJ (2010) Toxicity and cellular uptake of gold nanoparticles: what we have learned so far? Journal of nanoparticle research 12(7):2313-2333

Allan RS, Waithman J, Bedoui S, et al. (2006) Migratory dendritic cells transfer antigen to a lymph node-resident dendritic cell population for efficient CTL priming. Immunity 25(1):153-162

Atibalentja DF, Murphy KM, Unanue ER (2011) Functional redundancy between thymic CD8α+ and Sirpα+ conventional dendritic cells in presentation of blood-derived lysozyme by MHC class II proteins. The Journal of Immunology 186(3):1421-1431

Bangham A, Hill M, Miller N (1974) Preparation and use of liposomes as models of biological membranes Methods in membrane biology. Springer, p 1-68

Bankoti J, Burnett A, Navarro S, Miller AK, Rase B, Shepherd DM (2010a) Effects of TCDD on the fate of naive dendritic cells. Toxicol Sci 115(2):422-34 doi:10.1093/toxsci/kfq063

Bankoti J, Rase B, Simones T, Shepherd DM (2010b) Functional and phenotypic effects of AhR activation in inflammatory dendritic cells. Toxicol Appl Pharmacol 246(1-2):18-28 doi:10.1016/j.taap.2010.03.013

Bankoti J, Rase B, Simones T, Shepherd DM (2010c) Functional and phenotypic effects of AhR activation in inflammatory dendritic cells. Toxicology and applied pharmacology 246(1):18-28

Benson J, Beamer C, Seaver B, Shepherd D (2012a) Indole-3-Carbinol Exerts Sex-Specific Effects in Murine Colitis. European Journal of Inflammation 10(3):335-346

Benson JM, Beamer CA, Seaver BP, Shepherd DM (2012b) Indole-3-Carbinol Exerts Sex-Specific Effects in Murine Colitis. Eur J Inflamm 10(3):335-346 doi:Doi 10.1177/1721727x1201000309

Benson JM, Shepherd DM (2010) Aryl hydrocarbon receptor activation by TCDD reduces inflammation associated with Crohn's disease. Toxicological Sciences 120(1):68-78

Benson JM, Shepherd DM (2011a) Aryl hydrocarbon receptor activation by TCDD reduces inflammation associated with Crohn's disease. Toxicological sciences

: an official journal of the Society of Toxicology 120(1):68-78 doi:10.1093/toxsci/kfq360
Benson JM, Shepherd DM (2011b) Dietary ligands of the aryl hydrocarbon receptor induce anti-inflammatory and immunoregulatory effects on murine dendritic cells. Toxicological Sciences 124(2):327-338
Birnbaum LS (1986) Distribution and excretion of 2,3,7,8-tetrachlorodibenzo-p-dioxin in congenic strains of mice which differ at the Ah locus. Drug metabolism and disposition: the biological fate of chemicals 14(1):34-40
Bjeldanes LF, Kim J-Y, Grose KR, Bartholomew JC, Bradfield CA (1991) Aromatic hydrocarbon responsiveness-receptor agonists generated from indole-3-carbinol in vitro and in vivo: comparisons with 2, 3, 7, 8-tetrachlorodibenzo-p-dioxin. Proceedings of the national academy of sciences 88(21):9543-9547
Blackburn CC, Manley NR (2004) Developing a new paradigm for thymus organogenesis. Nature Reviews Immunology 4(4):278
Bonasio R, Scimone ML, Schaerli P, Grabie N, Lichtman AH, von Andrian UH (2006) Clonal deletion of thymocytes by circulating dendritic cells homing to the thymus. Nat Immunol 7(10):1092-100 doi:10.1038/ni1385
Boule LA, Burke CG, Jin G-B, Lawrence BP (2018a) Aryl hydrocarbon receptor signaling modulates antiviral immune responses: ligand metabolism rather than chemical source is the stronger predictor of outcome. Scientific reports 8(1):1826
Boule LA, Burke CG, Jin GB, Lawrence BP (2018b) Aryl hydrocarbon receptor signaling modulates antiviral immune responses: ligand metabolism rather than chemical source is the stronger predictor of outcome. Sci Rep 8(1):1826 doi:10.1038/s41598-018-20197-4
Bozzuto G, Molinari A (2015) Liposomes as nanomedical devices. International journal of nanomedicine 10:975
Çağdaş M, Sezer AD, Bucak S (2014) Liposomes as potential drug carrier systems for drug delivery Application of nanotechnology in drug delivery. InTech
Calabro S, Liu D, Gallman A, et al. (2016) Differential intrasplenic migration of dendritic cell subsets tailors adaptive immunity. Cell reports 16(9):2472-2485
Camacho IA, Nagarkatti M, Nagarkatti PS (2002) 2, 3, 7, 8-Tetrachlorodibenzo-p-dioxin (TCDD) induces Fas-dependent activation-induced cell death in superantigen-primed T cells. Archives of toxicology 76(10):570-580
Camacho IA, Nagarkatti M, Nagarkatti PS (2004) Evidence for induction of apoptosis in T cells from murine fetal thymus following perinatal exposure to 2, 3, 7, 8-tetrachlorodibenzo-p-dioxin (TCDD). Toxicological Sciences 78(1):96-106
Camacho IA, Singh N, Hegde VL, Nagarkatti M, Nagarkatti PS (2005a) Treatment of mice with 2,3,7,8-tetrachlorodibenzo-p-dioxin leads to aryl hydrocarbon receptor-dependent nuclear translocation of NF-kappaB and expression of Fas ligand in thymic stromal cells and consequent apoptosis in T cells. J Immunol 175(1):90-103
Camacho IA, Singh N, Hegde VL, Nagarkatti M, Nagarkatti PS (2005b) Treatment of mice with 2, 3, 7, 8-tetrachlorodibenzo-p-dioxin leads to aryl hydrocarbon receptor-dependent nuclear translocation of NF-κB and expression of Fas

ligand in thymic stromal cells and consequent apoptosis in T cells. The Journal of Immunology 175(1):90-103
Capini C, Jaturanpinyo M, Chang H-I, et al. (2009) Antigen-specific suppression of inflammatory arthritis using liposomes. The Journal of Immunology 182(6):3556-3565
Carlstedt-Duke JM (1979) Tissue distribution of the receptor for 2, 3, 7, 8-tetrachlorodibenzo-p-dioxin in the rat. Cancer research 39(8):3172-3176
Cepeda S, Griffith AV (2017) Thymic stromal cells: Roles in atrophy and age-associated dysfunction of the thymus. Experimental gerontology
Chung B, Montel‐Hagen A, Ge S, et al. (2014) Engineering the human thymic microenvironment to support thymopoiesis in vivo. Stem cells 32(9):2386-2396
Coder BD, Wang H, Ruan L, Su D-M (2015) Thymic involution perturbs negative selection leading to autoreactive T cells that induce chronic inflammation. The Journal of Immunology:1500082
Comment CE, Blaylock BL, Germolec DR, et al. (1992) Thymocyte injury after in vitro chemical exposure: potential mechanisms for thymic atrophy. J Pharmacol Exp Ther 262(3):1267-73
Connor K, Finley B (2003) Naturally occurring ah-receptor agonists in foods: Implications regarding dietary dioxin exposure and health risk. Human and Ecological Risk Assessment 9(7):1747-1763
De Heer C, Verlaan AP, Penninks AH, Vos JG, Schuurman HJ, Van Loveren H (1994) Time course of 2,3,7,8-tetrachlorodibenzo-p-dioxin (TCDD)-induced thymic atrophy in the Wistar rat. Toxicol Appl Pharmacol 128(1):97-104
Dencker L, Hassoun E, d'Argy R, Alm G (1985) Fetal thymus organ culture as an in vitro model for the toxicity of 2, 3, 7, 8-tetrachlorodibenzo-p-dioxin and its congeners. Molecular pharmacology 27(1):133-140
Denison MS, Nagy SR (2003) Activation of the aryl hydrocarbon receptor by structurally diverse exogenous and endogenous chemicals. Annual review of pharmacology and toxicology 43(1):309-334
Desai TR, Wong JP, Hancock RE, Finlay WH (2002) A novel approach to the pulmonary delivery of liposomes in dry powder form to eliminate the deleterious effects of milling. Journal of pharmaceutical sciences 91(2):482-491
Dolciami D, Gargaro M, Cerra B, et al. (2018) Binding Mode and Structure-Activity Relationships of ITE as an Aryl Hydrocarbon Receptor (AhR) Agonist. ChemMedChem 13(3):270-279 doi:10.1002/cmdc.201700669
Dolwick KM, Swanson HI, Bradfield CA (1993) In vitro analysis of Ah receptor domains involved in ligand-activated DNA recognition. Proceedings of the National Academy of Sciences 90(18):8566-8570
Ehrlich AK, Pennington JM, Bisson WH, Kolluri SK, Kerkvliet NI (2018) TCDD, FICZ, and Other High Affinity AhR Ligands Dose-Dependently Determine the Fate of CD4+ T Cell Differentiation. Toxicol Sci 161(2):310-320 doi:10.1093/toxsci/kfx215

Ema M, Ohe N, Suzuki M, et al. (1994) Dioxin binding activities of polymorphic forms of mouse and human arylhydrocarbon receptors. Journal of Biological Chemistry 269(44):27337-27343
Esser C, Rannug A (2015) The aryl hydrocarbon receptor in barrier organ physiology, immunology, and toxicology. Pharmacological reviews 67(2):259-279
Esser C, Welzel M (1993) Ontogenic development of murine fetal thymocytes is accelerated by 3, 3′, 4, 4′-tetrachlorobiphenyl. International journal of immunopharmacology 15(8):841-852
Faith RE, Luster MI (1979) Investigations on the effects of 2, 3, 7, 8‐tetrachlorodibenzo‐p‐dioxin (TCDD) on parameters of various immune functions. Annals of the New York Academy of Sciences 320(1):564-571
Fernandez-Salguero PM, Hilbert DM, Rudikoff S, Ward JM, Gonzalez FJ (1996) Aryl-hydrocarbon receptor-deficient mice are resistant to 2,3,7,8-tetrachlorodibenzo-p-dioxin-induced toxicity. Toxicol Appl Pharmacol 140(1):173-9 doi:10.1006/taap.1996.0210
Fisher MT, Nagarkatti M, Nagarkatti PS (2004) Combined screening of thymocytes using apoptosis-specific cDNA array and promoter analysis yields novel gene targets mediating TCDD-induced toxicity. Toxicol Sci 78(1):116-24 doi:10.1093/toxsci/kfh058
Foged C, Arigita C, Sundblad A, Jiskoot W, Storm G, Frokjaer S (2004) Interaction of dendritic cells with antigen-containing liposomes: effect of bilayer composition. Vaccine 22(15-16):1903-1913
Funatake CJ, Marshall NB, Steppan LB, Mourich DV, Kerkvliet NI (2005) Cutting edge: activation of the aryl hydrocarbon receptor by 2, 3, 7, 8-tetrachlorodibenzo-p-dioxin generates a population of CD4+ CD25+ cells with characteristics of regulatory T cells. The Journal of Immunology 175(7):4184-4188
Gagliani N, Vesely MC, Iseppon A, et al. (2015) Th17 cells transdifferentiate into regulatory T cells during resolution of inflammation. Nature 523(7559):221-5 doi:10.1038/nature14452
Gasiewicz TA, Geiger LE, Rucci G, Neal RA (1983) Distribution, excretion, and metabolism of 2,3,7,8-tetrachlorodibenzo-p-dioxin in C57BL/6J, DBA/2J, and B6D2F1/J mice. Drug metabolism and disposition: the biological fate of chemicals 11(5):397-403
Goettel JA, Gandhi R, Kenison JE, et al. (2016) AHR Activation Is Protective against Colitis Driven by T Cells in Humanized Mice. Cell Rep 17(5):1318-1329 doi:10.1016/j.celrep.2016.09.082
Goudot C, Coillard A, Villani A-C, et al. (2017) Aryl hydrocarbon receptor controls monocyte differentiation into dendritic cells versus macrophages. Immunity 47(3):582-596. e6
Gu Y-Z, Hogenesch JB, Bradfield CA (2000) The PAS superfamily: sensors of environmental and developmental signals. Annual review of pharmacology and toxicology 40(1):519-561

Hanieh H (2014) Toward understanding the role of aryl hydrocarbon receptor in the immune system: current progress and future trends. BioMed research international 2014:520763 doi:10.1155/2014/520763
Hao N, Whitelaw ML (2013) The emerging roles of AhR in physiology and immunity. Biochem Pharmacol 86(5):561-70 doi:10.1016/j.bcp.2013.07.004
Harper PA, Riddick DS, Okey AB (2006) Regulating the regulator: factors that control levels and activity of the aryl hydrocarbon receptor. Biochemical pharmacology 72(3):267-279
Harrill JA, Layko D, Nyska A, et al. (2016) Aryl hydrocarbon receptor knockout rats are insensitive to the pathological effects of repeated oral exposure to 2,3,7,8-tetrachlorodibenzo-p-dioxin. J Appl Toxicol 36(6):802-14 doi:10.1002/jat.3211
Harris M, Moore J, Vos J, Gupta B (1973) General biological effects of TCDD in laboratory animals. Environmental health perspectives 5:101
Hathout RM, Mansour S, Mortada ND, Guinedi AS (2007) Liposomes as an ocular delivery system for acetazolamide: in vitro and in vivo studies. AAPS pharmscitech 8(1):E1-E12
Haynes L, Swain SL (2006) Why aging T cells fail: implications for vaccination. Immunity 24(6):663-666
Henry EC, Bemis JC, Henry O, Kende AS, Gasiewicz TA (2006) A potential endogenous ligand for the aryl hydrocarbon receptor has potent agonist activity in vitro and in vivo. Arch Biochem Biophys 450(1):67-77 doi:10.1016/j.abb.2006.02.008
Henry EC, Welle SL, Gasiewicz TA (2010) TCDD and a putative endogenous AhR ligand, ITE, elicit the same immediate changes in gene expression in mouse lung fibroblasts. Toxicol Sci 114(1):90-100 doi:10.1093/toxsci/kfp285
Holladay S, Lindstrom P, Blaylock B, et al. (1991) Perinatal thymocyte antigen expression and postnatal immune development altered by gestational exposure to tetrachlorodibenzo‐p‐dioxin (TCDD). Teratology 44(4):385-393
Hubbard TD, Murray IA, Bisson WH, et al. (2016) Divergent Ah Receptor Ligand Selectivity during Hominin Evolution. Mol Biol Evol 33(10):2648-58 doi:10.1093/molbev/msw143
Hubert FX, Kinkel SA, Davey GM, et al. (2011) Aire regulates the transfer of antigen from mTECs to dendritic cells for induction of thymic tolerance. Blood 118(9):2462-72 doi:10.1182/blood-2010-06-286393
Jesorka A, Orwar O (2008) Liposomes: technologies and analytical applications. Annu Rev Anal Chem 1:801-832
Jin G-B, Moore AJ, Head JL, Neumiller JJ, Lawrence BP (2010) Aryl hydrocarbon receptor activation reduces dendritic cell function during influenza virus infection. Toxicological sciences 116(2):514-522
Kamath AB, Camacho I, Nagarkatti PS, Nagarkatti M (1999a) Role of Fas-Fas ligand interactions in 2,3,7,8-tetrachlorodibenzo- p-dioxin (TCDD)-induced immunotoxicity: increased resistance of thymocytes from Fas-deficient (lpr)

and Fas ligand-defective (gld) mice to TCDD-induced toxicity. Toxicol Appl Pharmacol 160(2):141-55 doi:10.1006/taap.1999.8753
Kamath AB, Camacho I, Nagarkatti PS, Nagarkatti M (1999b) Role of Fas–Fas ligand interactions in 2, 3, 7, 8-tetrachlorodibenzo-p-dioxin (TCDD)-induced immunotoxicity: increased resistance of thymocytes from Fas-deficient (lpr) and Fas ligand-defective (gld) mice to TCDD-induced toxicity. Toxicology and applied pharmacology 160(2):141-155
Kamath AB, Nagarkatti PS, Nagarkatti M (1998) Characterization of Phenotypic Alterations Induced by 2, 3, 7, 8-Tetrachlorodibenzo-p-dioxin on Thymocytesin Vivoand Its Effect on Apoptosis. Toxicology and applied pharmacology 150(1):117-124
Kamath AB, Xu H, Nagarkatti PS, Nagarkatti M (1997) Evidence for the induction of apoptosis in thymocytes by 2, 3, 7, 8-tetrachlorodibenzo-p-dioxinin vivo. Toxicology and applied pharmacology 142(2):367-377
Kambayashi T, Laufer TM (2014) Atypical MHC class II-expressing antigen-presenting cells: can anything replace a dendritic cell? Nature reviews Immunology 14(11):719
Kerkvliet NI (2002) Recent advances in understanding the mechanisms of TCDD immunotoxicity. International immunopharmacology 2(2-3):277-291
Kerkvliet NI (2012) TCDD: an environmental immunotoxicant reveals a novel pathway of immunoregulation—a 30-year odyssey. Toxicologic pathology 40(2):138-142
Kerkvliet NI, Steppan LB, Vorachek W, et al. (2009) Activation of aryl hydrocarbon receptor by TCDD prevents diabetes in NOD mice and increases Foxp3+ T cells in pancreatic lymph nodes. Immunotherapy 1(4):539-547
Knight SC, Iqball S, Roberts MS, Macatonia S, Bedford PA (1998) Transfer of antigen between dendritic cells in the stimulation of primary T cell proliferation. European journal of immunology 28(5):1636-1644
Kochiadakis GE, Kanoupakis EM, Kalebubas MD, et al. (2001) Sotalol vs metoprolol for ventricular rate control in patients with chronic atrial fibrillation who have undergone digitalization: a single-blinded crossover study. Europace 3(1):73-9 doi:10.1053/eupc.2000.0140
Kouri RE, Ratrie H, Atlas SA, Niwa A, Nebert DW (1974) Aryl hydrocarbon hydroxylase induction in human lymphocyte cultures by 2, 3, 7, 8-tetrachlorodibenzo-p-dioxin. Life sciences 15(9):1585-1595
Kraft JC, Freeling JP, Wang Z, Ho RJ (2014) Emerging research and clinical development trends of liposome and lipid nanoparticle drug delivery systems. Journal of pharmaceutical sciences 103(1):29-52
Kreitinger JM, Beamer CA, Shepherd DM (2016) Environmental immunology: lessons learned from exposure to a select panel of immunotoxicants. The Journal of Immunology 196(8):3217-3225
Lai ZW, Kremer J, Gleichmann E, Esser C (1994) 3, 3′, 4, 4′‐Tetrachlorobiphenyl Inhibits Proliferation of Immature Thymocytes in Fetal Thymus Organ Culture. Scandinavian journal of immunology 39(5):480-488

Laiosa MD, Wyman A, Murante FG, et al. (2003a) Cell proliferation arrest within intrathymic lymphocyte progenitor cells causes thymic atrophy mediated by the aryl hydrocarbon receptor. The Journal of Immunology 171(9):4582-4591
Laiosa MD, Wyman A, Murante FG, et al. (2003b) Cell proliferation arrest within intrathymic lymphocyte progenitor cells causes thymic atrophy mediated by the aryl hydrocarbon receptor. J Immunol 171(9):4582-91
Lee J, Prokopec SD, Watson JD, Sun RX, Pohjanvirta R, Boutros PC (2015a) Male and female mice show significant differences in hepatic transcriptomic response to 2, 3, 7, 8-tetrachlorodibenzo-p-dioxin. BMC genomics 16(1):625
Lee KD, Nir S, Papahadjopoulos D (1993) Quantitative analysis of liposome-cell interactions in vitro: rate constants of binding and endocytosis with suspension and adherent J774 cells and human monocytes. Biochemistry 32(3):889-899
Lee YH, Lin CH, Hsu PC, et al. (2015b) Aryl hydrocarbon receptor mediates both proinflammatory and anti‐inflammatory effects in lipopolysaccharide‐activated microglia. Glia 63(7):1138-1154
Lei Y, Ripen AM, Ishimaru N, et al. (2011) Aire-dependent production of XCL1 mediates medullary accumulation of thymic dendritic cells and contributes to regulatory T cell development. J Exp Med 208(2):383-94 doi:10.1084/jem.20102327
Lepletier A, Chidgey AP, Savino W (2015) Perspectives for improvement of the thymic microenvironment through manipulation of thymic epithelial cells: a mini-review. Gerontology 61(6):504-514
Lewinski N, Colvin V, Drezek R (2008) Cytotoxicity of nanoparticles. small 4(1):26-49
Li S, Pei X, Zhang W, Xie HQ, Zhao B (2014) Functional analysis of the dioxin response elements (DREs) of the murine CYP1A1 gene promoter: beyond the core DRE sequence. International journal of molecular sciences 15(4):6475-6487
Li X, Hu Z, Ma J, et al. (2018) The systematic evaluation of size-dependent toxicity and multi-time biodistribution of gold nanoparticles. Colloids and Surfaces B: Biointerfaces 167:260-266
Liu X, Huang N, Li H, Jin Q, Ji J (2013) Surface and size effects on cell interaction of gold nanoparticles with both phagocytic and nonphagocytic cells. Langmuir 29(29):9138-9148
Lundberg K, Grönvik K-O, Goldschmidt TJ, Klareskog L, Dencker L (1990) 2, 3, 7, 8-Tetrachlorodibenzo-p-dioxin (TCDD) alters intrathymic T-cell development in mice. Chemico-biological interactions 74(1-2):179-193
Lutz CT, Browne G, Petzold CR (1998) Methylcholanthrene causes increased thymocyte apoptosis. Toxicology 128(2):151-167
Masters A, Haynes L, Su DM, Palmer D (2017) Immune senescence: significance of the stromal microenvironment. Clinical & Experimental Immunology 187(1):6-15

Maswadeh H, Demetzos C, Daliani I, et al. (2002) A molecular basis explanation of the dynamic and thermal effects of vinblastine sulfate upon dipalmitoylphosphatidylcholine bilayer membranes. Biochimica et Biophysica Acta (BBA)-Biomembranes 1567:49-55
Mellman I, Steinman RM (2001) Dendritic cells: specialized and regulated antigen processing machines. Cell 106(3):255-258
Merad M, Sathe P, Helft J, Miller J, Mortha A (2013) The dendritic cell lineage: ontogeny and function of dendritic cells and their subsets in the steady state and the inflamed setting. Annual review of immunology 31:563-604
Mezrich JD, Fechner JH, Zhang X, Johnson BP, Burlingham WJ, Bradfield CA (2010) An interaction between kynurenine and the aryl hydrocarbon receptor can generate regulatory T cells. The Journal of Immunology:0903670
Miniero R, De Felip E, Ferri F, Di Domenico A (2001) An overview of TCDD half-life in mammals and its correlation to body weight. Chemosphere 43(4-7):839-844
Mizrahy S, Goldsmith M, Leviatan-Ben-Arye S, et al. (2014) Tumor targeting profiling of hyaluronan-coated lipid based-nanoparticles. Nanoscale 6(7):3742-3752
Mo R, Chen J, Han Y, et al. (2003) T cell chemokine receptor expression in aging. The Journal of Immunology 170(2):895-904
Murphy K, Weaver C (2016) Janeway's immunobiology. Garland Science
Murray JM, Kaufmann GR, Hodgkin PD, et al. (2003) Naive T cells are maintained by thymic output in early ages but by proliferation without phenotypic change after age twenty. Immunology and Cell Biology 81(6):487
Nault R, Fader KA, Harkema JR, Zacharewski T (2017) Loss of liver-specific and sexually dimorphic gene expression by aryl hydrocarbon receptor activation in C57BL/6 mice. PloS one 12(9):e0184842
Nebert D, Gelboin H (1968) Substrate-inducible microsomal aryl hydroxylase in mammalian cell culture I. Assay and properties of induced enzyme. Journal of Biological Chemistry 243(23):6242-6249
Nebert D, Gelboin H (1969) The in vivo and in vitro induction of aryl hydrocarbon hydroxylase in mammalian cells of different species, tissues, strains, and developmental and hormonal states. Archives of biochemistry and biophysics 134(1):76-89
Needham L, Gerthoux P, Patterson Jr D, et al. (1999) Exposure assessment: serum levels of TCDD in Seveso, Italy. Environmental research 80(2):S200-S206
Nguyen LP, Bradfield CA (2007) The search for endogenous activators of the aryl hydrocarbon receptor. Chemical research in toxicology 21(1):102-116
Nikolaidis E, Brunström B, Dencker L (1988) Effects of the TCDD congeners 3, 3′, 4, 4′-tetrachlorobiphenyl and 3, 3′, 4, 4′-tetrachloroazoxybenzene on lymphoid development in the bursa of Fabricius of the chick embryo. Toxicology and applied pharmacology 92(2):315-323
Nohara K, Suzuki T, Ao K, et al. (2009) Constitutively active aryl hydrocarbon receptor expressed in T cells increases immunization-induced IFN-gamma production in mice but does not suppress T(h)2-cytokine production or

antibody production. Int Immunol 21(7):769-77 doi:10.1093/intimm/dxp045
Nowell CS, Farley AM, Blackburn CC (2007) Thymus organogenesis and development of the thymic stroma Immunological Tolerance. Springer, p 125-162
Nugent LF, Shi G, Vistica BP, Ogbeifun O, Hinshaw SJ, Gery I (2013) ITE, a novel endogenous nontoxic aryl hydrocarbon receptor ligand, efficiently suppresses EAU and T-cell-mediated immunity. Invest Ophthalmol Vis Sci 54(12):7463-9 doi:10.1167/iovs.12-11479
Nukaya M, Bradfield CA (2009) Conserved genomic structure of the Cyp1a1 and Cyp1a2 loci and their dioxin responsive elements cluster. Biochemical pharmacology 77(4):654-659
Okey A, Bondy G, Mason M, et al. (1979) Regulatory gene product of the Ah locus. Characterization of the cytosolic inducer-receptor complex and evidence for its nuclear translocation. Journal of Biological Chemistry 254(22):11636-11648
Okey AB (2007) An aryl hydrocarbon receptor odyssey to the shores of toxicology: the Deichmann Lecture, International Congress of Toxicology-XI. Toxicol Sci 98(1):5-38 doi:10.1093/toxsci/kfm096
Olsen PC, Ferreira TP, Serra MF, et al. (2011) Lidocaine-derivative JMF2-1 prevents ovalbumin-induced airway inflammation by regulating the function and survival of T cells. Clin Exp Allergy 41(2):250-9 doi:10.1111/j.1365-2222.2010.03580.x
Olson JR, Holscher MA, Neal RA (1980) Toxicity of 2,3,7,8-tetrachlorodibenzo-p-dioxin in the golden Syrian hamster. Toxicol Appl Pharmacol 55(1):67-78
Pearse G (2006) Normal structure, function and histology of the thymus. Toxicologic pathology 34(5):504-514
Perdew GH, Murray IA, Hubbard TD (2015) Indole and tryptophan metabolism: endogenous and dietary routes to Ah receptor activation. Drug Metabolism and Disposition:dmd. 115.064246
Platt N, da Silva RP, Gordon S (1998) Recognizing death: the phagocytosis of apoptotic cells. Trends in cell biology 8(9):365-372
Platzer B, Richter S, Kneidinger D, Waltenberger D, Woisetschläger M, Strobl H (2009) Aryl hydrocarbon receptor activation inhibits in vitro differentiation of human monocytes and Langerhans dendritic cells. The Journal of Immunology:jimmunol. 0802997
Pohjanvirta R (2011) The AH receptor in Biology and Toxicology. John Wiley & Sons
Poland A, Glover E (1975) Genetic expression of aryl hydrocarbon hydroxylase by 2, 3, 7, 8-tetrachlorodibenzo-p-dioxin: evidence for a receptor mutation in genetically non-responsive mice. Molecular Pharmacology 11(4):389-398
Poland A, Glover E (1980) 2, 3, 7, 8-Tetrachlorodibenzo-p-dioxin: segregation of toxicity with the Ah locus. Molecular Pharmacology 17(1):86-94
Poland A, Glover E, Kende A (1976) Stereospecific, high affinity binding of 2, 3, 7, 8-tetrachlorodibenzo-p-dioxin by hepatic cytosol. Evidence that the binding species is receptor for induction of aryl hydrocarbon hydroxylase. Journal of Biological Chemistry 251(16):4936-4946

Poland A, Palen D, Glover E (1994) Analysis of the four alleles of the murine aryl hydrocarbon receptor. Molecular pharmacology 46(5):915-921
Prelog M (2006) Aging of the immune system: a risk factor for autoimmunity? Autoimmunity reviews 5(2):136-139
Proietto AI, van Dommelen S, Zhou P, et al. (2008a) Dendritic cells in the thymus contribute to T-regulatory cell induction. Proceedings of the National Academy of Sciences 105(50):19869-19874
Proietto AI, van Dommelen S, Zhou P, et al. (2008b) Dendritic cells in the thymus contribute to T-regulatory cell induction. Proc Natl Acad Sci U S A 105(50):19869-74 doi:10.1073/pnas.0810268105
Qiu J, Heller JJ, Guo X, et al. (2012) The aryl hydrocarbon receptor regulates gut immunity through modulation of innate lymphoid cells. Immunity 36(1):92-104 doi:10.1016/j.immuni.2011.11.011
Quintana FJ, Murugaiyan G, Farez MF, et al. (2010a) An endogenous aryl hydrocarbon receptor ligand acts on dendritic cells and T cells to suppress experimental autoimmune encephalomyelitis. Proceedings of the National Academy of Sciences 107(48):20768-20773
Quintana FJ, Murugaiyan G, Farez MF, et al. (2010b) An endogenous aryl hydrocarbon receptor ligand acts on dendritic cells and T cells to suppress experimental autoimmune encephalomyelitis. Proceedings of the National Academy of Sciences of the United States of America 107(48):20768-73 doi:10.1073/pnas.1009201107
Quintana FJ, Murugaiyan G, Farez MF, et al. (2010c) An endogenous aryl hydrocarbon receptor ligand acts on dendritic cells and T cells to suppress experimental autoimmune encephalomyelitis. Proc Natl Acad Sci U S A 107(48):20768-73 doi:10.1073/pnas.1009201107
Ramana LN, Sethuraman S, Ranga U, Krishnan UM (2010) Development of a liposomal nanodelivery system for nevirapine. Journal of biomedical science 17(1):57
Rhile MJ, Nagarkatti M, Nagarkatti PS (1996) Role of Fas apoptosis and MHC genes in 2, 3, 7, 8-tetrachlorodibenzo-p-dioxin (TCDD)-induced immunotoxicity of T cells. Toxicology 110(1-3):153-167
Sade A, Banerjee S, Severcan F (2010) Concentration-dependent differing actions of the nonsteroidal anti-inflammatory drug, celecoxib, in distearoyl phosphatidylcholine multilamellar vesicles. Journal of liposome research 20(2):168-177
Savino W (2006) The thymus is a common target organ in infectious diseases. PLoS pathogens 2(6):e62
Serro A, Galante R, Kozica A, et al. (2014) Effect of tetracaine on DMPC and DMPC+ cholesterol biomembrane models: Liposomes and monolayers. Colloids and Surfaces B: Biointerfaces 116:63-71
Silkworth J, Antrim L (1985) Relationship between Ah receptor-mediated polychlorinated biphenyl (PCB)-induced humoral immunosuppression and thymic atrophy. Journal of Pharmacology and Experimental Therapeutics 235(3):606-611

Silkworth JB, Antrim L, Sack G (1986) Ah receptor mediated suppression of the antibody response in mice is primarily dependent on the Ah phenotype of lymphoid tissue. Toxicology and applied pharmacology 86(3):380-390
Silverstone AE, Frazier DE, Jr., Fiore NC, Soults JA, Gasiewicz TA (1994a) Dexamethasone, beta-estradiol, and 2,3,7,8-tetrachlorodibenzo-p-dioxin elicit thymic atrophy through different cellular targets. Toxicol Appl Pharmacol 126(2):248-59 doi:10.1006/taap.1994.1114
Silverstone AE, Frazier DE, Jr., Gasiewicz TA (1994b) Alternate immune system targets for TCDD: lymphocyte stem cells and extrathymic T-cell development. Exp Clin Immunogenet 11(2-3):94-101
Simones T, Shepherd DM (2011) Consequences of AhR activation in steady-state dendritic cells. Toxicol Sci 119(2):293-307 doi:10.1093/toxsci/kfq354
Singh NP, Singh UP, Rouse M, et al. (2016) Dietary Indoles Suppress Delayed-Type Hypersensitivity by Inducing a Switch from Proinflammatory Th17 Cells to Anti-Inflammatory Regulatory T Cells through Regulation of MicroRNA. J Immunol 196(3):1108-22 doi:10.4049/jimmunol.1501727
Singh U, Abron J, Singh N, et al. (2014) An endogenous aryl hydrocarbon receptor (AhR) ligand, ITE induces regulatory T cells (Tregs) and ameliorates experimental colitis (IRC4P. 490). Am Assoc Immnol
Smith KJ, Murray IA, Boyer JA, Perdew GH (2018) Allelic variants of the aryl hydrocarbon receptor differentially influence UVB-mediated skin inflammatory responses in SKH1 mice. Toxicology 394:27-34
Song J, Clagett-Dame M, Peterson RE, et al. (2002) A ligand for the aryl hydrocarbon receptor isolated from lung. Proceedings of the National Academy of Sciences 99(23):14694-14699
Staples JE, Murante FG, Fiore NC, Gasiewicz TA, Silverstone AE (1998) Thymic alterations induced by 2,3,7,8-tetrachlorodibenzo-p-dioxin are strictly dependent on aryl hydrocarbon receptor activation in hemopoietic cells. J Immunol 160(8):3844-54
Stockinger B (2009) Beyond toxicity: aryl hydrocarbon receptor-mediated functions in the immune system. J Biol 8(7):61 doi:10.1186/jbiol170
Stockinger B, Meglio PD, Gialitakis M, Duarte JH (2014) The aryl hydrocarbon receptor: multitasking in the immune system. Annual review of immunology 32:403-432
Surh CD, Sprent J (2000) Homeostatic T cell proliferation: how far can T cells be activated to self-ligands? Journal of Experimental Medicine 192(4):F9-F14
Swanson HI, Chan WK, Bradfield CA (1995) DNA binding specificities and pairing rules of the Ah receptor, ARNT, and SIM proteins. Journal of Biological Chemistry 270(44):26292-26302
Tacken PJ, Zeelenberg IS, Cruz LJ, et al. (2011) Targeted delivery of Toll-like receptor ligands to human and mouse dendritic cells strongly enhances adjuvanticity. Blood:blood-2011-07-367615
Takenaka MC, Quintana FJ Tolerogenic dendritic cells. In: Seminars in immunopathology, 2017. vol 39. Springer, p 113-120

Temchura VV, Frericks M, Nacken W, Esser C (2005) Role of the aryl hydrocarbon receptor in thymocyte emigration in vivo. European journal of immunology 35(9):2738-2747
Tran TH, Tran TTP, Nguyen HT, et al. (2018) Nanoparticles for dendritic cell-based immunotherapy. International journal of pharmaceutics
Van Loveren H, Schuurman H-J, Kampinga J, Vos JG (1991) Reversibility of thymic atrophy induced by 2, 3, 7, 8-tetrachlorodibenzo-p-dioxin (TCDD) and bis (tri-n-butyltin) oxide (TBTO). International journal of immunopharmacology 13(4):369-377
Vecchi A, Mantovani A, Sironi M, Luini W, Cairo M, Garattini S (1980) Effect of acute exposure to 2, 3, 7, 8-tetrachlorodibenzo-p-dioxin on humoral antibody production in mice. Chemico-biological interactions 30(3):337-342
Vogel CF, Goth SR, Dong B, Pessah IN, Matsumura F (2008) Aryl hydrocarbon receptor signaling mediates expression of indoleamine 2, 3-dioxygenase. Biochemical and biophysical research communications 375(3):331-335
Vorderstrasse BA, Kerkvliet NI (2001) 2, 3, 7, 8-Tetrachlorodibenzo-p-dioxin affects the number and function of murine splenic dendritic cells and their expression of accessory molecules. Toxicology and applied pharmacology 171(2):117-125
Walisser JA, Glover E, Pande K, Liss AL, Bradfield CA (2005) Aryl hydrocarbon receptor-dependent liver development and hepatotoxicity are mediated by different cell types. Proceedings of the National Academy of Sciences of the United States of America 102(49):17858-17863
Wang C, Ye Z, Kijlstra A, Zhou Y, Yang P (2014) Activation of the aryl hydrocarbon receptor affects activation and function of human monocyte‐derived dendritic cells. Clinical & Experimental Immunology 177(2):521-530
Watson DS, Endsley AN, Huang L (2012) Design considerations for liposomal vaccines: influence of formulation parameters on antibody and cell-mediated immune responses to liposome associated antigens. Vaccine 30(13):2256-2272
Winans B, Nagari A, Chae M, et al. (2015) Linking the Aryl Hydrocarbon Receptor with Altered DNA Methylation Patterns and Developmentally Induced Aberrant Antiviral CD8+ T Cell Responses. The Journal of Immunology 194(9):4446-4457
Wright EJ, De Castro KP, Joshi AD, Elferink CJ (2017) Canonical and non-canonical aryl hydrocarbon receptor signaling pathways. Current Opinion in Toxicology 2:87-92
Wu L, Shortman K (2005) Heterogeneity of thymic dendritic cells. Seminars in immunology 17(4):304-12 doi:10.1016/j.smim.2005.05.001
Yang YY, Lee FY, Hsu HC, et al. (2011) Assessment of first-year post-graduate residents: usefulness of multiple tools. J Chin Med Assoc 74(12):531-8 doi:10.1016/j.jcma.2011.10.002
Yao EF, Denison MS (1992) DNA sequence determinants for binding of transformed Ah receptor to a dioxin-responsive enhancer. Biochemistry 31(21):5060-5067

Yeste A, Nadeau M, Burns EJ, Weiner HL, Quintana FJ (2012) Nanoparticle-mediated codelivery of myelin antigen and a tolerogenic small molecule suppresses experimental autoimmune encephalomyelitis. Proc Natl Acad Sci U S A 109(28):11270-5 doi:10.1073/pnas.1120611109

Zhang L, Ma J, Takeuchi M, et al. (2010) Suppression of experimental autoimmune uveoretinitis by inducing differentiation of regulatory T cells via activation of aryl hydrocarbon receptor. Investigative ophthalmology & visual science 51(4):2109-2117